Université catholique de Louvain
Faculté des Sciences
Institut de Recherche en Mathématique et Physique
Centre for Cosmology, Particle Physics and Phenomenology

Quarks beyond the Top

Doctoral dissertation presented by

Mathieu Buchkremer

in fulfilment of the requirements for the degree of Doctor in Sciences

Prof. Jean-Marc Gérard (Advisor)	UCL, Belgium
Prof. Fabio Maltoni (Advisor)	UCL, Belgium
Prof. Jan Govaerts (Chairman)	UCL, Belgium
Prof. Eduardo Cortina Gil	UCL, Belgium
Prof. Aldo Deandrea	Lyon 1, France
Prof. Jorgen D'Hondt	VUB, Belgium

August 2014

If, in some cataclysm, all of scientific knowledge were to be destroyed, and only one sentence passed on to the next generations of creatures, what statement would contain the most information in the fewest words? I believe it is the atomic hypothesis that all things are made of atoms. In that one sentence, you will see, there is an enormous amount of information about the world, if just a little imagination and thinking are applied.

Richard Feynman

Acknowledgements

A bit of advice given to a young Native American at the time of his initiation: "As you go the way of life, you will see a great chasm. Jump. It is not as wide as you think."

Joseph Campbell

Despite the obsctacles, making such a leap forward would not have been possible without the endless help and support of many people. While an obvious statement, I want here to testify how important it has been for me while going through such a memorable journey.

Foremost, I want to express my sincere gratitude to my "number 1" advisor, Prof. Jean-Marc Gérard, for offering me the opportunity to undertake and complete this thesis on such an enthralling and challenging topic. His enthusiasm and expertise constantly pushed me forward the past four years, and I would like to thank him for his careful supervision, not to mention the trust and support he gave me while conducting my research.

I am also indebted to my second “number 1” advisor, Prof. Fabio Maltoni. I cannot thank him enough for sharing his amazing expertise of the field, and teaching me the importance of being rigorous and thinking critically (also overcoming my tendency to take shortcuts). I am much obliged to him for making me realise the value of effective scientific communication, and for encouraging me to travel and build collaborations. Many thanks, Fabio.

I wish to thank all the members of my jury for their interest and accepting to read my manuscript. In particular, I am beholden to Profs. Jan Govaerts and Eduardo Cortina Gil for their attentive guidance throughout my studies. I would like to show my appreciation to Prof. Jorgen D’Hondt for his eye for detail, taking the opportunity here to thank all the IIHE members for these many enriching discussions at Vrije Universiteit Brussels. Proof, if any were required, that collaboration constantly leads to fruitful results. Dank u wel Petra, Freya, Gerrit, Bettina and Kentarou !

I am much grateful to Prof. Aldo Deandrea who kindly accepted to be part of my jury. Aldo, I cannot express how pleasant it has been to experience such an amazing collaboration with you, Giacomo, Luca, Daniele, Sasha, Stefania, Jad and Stefano. Thank you for these warm welcomes at IPNL in Lyon, not to mention this amazing cooperation we enjoyed with the rest of the “crew”: thanks for all the helpful physical discussions, and the neverending help on this exciting work done together (and still to be done). Whatever lies around the corner, I am much obliged to all of you who have been top partners on this journey (pun intended).

Completing this picture on a more international note, I must acknowledge Profs. Wei-Shu (George) Hou, Kai-Feng (Jack) Chen and P.Q. Hung, with whom I had so many valuable discussions in Taiwan and Quy Nhon: it has been a real pleasure to meet you and enjoy together this "pre-Higgs discovery" epoch in Asia. Last but not least, I wish to express my heartfelt appreciation to Alexander Schmidt and his team in Hamburg, who have been working hard (and keep working hard) on these impressive "post-Higgs" searches. To me, it comes as no surprise that CMS is performing so well, knowing that all of you are behind such a wonderful experiment.

On a more personal note, I would like to thank here all the CP3 people. To each of you who offered your time and talents, and in random order (my apologies if anyone has been forgotten on the list), thank you Michaël, Elvira, Philippe, Antoine, Marco, Michele, Alexandre, Gauthier, Elisa, Cen, Simone, Julien, Loic, Simon, Pierre, Laurent, Priscila, Olivier, Céline, Bob, Claude, Giacomo, Alban, Stéphane, Ludivine, Adrien, Camille, Nicolas, Federico, Roshan, Lucia, David, Eleni, Andrea, Tristan, Suzan, Christophe, Matthias, Andrey, Marcello, Vincent, Michel, Christophe, Ioannis, Brieuc, Antony, Benoît and all of you who have been in the same boat all these years: I wish you Godspeed ! Of course, a very special "thank you" goes to Ginette and Luc, for their support (both administrative and moral). Further thanks to the CP3 computing team: Vincent, Jérôme, Pavel and Juan for the patience they exercised while configuring my dual-booted machine, and not even considering asking me to buy another one. I also wish to personally thank my laptop for not exploding in a shower of fire and smoke before I completed the last page of this thesis.

Special thanks to Ivan, Philippe, Sébastien, Nabila, Jonathan, Arnaud, Nicolas, Michaël, Lise and Guillaume for your friendship and all the time spent together. It would not have been the same without you !

And finally, I conclude with a huge MERCI! to my whole family, for supporting me all over through this journey. Even light-years away from home, but always in my heart and thoughts, nothing of this could have been possible without your presence and encouragements.

This work has been supported by the National Fund for Scientific Research (F.R.S.-FNRS), under a FRIA grant.

Contents

Introduction

The goal of Particle Physics is to identify the ultimate building blocks of Nature, and to understand their fundamental interactions. In this context, there is no need to stress the importance and elegance of the Standard Model (SM) of particle physics as a remarkably successful theory. In a systematic and descriptive fashion, the electroweak theory with the Brout-Englert-Higgs mechanism and Quantum Chromo-Dynamics with confinement account together for the most prominent experimental observations in high energy physics. The recent observation of a new particle resembling the long-sought Higgs boson at the Large Hadron Collider (LHC) allowed to firmly establish the effective description of the SM, providing us with strong evidence for its validity.

But despite the fact that most of the current experimental results are consistent within this framework, several fundamental problems are still to be addressed. For instance, the theoretical motivation for having exactly three chiral generations of quarks and leptons is not explained by the theory, neither is the pattern of fermion masses and mixings. Another open issue is the origin of charge quantisation, intimately related to the electroweak quantum numbers of every matter particle through the Gell-Mann–Nishijima formula. The seemingly arbitrary origin of the Yukawa couplings, the existence of massive neutrinos, and the nature of the Cabibbo-Kobayashi-Maskawa mixing matrix also point at the need for new physics beyond the SM. From a larger perspective, we can also mention the absence of any quantum field theory of gravity, the lack of justifi-

cation for the baryonic asymmetry of the universe, and the unexplained nature of Dark Matter, if any.

As a straightforward illustration, one of the Holy Grails of contemporary particle physics is certainly the issue of naturalness. The discovery of a Higgs candidate at a mass of 125 GeV is actually understood as a realisation of the Hierarchy problem: why would the scalar mass be so close to the electroweak scale ? What symmetry, if any, is shielding it from large loop corrections at larger energy scales ? While the SM is expected to loose its predictive power as the experimental searches now reach the TeV scale, the quest for an answer to such questions has been the guiding principle behind the flourishing of model building in the past decades.

Appraising the impressive amount of experimental data that has been collected since the start of the LHC experiments in 2009, the past years have seen tremendous changes in the landscape of the new physics scenarios attempting to solve these problems. From direct searches, the CMS and ATLAS collaborations now put stringent constraints on the parameter space of many scenarios going beyond the Standard Model, including Supersymmetry (SUSY). Likewise, flavour and electroweak precision constraints have been shown to be consistent with the Standard Model expectations with an unprecedented accuracy, especially in B-physics.

Models of supersymmetry are arguably among the best-motivated theories to solve the gauge hierarchy problem and explain a light SM-like Higgs boson. Yet, simpler models may also offer interesting clues about the naturalness issue. A common ingredient of these scenarios is the presence of new weakly coupled states, which effectively cut-off the divergent loop contributions to the Higgs mass by mixing with the Standard Model states. As the top quark is known to have the largest Yukawa coupling to the Higgs field, it is also a natural expectation that the lightest new states mix with the top itself, regulating the large quantum corrections to the Higgs boson mass.

While SUSY theories introduce new symmetries and numerous scalar degrees of freedom, the case for tentative new coloured fermions requires different search strategies, which must be treated with care at the LHC. Even though it is acknowledged that a new chiral family of fermions is now ruled out by the recent Higgs searches results obtained by the ATLAS and CMS collaborations,

this does not embed all the possibilities of having new massive fermions beyond the top. In particular, vector-like representations of top partners remain a crucial issue that we will investigate in this work. From a bottom-up perspective, non-chiral quarks can naturally exist near the electroweak scale without upsetting the existing measurements. Since their left- and right-handed components transform in the same way under the electroweak gauge group, their mass terms are neither forbidden nor bounded by any symmetry. While their masses decouple when they are taken to infinity, the low-energy phenomenology of the SM is barely affected. Furthermore, their presence automatically breaks the Glashow-Iliopoulos-Maiani mechanism giving rise to flavour-changing neutral currents at tree-level. In this respect, new vector-like quarks might imply unitarity violations of the CKM matrix, as well as potential new sources of CP violation.

In a top-down approach, the possibility for vector-like quarks close to the TeV scale is a common feature of many scenarios going beyond the SM. Prominent examples include Little Higgs and composite Higgs models, extra-dimensional and grand-unified theories, as well as scenarios with gauged flavour groups. If the Higgs occurs to be a pseudo-Goldstone boson, new fermions could help to induce the breaking of the electroweak symmetry, explaining the observed lightness of the Higgs. As another example, theories of flavour with partial-compositeness predict new heavy fermions to mix sizeably with the third family of SM quarks, explaining the large size of the top quark Yukawa coupling. While such motivations might not seem compelling with respect to the very good agreement between the SM predictions and the LHC measurements, they are suggestive in encouraging new physics extensions.

As a key strategy, the premise defended in this thesis is that narrowing down the large number of proposed scenarios appears to be the most efficient way to make progress in the next decade. As the huge amount of literature on BSM scenarios proves, a full scan of the parameter spaces associated to these models is too ambitious to be tackled in full generality. Given the unprecedented sensitivity currently reached in Flavour and Collider Physics, both approaches will provide invaluable insights into their couplings and mixing patterns. We argue that model independent approaches should be privileged in that perspective. Ensuring proper communication between theoretical models and the LHC

collaborations then becomes a task more important than ever given the large amount of new physics extensions that have to be compared with experimental data.

In this context, the present work provides an overview of the current phenomenology of heavy quarks above the top at the LHC. Our objective is to analyse the implications of new quarks with a mass close to the TeV scale, and investigate the processes in which they could possibly be put in evidence. As we will establish, the forthcoming measurements at the LHC yield strong potential for the discovery or exclusion of such new particles.

The outline is as following. In **Chapter 1** we present a brief overview of the Standard Model. After introducing its basic ingredients, the theoretical picture of the gauge interactions and elementary particles is considered, with a specific focus on the fundamental origins of massive particles in nature. **Chapter 2** is dedicated to a systematic analysis of the constraints set on a sequential fourth generation of quarks and leptons. The implications of the direct limits set from the recent LHC results are then discussed, together with the Higgs search constraints and Electroweak precision observables. In synergy with the CMS collaboration, these results helped to develop an inclusive search strategy for a new sequential quark family, produced either singly or in pairs. Assuming a minimal off-diagonal mixing between the fourth and the third generation quarks, the obtained results now rule out t' and b' chiral quark masses below the unitarity and perturbativity bounds.

In **Chapter 3**, we introduce a model-independent framework to study the LHC phenomenology of vector-like top partners, and perform a comprehensive analysis of the various production modes of these new states. Considering non-chiral states embedded in general representations of the weak $SU(2)_L$, we detail how new heavy quarks can be studied in terms of few parameters in an effective description with a clear and simple connection with the experimental observables. The key note of our approach relies on the introduction of a model-independent and general Lagrangian, allowing for couplings to the three known Standard Model quark generations. Based on this parametrisation, we probe the possibility for new top partners to be singly produced at the LHC, in conjunction with the constraints obtained from Flavour Physics. Our main results are a clear connection between branching ratios and single production

channels, and the identification of novel interesting channels to be studied at the LHC. Further, our analysis indicates that new exotic quarks are likely to be produced electroweakly and with significant cross-sections, at large center of mass energies.

Experimental searches for new heavy quarks are generally undertaken under the simplifying assumption that only one new state beside the Standard Model is present. The obtained bounds, however, cannot be easily reinterpreted in models which contain multiple top partners, with possibly different charges. In this context, **Chapter 4** presents a dedicated tool, aiming at setting conservative bounds on scenarios involving one or multiple heavy extra quarks, with generic assumptions on their decay modes. For that purpose, we designed, validated and applied a software package called `XQCAT` (eXtra Quark Combined Analysis Tool), which determines the exclusion confidence level based on publicly available experimental data from direct searches for top partners and from Supersymmetry inspired searches. Based on these results, the mass limits set on a simplified benchmark scenarios, with general coupling assumptions, are briefly discussed in this framework. Finally, we conclude with possible prospects and future strategies, highlighting the interest of combining multiple searches so as to set bounds on extended fermion sectors at the TeV scale, and beyond.

The work presented in this thesis is based on the following publications:

- M. Buchkremer, J.-M. Gérard, F. Maltoni, "Closing in on a perturbative fourth generation", *JHEP*, vol. 1206, pp. 135, 2012, 1204.5403.

- M. Buchkremer, G. Cacciapaglia, A. Deandrea, L. Panizzi, "Model Independent Framework for Searches of Top Partners", *Nucl.Phys.*, vol. B876, pp. 376-417, 2013, 1305.4172.

- D. Barducci, A. Belyaev, M. Buchkremer, G. Cacciapaglia, A. Deandrea, S. De Curtis, J. Marrouche, S. Moretti, L. Panizzi, "Model Independent Framework for Analysis of Scenarios with Multiple Heavy Extra Quarks", submitted for publication in *JHEP*, 1405.0737.

Some of the presented results have also been published in:

- M. Buchkremer, A. Schmidt, "Long-lived heavy quarks : a review", *Adv. High Energy Phys.*, vol. 2013, pp. 690254, 2013, 1210.6369.

- G. Brooijmans *et al.*, "Les Houches 2013: Physics at TeV Colliders: New Physics Working Group Report", 1405.1617.

- M. Buchkremer, "Model-independent analysis of scenarios with heavy vector-like top partners", *proceedings contribution to the XLIXth Rencontres de Moriond session devoted to electroweak interactions and unified theories (La Thuile, March 15th - March 22th, 2014)*, 1405.2586.

Chapter 1

The Standard Model

"Nature uses only the longest threads to weave her patterns, so each small piece of her fabric reveals the organization of the entire tapestry"

Richard Feynman

In this chapter we present a brief summary of the Standard Model (SM) and of its theoretical framework. After the introduction of its matter content, the gauge structure of the fundamental interactions is discussed. Based on these basic ingredients, we then review the major role played by the spontaneous breaking of the electroweak symmetry and the Brout-Englert-Higgs mechanism, and how the latter explains the observation of massive particles in the SM. Finally, we conclude with one of the main issues left open by the theory, namely, the hierarchy problem.

1.1 Particle content

One of the most successful theories of physics up to date, the Standard Model describes three of the four fundamental interactions observed in nature. It consists of two theories formulated during the second half of the 20th century,

namely, the electroweak theory of Glashow, Weinberg and Salam based on the gauge symmetry group $SU(2)_L \times U(1)_Y$ [1, 2], together with Quantum Chromo-Dynamics (QCD), the theory of strong interactions based associated to the $SU(3)_c$ group [3, 4, 5, 6] [1].

A theory of quarks and leptons, the Standard Model (SM) describes the electromagnetic and weak interactions within a single framework. At the particle level, the model includes two kinds of fields: the matter and the gauge fields. Classifying all elementary particles according to their quantum numbers, they can be distinguished in two groups. The matter particles, called *fermions*, carry a half-integer spin, whereas the mediators of the fundamental forces, the *bosons*, have an integral spin. For every fermion, there exists an antiparticle partner with identical mass, but differing from its counterpart by opposite signs of its quantum numbers.

In this framework, matter fields consist of three distinct generations of Dirac fermions, classified into chiral *quarks* and *leptons*. The left-handed components of the fields transform as doublets under the weak isospin group $SU(2)_L$, while the right handed components transform as singlets. The upper and lower partners of each doublet have a weak isospin equal to $1/2$ and $-1/2$ respectively, whereas the third axis projection of the weak isospin T_3 vanishes for singlets.

Quarks are the fundamental particles of matter. They are grouped together to form three sets called *generations* with identical properties except for their mass. Each of these three families consists of two types of quarks, carrying an electric charge $\mathrm{Q}_{up} = 2/3$ and $\mathrm{Q}_{down} = -1/3$, respectively. Up, down quarks (u, d) are forming the lightest generation, while the two other families contain corresponding heavier quarks, i.e., charm, strange (c, s) and top, bottom (t, b) pairs. We can readily emphasise the particular role played by the top quark in the SM: due to its large mass $m_t = 173.3$ GeV [7, 8], the top is the heaviest elementary particle known in nature. As observed, all these six quarks possess an additional quantum number: colour. As a consequence, quarks are the only

[1] The only fundamental force absent from this framework is that of gravity ; including the latter in a consistent quantum field theory remains a difficult challenge which is still to be resolved.

	$i=1$	$i=2$	$i=3$	Q	T_3	Y
Q_L^i	$\begin{pmatrix} u \\ d \end{pmatrix}_L$	$\begin{pmatrix} c \\ s \end{pmatrix}_L$	$\begin{pmatrix} t \\ b \end{pmatrix}_L$	$\begin{pmatrix} 2/3 \\ -1/3 \end{pmatrix}$	$\begin{pmatrix} +1/2 \\ -1/2 \end{pmatrix}$	$\begin{pmatrix} 1/3 \\ 1/3 \end{pmatrix}$
u_R^i	u_R	c_R	t_R	$2/3$	0	$4/3$
d_R^i	d_R	s_R	b_R	$-1/3$	0	$-2/3$
L_L^i	$\begin{pmatrix} \nu_e \\ e \end{pmatrix}_L$	$\begin{pmatrix} \nu_\mu \\ \mu \end{pmatrix}_L$	$\begin{pmatrix} \nu_\tau \\ \tau \end{pmatrix}_L$	$\begin{pmatrix} 0 \\ -1 \end{pmatrix}$	$\begin{pmatrix} +1/2 \\ -1/2 \end{pmatrix}$	$\begin{pmatrix} -1 \\ -1 \end{pmatrix}$
l_R^i	e_R	μ_R	τ_R	-1	0	-2

Table 1.1: The matter fields have fixed quantum numbers under the electroweak gauge group. Depending in the chirality, the left-handed fermions transform as doublets under the weak isospin group $SU(2)_L$, while the right-handed degrees-of-freedom transform as singlets. The electric charge of each field is the sum of the third component of the weak isospin T_3 of of the weak hypercharge Y, to which each quark and lepton belongs. Note that both members of a same SU(2)$_L$ doublet have the same weak hypercharge to satisfy gauge invariance. Not listed above, antiparticles partners have identical mass, but differ from their counterparts by opposite signs of their quantum numbers.

known matter particles sensitive to the strong interaction, and transform as triplets under $SU(3)_c$. Leptons are likewise fermionic particles that have an integral electric charge $Q = 0, -1$. As they do not carry colour, they are only affected by the electromagnetic and weak forces. The electron (e) and the electron-neutrino (ν_e) compose the first generation, while the muon (μ) and the tau (τ) are similarly arranged with the corresponding neutrinos (ν_μ and ν_τ) to form the second and third generations. The particle content of these three families, the associated fields and their quantum numbers are summarised in Tab. 1.1.

It is interesting to observe that the value of the charge assignments for $2(Q - T_3)$ are identical for all members inside a given multiplet. In the following, we will denote the latter quantity as the hypercharge Y, namely, the conserved charge associated to the abelian group $U(1)_Y$. Consequently, we can check that the so-called Gell-Mann-Nishijima relation holds for all the generators of the groups, as originally introduced in the context of the strong interaction:

$$Q = T_3 + \frac{Y}{2}, \tag{1.1.1}$$

1.2 Gauge symmetries

The dynamics of any quantum theory of fields are described by a Lagrangian which specifies all the allowed interactions between the various degrees of freedom of the theory. Besides the matter fields, gauge bosons must be introduced so as to mediate the fundamental interactions of the electroweak Standard Model. By construction, the electroweak part of the SM is required to be gauge invariant under the symmetry group $SU(2)_L \times U(1)_Y$, combining the weak and the electromagnetic interactions into a single and unified framework. The original motivation for this unification is related to the experimental observation that parity is violated in the electroweak decays, generating an asymmetry between the left- and the right-handed components of the fermions.

According to the theory of Yang and Mills [9], to each non-abelian symmetry group $SU(N)$ corresponds a number $N^2 - 1$ of massless vector fields carrying the interaction, and corresponding to the generators of the group. The abelian subgroup $U(1)_Y$ is associated to the hyperphoton field B_μ, and consists of a single generator proportional to the identity, the weak hypercharge Y. The $SU(2)_L$, known as the weak isospin group, is related to the coupling constant g. It is of dimension $2^2 - 1 = 3$, and is associated to the corresponding vector fields W_μ^i with $i = 1, 2, 3$. The three generators of $SU(2)_L$ acting on these fields are proportional to the traceless Pauli matrices

$$\sigma_1 = \begin{bmatrix} 0 & 1 \\ 1 & 0 \end{bmatrix}; \sigma_2 = \begin{bmatrix} 0 & -i \\ i & 0 \end{bmatrix}; \sigma_3 = \begin{bmatrix} 1 & 0 \\ 0 & -1 \end{bmatrix} \quad \text{with} \quad [\sigma_i, \sigma_j] = 2i\varepsilon^{ijk}\sigma_k \tag{1.2.2}$$

As we will see, an additional theoretical principle will be required to explain how the particles corresponding to the fields B_μ and W^i_μ gain their masses, as observed.

Following the general properties of Yang-Mills gauge theories [9], the interactions of the gauge part of the $SU(2)_L \times U(1)_Y$ Lagrangian are given by

$$\mathcal{L}_{gauge} = -\frac{1}{4} B^{\mu\nu} B_{\mu\nu} - \frac{1}{4} W_i^{\mu\nu} W^i_{\mu\nu}, \tag{1.2.3}$$

where $B_{\mu\nu}$ and $W^i_{\mu\nu}$ are the field-strength tensors

$$\begin{aligned} B_{\mu\nu} &= \partial_\mu B_\nu - \partial_\nu B_\mu, \\ W^i_{\mu\nu} &= \partial_\mu W^i_\nu - \partial_\nu W^i_\mu - g\varepsilon^{ijk} W^j_\mu W^k_\nu, \end{aligned} \tag{1.2.4}$$

The quantities g and ε^{ijk} correspond to the coupling and to the antisymmetric structure constants of the $SU(2)_L$ gauge group, respectively. Expanding Eq.(1.2.3) explicitly, $\mathcal{L}_{gauge}$ will provide the kinetic terms for the vector fields, as well as the interactions between them. The local gauge invariance of the electroweak SM is imposed through the covariant derivative

$$\partial_\mu \rightarrow D_\mu = \partial_\mu - i\frac{g}{2}\sigma^i W^i_\mu - i\frac{g'}{2} B_\mu, \tag{1.2.5}$$

in the Lagrangian. Reminding that the SM is a chiral theory, all matter fields are minimally coupled to the electroweak gauge fields W^i_μ and B_μ by means of

$$\begin{aligned} D^L_\mu &= \partial_\mu \begin{pmatrix} 1 & 0 \\ 0 & 1 \end{pmatrix} - \frac{i}{2} \begin{pmatrix} gW^3_\mu - g'YB_\mu & W^1_\mu - iW^2_\mu \\ W^1_\mu + iW^2_\mu & -gW^3_\mu - g'YB_\mu \end{pmatrix}, \\ D^R_\mu &= \partial_\mu - \frac{i}{2} g'YB_\mu, \end{aligned} \tag{1.2.6}$$

as only the isospin term is present when considering right-handed particles. As far as the matter fields are concerned, the SM Lagrangian including the fermions and the gauge bosons interactions reads

$$\begin{aligned}\mathcal{L}_{SM} &= -\frac{1}{4}B^{\mu\nu}B_{\mu\nu} - \frac{1}{4}W_i^{\mu\nu}W^i_{\mu\nu} - \frac{1}{4}G_a^{\mu\nu}G^a_{\mu\nu} \\ &\quad + i\bar{Q}_L^j D_\mu \gamma^\mu Q_L^j + i\bar{u}_R^j D_\mu \gamma^\mu u_R^j + i\bar{d}_R^j D_\mu \gamma^\mu d_R^j \\ &\quad + i\bar{Q}_L^j D_\mu \gamma^\mu Q_L^j + i\bar{u}_R^j D_\mu \gamma^\mu u_R^j + i\bar{d}_R^j D_\mu \gamma^\mu d_R^j + h.c.,\end{aligned} \tag{1.2.7}$$

which is invariant under the local $SU(2)_L \times U(1)_Y$ gauge transformations. Related to the fact that the SM is a chiral theory, right-handed neutrinos neutrinos are absent from this picture.

1.3 The Brout-Englert-Higgs mechanism

Building a gauge invariant theory on the basis of $SU(2)_L \times U(1)_Y$, one has uniquely specified the structure of the theory in terms of matter content and force carriers. This leaves however no room for gauge boson mass terms in the Lagrangian, given that such terms would be quadratic in the field in question, breaking the gauge invariance of the theory. This is obviously in contrast with the experiments, as the limited range of the weak interaction imposes that the associated gauge bosons must be massive. This can be achieved through the introduction of an additional theoretical principle, as we will now explain.

The Brout-Englert-Higgs (BEH) mechanism, developped by Higgs in [10, 11], and originally proposed by Brout and Englert in [12], predicts that the masses of the electroweak gauge bosons arise dynamically from the interactions of the bosonic fields with a new scalar field, without spoiling the gauge invariance of the theory. After this procedure, the remaining unbroken symmetry will be that of the electromagnetic gauge group $U(1)_{EM}$, with

$$SU(2)_L \times U(1)_Y \to U(1)_{EM}$$

The presence in the theory of the massive weak bosons W and Z, together with the massless photon γ is a consequence of the Goldstone theorem [13, 14]. Since the theory must also explain the experimental fact that the electroweak

interaction is parity-violating while electromagnetism is not, charged bosons can only couple to left-handed fermions and right-handed antifermions. As observed, the neutral weak boson couples differently to the two chiralities, while the photon field interacts with all particles proportionally to their electric charge.

As the simplest realisation of a scalar field theory consistent with gauge invariance and renormalisability, the Lagrangian describing the dynamics reads

$$\mathcal{L} = \frac{1}{2}\partial_\mu\phi\partial^\mu\phi - V(\phi), \quad \text{with } V(\phi) = \frac{1}{2}\mu^2\phi^2 + \frac{1}{4}\lambda\phi^4, \tag{1.3.8}$$

where the choice $\lambda > 0$ bounds the potential $V(\phi)$ from below. To extremise the action, we look for the minima of Eq.(1.3.8), which can be computed through

$$\frac{\partial V}{\partial \phi} = \mu^2\phi + \lambda\phi^3 = 0. \tag{1.3.9}$$

Solving this equation, two separate situations arise:

1. if $\mu^2 > 0$, the lowest energy state is located at $\phi = 0$, and both the Lagrangian and the lowest energy state of the theory are invariant under the reflection symmetry $\phi \to -\phi$. The symmetry is said to be explicitly realized, and the corresponding field remains massless.

2. if $\mu^2 < 0$, the vacuum state of the field ϕ becomes non-zero. The latter is actually degenerated, as it depends on the choice $+v$ or $-v$, where v corresponds to the Vacuum Expectation Value (VEV) of the field that minimises $V(\phi)$,

$$\phi_0 = \pm\sqrt{-\frac{\mu^2}{\lambda}} \equiv \pm v. \tag{1.3.10}$$

   The two corresponding situations are illustrated in Fig. 1.1.

To provide a correct interpretation of the corresponding dynamics, the Lagrangian (1.3.8) can be rescaled in terms of a new field, $\sigma = \phi - v$, so that

$$L = \frac{1}{2}\partial_\mu\sigma\partial^\mu\sigma - V(\sigma), \quad \text{with } V(\sigma) = \lambda v^2\sigma^2 + \lambda v\sigma^3 + \frac{\lambda}{4}\sigma^4. \tag{1.3.11}$$

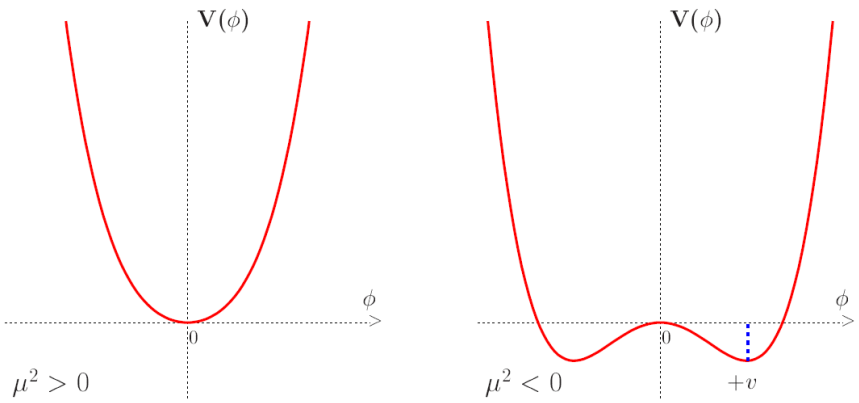

Figure 1.1: The minimum of the potential $V(\phi)$ yields two different solutions depending on the sign of μ^2: if $\mu^2 > 0$ (left) there is a single global minimum at the origin $\phi_0 = 0$, if $\mu^2 < 0$ (right) the potential exhibits a degenerate vacuum state, given by two local minima in $\phi_0 = v$ and $\phi_0 = -v$. Adapted from [15].

Following this redefinition, we end up with a massive scalar field σ, with $m_\sigma = \sqrt{-2\mu^2}$. This follows from the spontaneous breaking of the original symmetry in Eq.(1.3.8), while the choice $\mu^2 > 0$ was leading to a degenerate vacuum.

In the electroweak Standard Model, a similar mechanism has been proposed to generate the masses of the weak bosons. For that purpose, one can introduce a scalar field Φ, transforming as a complex doublet of SU(2)$_L$ with non-zero weak hypercharge $Y = +1/2$, namely

$$\Phi = \begin{pmatrix} \phi^+ \\ \phi^0 \end{pmatrix} = \frac{1}{\sqrt{2}} \begin{pmatrix} \phi_1 + i\phi_2 \\ \phi_3 + i\phi_4 \end{pmatrix}. \tag{1.3.12}$$

The corresponding Lagrangian reads

$$L^{SM} = L^{gauge} + D_\mu \Phi^\dagger D^\mu \Phi - \mu^2 \Phi^\dagger \Phi - \lambda (\Phi^\dagger \Phi)^2. \tag{1.3.13}$$

In a local theory, the combinations $\Phi^\dagger\Phi$ and $D_\mu\Phi^\dagger D^\mu\Phi$ are singlets under $SU(2)_L \times U(1)_Y$, so that the theory is effectively gauge invariant. Considering

the case $\mu^2 < 0$ as previously, the electromagnetic $U(1)_{EM}$ is unbroken, while we can check that the field Φ acquires the non-zero expectation value

$$|\langle 0|\Phi|0\rangle| = \frac{v}{\sqrt{2}}. \tag{1.3.14}$$

Using gauge invariance, we choose the position of the minimum in Eq.(1.3.13) so that $\phi_1 = \phi_2 = \phi_4 = 0$ and $\phi_3 = v$, where v is here the VEV of the scalar field Φ. Doing so, the vacuum takes the value $v = \sqrt{-\mu^2/\lambda}$, and the electroweak symmetry $SU(2)_L \times U(1)_Y$ is said to be broken down to $U(1)_{em}$. To reinterpret the dynamics, the scalar field can be defined perturbatively around the VEV,

$$\Phi = \frac{1}{\sqrt{2}} \begin{pmatrix} 0 \\ v + H \end{pmatrix}, \tag{1.3.15}$$

for the vacuum to lie at the origin. The scalar potential then becomes

$$V(H) = \frac{1}{4}\lambda v^4 + \lambda v^2 H^2 + \lambda v H^3 + \frac{1}{4}\lambda H^4, \tag{1.3.16}$$

where the second term provides the mass of the scalar field, while the third and the fourth terms give its cubic and quartic self-couplings, respectively. The expansion of the kinetic term of the scalar field displays the mass terms of the electroweak gauge bosons:

$$\begin{aligned} |D_\mu \Phi|^2 &= |(\partial_\mu - i\frac{g}{2}\sigma^i W_i^\mu - i\frac{g'}{2}B^\mu)\Phi|^2 \\ &\supset \frac{(v+H)^2}{8}[g^2(W_\mu^1)^2 + (W_\mu^2)^2 + (-gW_\mu^3 + g'B_\mu)^2]. \end{aligned} \tag{1.3.17}$$

It can be checked that $(W_\mu^1 - iW_\mu^2)$ carries electric charge $+e$ and $(W_\mu^1 + iW_\mu^2)$ carries electric charge $-e$. Denoting these combinations as the mass eigenstates

$$\begin{aligned} W_\mu^+ &= \frac{1}{\sqrt{2}}(W_\mu^1 - iW_\mu^2), \\ W_\mu^- &= \frac{1}{\sqrt{2}}(W_\mu^1 + iW_\mu^2), \end{aligned} \tag{1.3.18}$$

these fields can be readily identified with the fields $W^{\pm}$ mediating the charged current of the weak interaction. The vector bosons B_μ and W^3_μ, on the other hand, are electrically neutral. After breaking the electroweak symmetry, the two gauge fields can be rotated in field space so that

$$\begin{pmatrix} Z_\mu \\ A_\mu \end{pmatrix} = \begin{pmatrix} \cos\theta_W & -\sin\theta_W \\ \sin\theta_W & \cos\theta_W \end{pmatrix} \begin{pmatrix} W^3_\mu \\ B_\mu \end{pmatrix}, \tag{1.3.19}$$

where θ_W is known as the weak angle, with $\cos\theta_W = m_W/m_Z$. The neutral mass eigenstate Z_μ then corresponds to the vector field Z, while A_μ is to be identified to the photon field γ. Rewriting Eq.(1.3.17) as

$$|D_\mu\Phi|^2 \supset \frac{(gv)^2}{2} W^+_\mu W^{-\mu} + \frac{1}{2}(\frac{v}{2})^2(g^2+g'^2) Z_\mu Z^\mu + \frac{1}{2}(0) A_\mu A^\mu, \tag{1.3.20}$$

we conclude immediately that the photon remains a massless particle, accordingly to the application of the Goldstone theorem to the spontaneous symmetry breaking of $SU(2)_L \times U(1)_Y$ [13, 14]. The masses of the W and Z fields are non-zero and are related through the expressions

$$\begin{aligned} m_W &= \frac{gv}{2}, \\ m_Z &= \frac{\sqrt{g^2+g'^2}}{2} v = \frac{m_W}{\cos\theta_W}. \end{aligned} \tag{1.3.21}$$

Remarkably, the values of the $W^{\pm}$ and Z boson masses predicted by the theory are in excellent agreement with the experimental values, $m_W = 80.385$ GeV and $m_Z = 91.1876$ GeV [7]. The numerical value for the Higgs VEV, $v = 246$ GeV, can also be obtained from these results by replacing (1.3.21) into the definition of the Fermi coupling constant G_F, measured experimentally in muon decays to a very good accuracy as $G_F = 1.16637 \times 10^{-5}$ GeV^{-2} [16], with $v = (\sqrt{2}G_F)^{-1/2}$. We also highlight the following relation, obtained between the couplings of the electroweak Standard Model,

$$e = g\sin\theta_W = g'\cos\theta_W. \tag{1.3.22}$$

To sum up, from the combinations of the four fields B_μ and W^i_μ after the spontaneous breaking of the electroweak symmetry, we have obtained three

massive vector bosons $W_\mu^\pm$ and Z_μ. Orthogonal to the latter, the field A_μ can be identified with the photon γ, as it must be a massless and electrically neutral boson. In the process, an additional massive scalar field H, the so-called Higgs particle, had to be introduced in the theory. Its corresponding mass, $m_H = \sqrt{2\lambda v^2}$, can be read from Eq.(1.3.16), but cannot be evaluated numerically, due to the fact that the value of the λ parameter is not predicted by the theory.

On 4 July 2012, the ATLAS and CMS collaborations of the Large Hadron Collider jointly announced that they had observed a new boson in the mass region of 125 GeV [17, 18]. On 14 March 2013, CERN officially confirmed the existence of the Higgs particle. On 8 October 2013, the Nobel prize in physics was awarded jointly to François Englert and Peter Higgs for "the theoretical discovery of a mechanism that contributes to our understanding of the origin of mass of subatomic particles", and which has recently been confirmed through the discovery of the predicted fundamental particle. As of 2014, it is now acknowledged that the properties of this scalar particle are consistent with those predicted by the Standard Model and the BEH mechanism. With the impressive amount of data collected since the start of the LHC, the ATLAS and CMS collaborations put a final end to a 40 years effort for proving the existence of the ultimate building block of the standard electroweak theory.

1.4 Origin of the fermion masses in the SM

Gauge symmetries, as we discussed, require all particles to be massless. Although the spontaneous breaking of the electroweak symmetry allows the W, Z and H bosons to acquire a mass through the BEH mechanism, the experimental observation of massive quarks and leptons must still be explained in the SM.

Chiral fields, by definition, belong to inequivalent representations of $SU(2)_L \times U(1)_Y$, and cannot be massive in the Standard Model. Indeed, Dirac mass terms are not gauge invariant given that they systematically mix fermions with opposite chirality, and since left- and right-handed fermions carry unequal charges under the same symmetry group.

In [2], Weinberg extended the mechanism of spontaneous symmetry breaking to provide masses to the fermions, in the context of a renormalisable gauge theory. Even if explicit mass terms are known to be forbidden for Dirac fields, couplings between chiral fermions and scalar doublets, i.e., Yukawa interactions, can always be added by hand. The corresponding $SU(2)_L \times U(1)_Y$ invariant Lagrangian reads

$$L^{Yukawa} = -Y^u_{ij}\bar{Q}^i_L\tilde{\Phi}u^j_R - Y^d_{ij}\bar{Q}^i_L\Phi d^j_R - Y^e_{ij}\bar{L}^i_L\Phi e_R + h.c., \quad (1.4.23)$$

where Q_L and L_L are the isospin doublets that contain the left-handed quarks and leptons, respectively, while u_R, d_R and e_R are their corresponding right-handed singlet partners. The field $\tilde{\Phi}$ here represents the conjugate doublet $\tilde{\Phi} = i\sigma^2\Phi^*$, where the scalar field Φ can be identified with the Higgs field itself. The Y_{ij} here denote arbitrary 3×3 complex matrices that mix the flavour eigenstates i and j, and define their so-called Yukawa couplings. Substituting Φ with the vacuum state, one obtains the mass terms

$$L^{Yukawa} \supset -M^u_{ij}\bar{Q}^i_L u^j_R - M^d_{ij}\bar{Q}^i_L d^j_R - M^e_{ij}\bar{L}^i_L e_R + h.c., \quad (1.4.24)$$

wherein we can identify the masses of the charged fermions [2], as corresponding to the constants in front of each term,

$$M^{u,d,e}_{ij} = \frac{Y^{u,d,e}_{ij}v}{\sqrt{2}}. \quad (1.4.25)$$

After electroweak symmetry breaking, the fermion masses may thus be generated as a 'byproduct' of the same scalar doublet which is responsible for the gauge boson masses, the recently discovered Higgs particle. Due to the arbitrariness of the Yukawa matrices, it it however important to notice that these relations imply that the above eigenstates are not diagonal in the mass basis. In other words, the fields Q_L, L_L, u_R, d_R and e_R are not readily identifiable to the mass eigenstates of the fermions. Denoting the interaction eigenstates with primes, we have

$$\mathcal{L}_{mass} = -\sum_{i,j=1}^{3} \bar{u}^{i'}_L M^u_{ij} u'_{Rj} - \bar{d}^{i'}_L M^d_{ij} d'_{Rj} - \bar{e}^{i'}_L M^e_{ij} e'_{Rj} + h.c., \quad (1.4.26)$$

[2] Note that due to the seemingly absence of right-handed neutrinos in nature, neutral leptons are predicted to be massless in the SM, which is in conflict with the experimental observations. While this issue is not be discussed in the following, we comment, however, that the mechanism of mass generation for the charged leptons is similar to that of the quarks.

where the mass matrices are *not* diagonal. Using on the property that any arbitrary complex matrix M^f can be diagonalized by two unitary matrices V_L^f and V_R^f such that $M_{diag}^f = V_L^f M^f V_R^{f\dagger}$, we obtain

$$M^{u,d} = V_L^{u,d} Y^{u,d} \frac{v}{\sqrt{2}} V_R^{u,d\dagger}. \tag{1.4.27}$$

The same unitary matrices $V_{L,R}^{u,d}$ can also be used to rotate the flavour eigenstates into the mass eigenstate basis. The fermion fields in the mass basis are then defined as

$$\begin{aligned} u_R &= V_R^u u'_R \ ; \ u_L = V_L^u u'_L, \\ d_R &= V_R^d d'_R \ ; \ d_L = V_L^d d'_L. \end{aligned} \tag{1.4.28}$$

By convention, the flavour and the mass eigenstates will be choosen to be the same for up-type quarks, so that $V_L^u = V_R^u = 1$. Inserting the above transformation rules into the interaction terms for $W^\pm$ gauge bosons and quarks in the mass basis, we have from Eq.(1.3.17)

$$\mathcal{L}_W = \frac{g}{\sqrt{2}} \bar{u}_L^{i'} \gamma^\mu V_{CKM}^{ij} d'_{Rj} W_\mu^+ + h.c., \tag{1.4.29}$$

where we introduced the unitary 3×3 V_{CKM} matrix

$$V_{CKM} = (V_L^u)^\dagger V_L^d. \tag{1.4.30}$$

called the Cabibbo-Kobayashi-Maskawa (CKM) mixing matrix V_{CKM} [19, 20] [3], the elements of which encode the transition probabilities between the different quark flavours through the weak interaction. As Kobayashi and Maskawa established, Eq.(1.4.30) also embeds one complex phase δ in the presence of three quark generations, underlying the mechanism of CP violation. Since it is a product of two unitary matrices, we further emphasise that the CKM matrix must be unitary as well.

Coming back to the aforementioned convention $V_L^u = V_R^u = 1$, the down type quarks are rotated from the flavour basis to the mass basis by (1.4.30).

[3] A lepton analogue of the CKM matrix, the Pontecorvo-Maki-Nakagawa-Sakata (PMNS) matrix [21, 22], can be introduced in the same way as the CKM matrix above.

The matrix V_{CKM} thus translates the misalignment between the mass eigenstates of the down d, strange s and bottom b quarks with their weak interaction eigenstates d', s' and b', so that

$$\begin{pmatrix} d \\ s \\ b \end{pmatrix} = \begin{pmatrix} V_{ud} & V_{us} & V_{ub} \\ V_{cd} & V_{cs} & V_{cb} \\ V_{td} & V_{ts} & V_{tb} \end{pmatrix} \begin{pmatrix} d' \\ s' \\ b' \end{pmatrix} = V_{CKM} \begin{pmatrix} d' \\ s' \\ b' \end{pmatrix}. \tag{1.4.31}$$

According to the above relations, the charged-current interactions between up- and down-type quarks systematically involve a combination of matrices $V_L^{u\dagger} V_L^d$. Inserting Eqs.(1.4.28) into the Lagrangian describing the currents mixing with the Z-boson and the photon, it can be checked that $V_{L,R}^{u\dagger} V_{L,R}^u = 1$ and $V_{L,R}^{d\dagger} V_{L,R}^d$ will appear in the corresponding couplings. This implies that the neutral current couplings do not allow for flavour-changing processes, as they can only couple a fermion to its corresponding antifermion. This is summarised by the so-called Glashow-Iliopoulos-Maiani (GIM) mechanism [23], which states that there are no flavour-changing neutral currents (FCNC) among chiral quarks at the tree-level in the SM. The values of the mixing elements and the CP violating phase of V_{CKM} are provided by the experiments [7], and are typically calculated under the assumption that the CKM matrix is unitary, and that there are no more than three generations.

Note that there is in principle no natural explanation for the hierarchy observed in the CKM matrix elements. Although the SM fermion masses are generated from the same mechanism, the original Yukawa matrices from which they originate are arbitrarily free. This issue, which is known as the fermionic mass hierarchy, could be the indication for new physics beyond the electroweak scale. For instance, deviations from these values could be a hint of the existence of new fermions.

1.5 The Hierarchy problem

Previously, we presented the SM of particle physics as a consistent theory, describing all the known matter particles and fundamental interactions between them, except for the gravity. But however successful as it has been in describing the electroweak and strong interactions in the past decades, compelling

arguments indicate that new physics might show up at the TeV scale. In this section, we review two features that the SM still needs to address, and which may be settled by extending the fermion sector of the SM so as to solve the so-called Hierarchy problem.

A first fundamental observation that can be made is the remarkable feature that not only the masses of the electroweak gauge bosons but also the masses of the fermions seem to originate from one and same scalar particle, the Higgs boson. While all the charged fermion masses and mixings arise from the arbitrary Yukawa couplings, no theoretical argument can explain the apparent mass hierarchy between the three fermion generations, namely

$$m_e \ll m_\mu \ll m_\tau \ ; m_u \ll m_c \ll m_t \ ; m_d \ll m_s \ll m_b, \tag{1.5.32}$$

nor the large mass splitting within the third and heaviest family,

$$m_\tau \sim m_b \ll m_t. \tag{1.5.33}$$

In such a framework, the only natural mass scale appears to be the one given by the top quark, as it is the only observed particle of the SM with a Yukawa coupling of order unity,

$$y_t \equiv \frac{m_t\sqrt{2}}{v} \simeq 1. \tag{1.5.34}$$

In that sense, the masses of the other particles, as well as the differences between sequential generations, seem 'unnatural'. Considering that all the fermion masses should be proportional to the VEV of the Higgs field, such a hierarchy is still to be understood. Despite the elegance of the BEH mechanism and the discovery of the Higgs particle, the origin of the fermion masses and mixings thus remains an unexplained feature in particle physics.

A second important observation is that the Standard Model cannot explain the huge gap between the weak scale ($\simeq 10^2$ GeV) of electroweak unification and the Planck scale ($\simeq 10^{19}$ GeV) at which the quantum effects of gravity can be expected to become strong. In itself, this is not a problem of the Standard Model, but more about the assumption that more structures should be included in the theory at higher energies. One of the main consequences of this is

that the BEH mechanism actually predicts the existence of a scalar particle which mass is very sensitive to whatever may lie at higher energies. Because of the presence of an implicit ultraviolet divergency in the scalar sector, possibly large quantum corrections are expected to contribute to the mass of the Higgs boson particle, measured as $m_H = 125$ GeV.

By definition, the square of the mass m_H corresponds to the pole of the free propagator of the H boson in momentum space

$$\frac{i}{k^2 - m_H^2}. \tag{1.5.35}$$

Not being protected by any symmetry, m_H^2 receives quadratically divergent corrections at the quantum level, namely

$$\delta m_H^2 = m_H^2 - m_H^{(0)2}, \tag{1.5.36}$$

arising from the higher orders of the perturbative expansion of the Higgs two-point function.

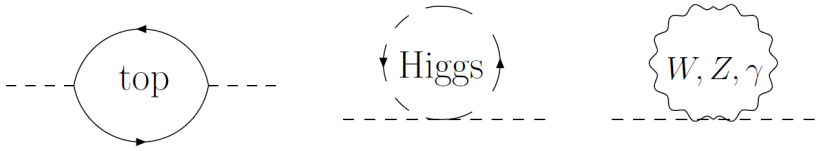

Figure 1.2: The most significant quadratically divergent contributions to the Higgs mass in the Standard Model. Adapted from [24].

We can consider explicitly the problem of quadratic divergences in the scalar sector through the calculation of the corresponding mass corrections at the one-loop level. As shown in Fig. 1.2, the three most significant loop corrections to the Higgs mass are given by the top quark, the quartic Higgs vertex and the electroweak gauge boson loop contributions. Assuming the possibility for new physics above a given scale Λ, we can adopt the cut-off regularisation scheme and evaluate the corresponding amplitudes at large momentum, $\Lambda \gg m_t$. Computed in the unitary gauge (see, e.g., [25, 24, 26]), the largest contribution to the Higgs mass self-energy originates from the top quark loop

$$\delta m_H^2|_t = -\frac{3m_t^2}{4\pi^2 v^2}[\Lambda^2 - 3m_t^2 \ln(\frac{\Lambda^2}{m_t^2}) + ...], \tag{1.5.37}$$

where the first term gives a quadratic divergence while the second gives a logarithmic divergence, that we will neglect in the following. What is remarkable from this result is that the correction $\delta m_H^2|_t$ depends explicitly on the mass of the top quark [4].

Similar results hold for the divergent pieces that appear from the quartic Higgs vertex and the gauge boson contributions. Even though the top quark loop is the most important contribution to the Higgs mass squared, they provide further quadratically divergent graphs that are to be included in the computation of δm_H^2. Writing explicitly these divergent pieces, we have

$$\delta m_H^2 = \frac{-3}{8\pi^2 v^2}(m_H^2 + 2m_W^2 + 4m_Z^2 - 4m_t^2)\,\Lambda^2, \tag{1.5.38}$$

where the magnitude of the Yukawa coupling of the top quark, $y_t \simeq 1$, can be shown to give the largest contribution. Here above, the cut-off Λ can be interpreted as the energy scale up to which the SM theory can be naturally extrapolated.

In order for all the above contributions to add up to a Higgs mass of 125 GeV, a large amount of fine-tuning is obviously required to avoid ridiculously large values of δm_H^2 with respect to m_H^2. This problem, known as the hierarchy problem, is one of the most common motivations for introducing new scenarios beyond the Standard Model. The latter argument can indeed be turned around to predict the scale Λ at which new physics should appear to cancel unwanted divergences in the radiative corrections to the Higgs mass. Based on this reasoning, tentative new physics could thus be observed above the electroweak, introducing novel particles stabilising the SM scalar boson mass. If such regimes exist at large scales and couple to the Higgs, then m_H might also not be protected by any mechanism, but simply fine-tuned to a very large accuracy.

While we will not discuss them in detail, many proposals have been made following naturalness as a guiding principle, addressing the hierarchy problem in various ways. A common approach consists in assuming that the radiative stability of m_H is attributed to new symmetries. In the limit where all the fermion

[4] In principle, all the other quark loops must be accounted for in the calculation, though the next-to-largest contribution from the bottom quark is already relatively small ($m_b/m_t \simeq 0.025$).

masses vanish, it was established previously that the underlying Lagrangian is invariant under chiral transformations [5]. No such property, however, holds for scalar particles in the SM, so that the ultraviolet divergence present in δm_H^2 appears as a physical issue of the theory, dominated by the mass of the top quark. Yet, it is interesting to notice that the scalar, the gauge and the fermion sectors appear to be intertwined at the level of δm_H^2 through (1.5.38).

In this context, supersymmetric theories have been developped to solve the hierarchy problem in an elegant way. As their simplest realisation, unbroken supersymmetry (SUSY) relates the bosons and fermions through a new symmetry. To every field present in the SM then corresponds a new partner, whose spin differs by a half-integer, but shares the same mass and quantum numbers. The introduction of those particles then solves the instability of the Higgs mass, due to the fact that all fermionic particles entering with a negative sign in the final contribution to Eq.(1.5.38) systematically cancel against the positive correction arising from their bosonic super-partners, and vice-versa. This guarantees that all the corrections to the Higgs boson mass diverge at most logarithmically, thus curing the quadratic divergence in δm_H^2. Further, if supersymmetry is softly broken in a soft way, realistic masses can be considered for the corresponding partners without spoiling the protection of the Higgs mass. As these approaches go beyond the scope of our work, supersymmetric theories will not be discussed in the following (see e.g., [27], for an introduction on the subject).

Beyond supersymmetry, we can mention a large number of models which also address the naturalness issue. Well-known examples include extra fermion generations, new gauge bosons, or extended Higgs sectors. Some are based on the effective Lagrangian approach, others introduce extended global symmetries like Little Higgs models [28], extra dimensional space symmetries or Gauge-Higgs Unification [29, 30, 31]. In models of extra dimensions [32, 33, 34], so-called Kaluza-Klein states are needed to complete a full representation of the extended symmetries. Other scenarios assume that the breaking of the electroweak symmetry is due to new strongly interacting dynamics, like in Composite Higgs models [35, 36]. Composite Higgs theories assume that the Higgs particle is not a fundamental scalar, but instead, is a bound state result-

[5] Fermionic masses are then said to be protected by the chiral symmetry.

ing from strongly interacting dynamics. In this case large corrections to m_H can be avoided due to the finite size of the Higgs, which becomes insensitive to virtual corrections arising from regimes above its confining scale. Models of Technicolour, which predict the existence of light Higgs-like scalars, are also part of this class of scenarios [37, 38, 39]. In all the above cases, a common prediction is the presence of new fermionic partners with quantum numbers similar to that of the top quark, as the simplest solution addressing the hierarchy problem.

Chapter 2

Closing in on a perturbative fourth generation

"Nulla poena sine lege"
Paul Johann Anselm Ritter von Feuerbach

"Nemo censetur ignorare legem"
Citation latine

Based on:

M. Buchkremer, J.-M. Gérard, F. Maltoni, "Closing in on a perturbative fourth generation", *JHEP*, vol. 1206, pp. 135, 2012, 1204.5403.

It is generally claimed that the Standard Model (SM) comprises at least three generations of fermions. However, many fundamental problems do not find an answer into this framework, and the possibility of additional massive fermions, such as a new sequential family of quarks, has been among the models in the spotlight of the first searches for new physics at the Large Hadron Collider (LHC).

In this chapter, we review the limits on a non-degenerate fourth generation of chiral quarks t' and b', considering the corresponding parameter space for non-zero CKM mixing with the third family. We present representative benchmark points for normal ($m_{t'} > m_{b'}$) and inverted ($m_{t'} < m_{b'}$) quark mass hierarchies, in light of the observation of a Higgs boson at a mass of 125 GeV. Based on the results of our original publications [40, 41], we show that a sizeable 3-4 CKM mixing is unlikely to be allowed when considering the various bound dependencies on the fourth generation parameters. Eventually, we detail the production and experimental signatures corresponding to these scenarios, and review the main arguments which exclude a perturbative fourth generation in the context of a single Higgs doublet.

2.1 Introduction

Over the past decades, we have discovered that nature consists of a given number of elementary particles, deeply connected with the known fundamental forces driving our universe. The recent observation of a new particle resembling the long-sought Higgs boson at the LHC now provides us with strong evidence for the validity of the Standard Model (SM) [17, 18]. Yet, while it is generally acknowledged that the latter comprises three generations of chiral quarks and leptons, various fundamental problems remain unexplained within this framework. For instance, long-standing issues such as the baryon asymmetry of the universe, the origin of the fermion mass hierarchy or the nature of the CKM mixing matrix hint at the possible need for new physics. As it is, the SM does not give any theoretical prediction for the number of quark and lepton families. The observed asymptotic freedom in Quantum Chromo-Dynamics (QCD) only puts an upper bound on the number of generations, which must be smaller or equal to eight.

While the SM is expected to loose its predictive power as the experimental searches now reach the TeV scale, models suggesting new heavy fermions might offer solutions to these problems (see, e.g., [42]). As one of the simplest extension of new physics, the possibility for a fourth sequential family of quarks (hereafter SM4) also serves as a template for new physics models for which the unitarity of the 3×3 CKM matrix might be violated [43]. In the

following, we denote SM4 as the extension of the Standard Model simply by an additional family of chiral matter. Its fermionic content reads

$$\begin{pmatrix} u \\ d \end{pmatrix} \begin{pmatrix} c \\ s \end{pmatrix} \begin{pmatrix} t \\ b \end{pmatrix} \begin{pmatrix} t' \\ b' \end{pmatrix} \; ; \; \begin{pmatrix} \nu_e \\ e^- \end{pmatrix} \begin{pmatrix} \nu_\mu \\ \mu^- \end{pmatrix} \begin{pmatrix} \nu_\tau \\ \tau^- \end{pmatrix} \begin{pmatrix} \nu_{\tau'} \\ \tau'^- \end{pmatrix} \tag{2.1.1}$$

where Dirac masses will be assumed in the following for the new heavy neutrino. The left- and right-handed components of the above fermions transform respectively as doublets and singlets under the electroweak $SU(2)_L \times U(1)_Y$ gauge group. All the associated fermion masses are assumed to originate from the Higgs mechanism through Yukawa interactions.

As an additional fermion generation might affect many observables directly, but also indirectly via loop processes, the SM4 is subjected to various types of constraints. At the time of the publication of the work [40] which is reported in this chapter, the possibility remained that specific regions of the still allowed SM4 parameter space could evade the direct searches if a sizeable mixing between the third and the fourth generation was allowed. The mass difference between the new heavy quarks also requires specific attention. In their seminal paper [44], Kribs *et al.* proposed the correlation

$$\Delta m_{q'} \simeq \left(1 + \frac{1}{5} \ln \frac{m_H}{115 \text{ GeV}}\right) \times 50 \text{ GeV} \tag{2.1.2}$$

between the SM4 Higgs boson mass and the quark mass difference, $\Delta m_{q'} = m_{t'} - m_{b'}$. Though simple, this approximation was previously known to overconstrain the SM4 parameter space [45], while the experimental searches usually require more refined predictions. In this chapter we argue that a better description of the fourth generation parameter space is provided by

$$\Delta m_{q'} \lesssim \left(1 + \frac{1}{5} \ln \frac{m_H}{125 \text{ GeV}} - 15 \, |V_{t'b}|^2\right) \times m_W. \tag{2.1.3}$$

where $|V_{t'b}| \simeq |V_{tb'}|$ is the CKM mixing element between the two heaviest quark families.

2.2 Current bound dependencies on the fourth generation parameters

While strong pair production at the LHC only depends on the new heavy quark masses, the electroweak production and decay modes are mainly sensitive to their mass difference and CKM mixings. As our purpose is to provide representative benchmark scenarios, the relations between the various SM4 parameters must be investigated carefully. As summarised in Tab. 2.1, the direct searches only constrain the fourth generation fermion masses. The Higgs direct hints provide an independent constraint on the allowed parameter space due to the decoupling of the new heavy fermion masses. The electroweak precision parameters are then considered, with the non-oblique correction to the $Z \to b\bar{b}$ vertex setting a stringent upper bound on $|V_{t'b}|$ as a function of the quark masses. As we will see, a careful treatment of the oblique parameters S and T can be used to derive (2.1.3) as a function of all previous constraints. In the following, we review these bounds and their various dependencies.

	$m_{q'}$	$\Delta m_{q'}$	$\lvert V_{t'b}\rvert$	$m_{l'}$	$\Delta m_{l'}$	m_H
Direct searches	✓			✓		
Higgs searches						✓
$Z \to b\bar{b}$	✓	✓	✓			
S, T	✓	✓	✓	✓	✓	✓
Strong production	✓					
Electroweak production	✓	✓	✓			
Branching Ratio		✓	✓			

Table 2.1: Summary of the relevant fourth generation parameters for the LHC searches, with the fourth generation fermions $q' = t', b'$ and $l' = \tau', \nu'$ ($\Delta m_{l'} = m_{\nu'} - m_{\tau'}$). The marks denote the dependencies on the constraints considered in our analysis.

2.2.1 Direct limits

The past few years, an impressive amount of experimental data has been collected at the LHC on new heavy fermions. Fourth generation quarks, in particular, are now among the most constrained New Physics (NP) extensions which have been looked for at the LHC. Previously, the CDF and D0 experiments set the limits $m_{t'} > 335$ GeV [46] and $m_{b'} > 385$ GeV [47] at the 95% Confidence Level (CL) for the masses of new up- and down-type heavy quarks. Direct searches at the LHC hinted at even more stringent constraints. Searching for short-lived b' quarks in the signature of trileptons and same-sign dileptons, CMS ruled out $m_{b'} < 495$ GeV at 95% CL assuming BR$(b' \to tW) \simeq 100$ $\%$ [48]. A search for heavy pair-produced top-like quarks has also been conducted considering $t' \to bW$ as a prompt exclusive decay: no excess over the SM expectations has been observed, excluding a t' quark with a mass below 557 GeV [49]. The ATLAS collaboration ruled out $m_Q < 350$ GeV at 95% CL by searching for pair-produced heavy quarks $Q\bar{Q}$ in the two-lepton channel [50], with BR$(Q \to qW) \simeq 100$ $\%$, where $q = u, d, c, s, b$. This last analysis does not rely on b-tagging and provides a rather conservative bound.

In parallel to our publication [40], the CMS collaboration [51] searched for SM4 quarks produced singly or in pairs, with an integrated luminosity of 5 inverse femtobarn at $\sqrt{s} =$ 7 TeV. Accounting for the extended CKM mixing matrix element $|V_{t'b}|$, limits have been set on up- and down-type fourth generation quarks combining electroweak and strong production mechanisms. Assuming minimal off-diagonal mixing between the third- and the fourth-generation quarks, [51] excluded $m_{t'} = m_{b'} < 685$ GeV in decay channels with at least one isolated muon or electron at 95% CL. Lifting the degeneracy between the t' and b' masses up to a mass difference of 25 GeV, the obtained limit shifts by about 20 GeV. In [52], the CMS collaboration searched for heavy quarks decaying into tops and electroweak bosons at $\sqrt{s} =$ 7 TeV, with a 5 fb^{-1} dataset. No deviations from the Standard Model expectations were observed, and the resulting upper limit on the production cross section times branching fraction excludes the existence of a down-type sequential fourth-generation quark with a mass below 675 GeV at 95% CL.

The current limits thus lie above the unitary bound, $m_{t'} \simeq 550$ GeV, required from the unitarity for the partial S-wave amplitude in $t'\bar{t}'$ scattering at tree-

level [53]. Additionally, perturbative methods are known to become inadequate above such a scale, if considering a single Higgs doublet[1]. However, we emphasise that most of the aforementioned limits are model-dependent. Direct searches indeed rely on the hypothesis that new heavy quarks are close in mass and mix predominantly with the third generation, which implies short lifetimes and prompt decays in the beampipe. While the former condition is well motivated by the precision electroweak measurements, as we will see, a small yet non-zero 3-4 family mixing element must be considered very carefully.

Regarding the fourth generation lepton sector, LEP obtained the lower bound $m_{\tau'} > 100$ GeV for new heavy charged leptons [55]. Assuming Dirac masses, the Z invisible width set $m_{\nu'} > 45$ GeV for new heavy stable neutrinos [16]. Although the off-diagonal lepton mixings are required to be smaller than 0.115 to be consistent with the recent global fits [56], a trivial 4×4 PMNS unitary matrix is considered throughout this analysis, namely a long-lived Dirac neutrino with $|U_{\nu'\tau'}| = 1$. As far as the Majorana case is concerned, we refer the reader to the exhaustive study [57].

2.2.2 Higgs search constraints

A new family of fermions implies important consequences for collider phenomenology, as it significantly modifies the Higgs production and decay rates with respect to the SM. At Leading Order (LO), the Higgs production cross-section via gluon-gluon fusion increases by a factor of about 9 due to the additional t' and b' fermion loops arising from the contribution of the two new heavy quarks. The same enhancement in $H \to gg$ increases the Higgs total width by a factor of about 1.6. On the other hand, the $H \to \gamma\gamma$ width suffers a factor of about 5 suppression due to the new heavy fermion loops involving t', b' and τ'. This accidental cancellation against the W contribution in the $H \to \gamma\gamma$ amplitude results in a comparable number of diphoton events. This accidental cancellation was previously recovered in [58], wherein the inclusive signal $gg \to H \to \gamma\gamma$ was confirmed to be similar to the SM one, indepen-

[1] As shown in [54] from the 2-loop renormalisation group equations, the fourth generation Yukawa couplings lead to the breakdown of perturbativity below the TeV scale if $m_{t',b'} > 375$ GeV.

dently from the masses and the Yukawa couplings of the new chiral quarks. The situation for a Higgs boson lighter than 200 GeV is summarised in [44] as

$$\begin{aligned}
\sigma(gg \to H)\ \mathrm{BR}(H \to \gamma\gamma)|_{SM4} &\simeq \sigma(gg \to H)\ \mathrm{BR}(H \to \gamma\gamma)|_{SM}, \\
\sigma(gg \to H)\ \mathrm{BR}(H \to ZZ)|_{SM4} &\simeq (5...8)\ \sigma(gg \to H)\ \mathrm{BR}(H \to ZZ)|_{SM}, \\
\sigma(gg \to H)\ \mathrm{BR}(H \to f\bar{f})|_{SM4} &\simeq 5\ \sigma(gg \to H)\ \mathrm{BR}(H \to f\bar{f})|_{SM}.
\end{aligned} \tag{2.2.4}$$

Given the recent discovery of a new scalar particle consistent with the Standard Model Higgs boson by the ATLAS and CMS collaborations [17, 18], the above predictions appear to be in strong disagreement with the SM expectations. At the time of our original publication [40], there were however two possible flaws with respect to this argument. The first loophole, emphasised by the studies [59, 60], was that the excluded parameter space for a SM4 Higgs boson did not take into account the possibility for a stable fourth generation neutrino. If such new neutral leptons are lighter than half the Higgs boson mass, the opening of the new invisible mode $H \to \nu'\bar{\nu}'$ increases the Higgs total width, and overtakes the $H \to WW^{(*)}, ZZ^{(*)}$ and $f\bar{f}$ rates with a substantial branching ratio in the low mass region. However, it is straightforward to check that the recent hints of a 125 GeV scalar boson fine tune $m_{\nu'}$ to a value very close to half the Higgs boson mass. Given that $H \to b\bar{b}$ is the dominant visible signal for a light SM-like Higgs boson with respect to $H \to \nu'\bar{\nu}'$ in SM4, the ratio

$$\frac{\Gamma_H^{SM4}}{\Gamma_H^{SM}} \simeq \frac{\Gamma(H \to \nu'\bar{\nu}')_{SM4}}{\Gamma(H \to b\bar{b})_{SM}} \simeq \frac{m_{\nu'}^2}{3m_b^2}\left(1 - 4\frac{m_{\nu'}^2}{m_H^2}\right)^{3/2} \tag{2.2.5}$$

must be of order unity. Combining Eq.(2.2.5) with the assumption that the Higgs invisible branching ratio does not excess 50%, the new neutral lepton mass must lie between 61 and 62.5 GeV. Were direct searches to exclude $m_{\nu'} \lesssim m_H/2$, the Higgs decay patterns would not be affected by the neutrino mass. If $m_{\nu'} > m_H/2$, a light SM4 Higgs boson would lead to significantly more events. In particular, the $H \to f\bar{f}$ and $H \to ZZ^{(*)}$ signal strengths are enhanced by a factor of about 5 to 6 for $m_H \simeq 125$ GeV [61], given the aforementioned gluon fusion enhancement.

The second loophole in this argumentation was the possibility for large Next-to-Leading Order (NLO) contributions to Higgs production whenever considering new heavy chiral quarks. Interestingly, the NLO calculations hinted at very large electroweak radiative corrections to the Higgs decay amplitudes in SM4 [62]. Considering fourth generation quark masses larger than 450 GeV (600 GeV), the Higgs branching ratios into WW and ZZ pairs are suppressed by corrections of the order of -40% (-60%), whereas BR($H \to f\bar{f}$) is enhanced by 30% (60%) in SM4. Additionally, the rate $\sigma(gg \to H)\times$ BR$(H \to \gamma\gamma)_{|SM4}$ is further suppressed by one order of magnitude with respect to the LO result, which hardly accomodates the fourth generation fermion scenario [63, 64, 65]. Considering these results, the following expectations are obtained [66]:

$$\begin{aligned}
\sigma(gg \to H)\ \text{BR}(H \to \gamma\gamma)|_{SM4} &< 0.27\sigma(gg \to H)\ \text{BR}(H \to \gamma\gamma)|_{SM}, \\
\sigma(gg \to H)\ \text{BR}(H \to ZZ)|_{SM4} &\simeq (1.35...9)\ \sigma(gg \to H)\ \text{BR}(H \to ZZ)|_{SM}, \\
\sigma(gg \to H)\ \text{BR}(H \to f\bar{f})|_{SM4} &\simeq (6.3...27)\ \sigma(gg \to H)\ \text{BR}(H \to f\bar{f})|_{SM}.
\end{aligned} \tag{2.2.6}$$

Therefore, any analysis not accounting for these corrections is unlikely to provide reliable constraints on SM4. As computed in [63], the full NLO expression for the rate into diphotons gives a further suppression by a factor of about six [63],

$$\sigma(gg \to H)\ \text{BR}(H \to \gamma\gamma)|_{SM4} < (0.09...0.2)\ \sigma(gg \to H)\ \text{BR}(H \to \gamma\gamma)|_{SM}, \tag{2.2.7}$$

if considering a Higgs mass of 125 GeV. Therefore, the SM4 could be in principle excluded due to a predicted *underproduction* of Higgs bosons at the LHC, given that at most 20 % of the expected events in the two-photon channel should be observed.

2.2.3 Electroweak precision observables

The electroweak precision observables are well known to yield stringent limits on the possible extensions of the SM. In the present framework, they can be

used to set up compelling bounds on the allowed mixings between a sequential fourth generation and the lighter fermion families. Considering a generic flavour structure, the addition of a new quark doublet requires to extend the CKM mixing sector to a 4×4 unitary matrix, whose entries depend upon three additional mixing angles and on two new CP-violating phases. Assuming a non-zero 3-4 family CKM mixing, the R_b ratio $\Gamma(Z \to b\bar{b})/\Gamma(Z \to \text{hadrons})$ can be shown to provide a solid constraint on a non-degenerate fourth generation, independently of the Higgs and leptonic sectors. On the one hand, the non-oblique corrections to R_b are known to remain below several permille for $m_{\nu'} < 100$ GeV [67]. On the other hand, the nondecoupling effects present in the $Zb\bar{b}$ vertex turn out to be slightly sensitive to non-zero $m_{t'} - m_{b'}$ quark mass splittings due to non-negligible $O(\alpha_s^2)$ QCD corrections. Following the derivation given in [68] and [69], their effect on the Z decay rate depends on the two quantities δ_b and δ^q_{tQCD}. While vanishing for light quarks, δ_b is sensitive to t and t' loop corrections in $Z \to b\bar{b}$, and reads

$$\delta_b \simeq \Big[\Big(0.2 - \frac{m_t^2}{2m_Z^2} \Big) |V_{tb}|^2 + \Big(0.2 - \frac{m_{t'}^2}{2m_Z^2} \Big) |V_{t'b}|^2 \Big] \times 10^{-2}. \quad (2.2.8)$$

Conversely, δ^q_{tQCD} includes the QCD contributions to the axial part of the decay. As computed in [70], the induced axial and vector currents corrections to the Z boson decay rate receive significant $O(\alpha_s^2)$ corrections due to the possible large splitting of heavy quark doublets. They stem from the absorptive part of the diagram obtained by squaring the tree-level decay $Z \to q\bar{q}$ with the real emission of 2 gluons $Z \to q\bar{q} \to gg$ via a triangle loop. In the context of four quark generations, the incomplete cancellation between the various heavy doublets gives rise to

$$\delta^f_{tQCD} \;=\; -\frac{\hat{a}_f}{\hat{v}_f^2 + \hat{a}_f^2} \Big(\frac{\alpha_s}{\pi} \Big)^2 [\hat{a}_t \; f(\mu_t) + \hat{a}_{t'} \; f(\mu_{t'}) - \hat{a}_{b'} \; f(\mu_{b'})] \quad (2.2.9)$$

where α_s is the QCD coupling constant evaluated at the Z pole (i.e. $\alpha_s(M_Z^2) = 0.119$) and $a_q = 2I_3^q$, $v_q = 2I_3^q - 4Q_q \hat{s}_W^2$ are the vector and axial vector couplings of the q quark, respectively. The quark masses $\bar{m}_i$ are defined in the $\overline{MS}$ scheme, with $\mu_i^2 = 4\bar{m}_i^2/M_Z^2$.

The function f reads [69]

$$f(\mu_i) = \ln\left(\frac{4}{\mu_i^2}\right) - 3.083 + \frac{0.346}{\mu_i^2} + \frac{0.211}{\mu_i^4}. \tag{2.2.10}$$

The δ^f_{tQCD} correction depends explicitely on *both* fourth generation quark masses, providing an additional constraint on the 3-4 family mixing as a function of the mass splitting. Using the exact expressions given in [68], we obtain

$$R_b = \frac{1.594(1+\delta_b)}{5.722 + 1.594(1+\delta_b)} \tag{2.2.11}$$

for $m_{t'} = 500$ GeV, which we can compare to the experimental value $R_b^{\rm exp} = 0.21629 \pm 0.00066$ [16]. We estimate that δ^f_{tQCD} yields a -5% ($+4\%$) correction for $m_{t'} = 500$ GeV if $\Delta m_{q'} = 80$ GeV (-80 GeV), which effect becomes weaker for larger $m_{t'}$ masses. While this implies a measurable effect in R_b, it depends sensitively on our choice of the $\overline{MS}$ top quark mass, here taken as $\bar{m}_t = 163.5$ GeV. Combining Eq.(2.2.11) with the condition $R_b > R_b^{\rm exp}$ at the 2σ level, we obtain the following upper bound on the 3-4 CKM mixing (for $\Delta m_{q'} = 0$ GeV) :

$$(|V_{t'b}|)_{R_b} \leq \begin{cases} 0.17 \text{ if } m_{t'} = 400 \text{ GeV} \\ 0.13 \text{ if } m_{t'} = 500 \text{ GeV} \\ 0.11 \text{ if } m_{t'} = 600 \text{ GeV} \end{cases} \tag{2.2.12}$$

which can be approximated by

$$(|V_{t'b}|)_{R_b} \lesssim 0.8\, \frac{m_W}{m_{t'}}. \tag{2.2.13}$$

Additionally, such bounds occur to be sensitive to the quark mass splitting when accounting for the $O(\alpha_s^2)$ QCD corrections in the $Z \to b\bar{b}$ decay rate. Most important, larger quark masses favour smaller $t - b'$ and $t' - b$ mixings, independently of the Higgs boson and heavy neutrino masses.

The oblique parameters originally introduced by Peskin and Takeuchi [71] lead to similar, albeit less model independent conclusions. Including all one-loop self-energy contributions of the electroweak vector bosons W, Z and γ arising from new heavy chiral fermions, the S, T and U have been evaluated in the

presence of a perturbative fourth family of fermions in [72]. Assuming that the corresponding new physics scale is much larger than the electroweak scale and that additional couplings to the SM fermions are suppressed, the contributions from a fourth fermion family to the oblique parameters read

$$S_4 = \frac{1}{3\pi}\Big(2 + \ln\frac{m_{b'}\, m_{\nu'}}{m_{t'}\, m_{\tau'}}\Big), \tag{2.2.14}$$

$$T_4 = \frac{3\,[m_{t'}^2 + m_{b'}^2 + |V_{t'b}|^2(F_{t'b'} - F_{tb'}) - F_{t'b'}] + [m_{\tau'}^2 + m_{\nu'}^2 - F_{\tau'\nu'}]}{16\pi\, s_W^2\, c_W^2\, M_Z^2}, \tag{2.2.15}$$

where s_W and c_W define the sine and cosine of the weak mixing angle respectively, and

$$F_{ij} = \frac{2m_i^2 m_j^2}{m_i^2 - m_j^2}\ln\frac{m_i^2}{m_j^2}. \tag{2.2.16}$$

We observe that large quark mass differences increase the T_4 contribution, while small $|V_{t'b}|$ values balance this effect. Assuming $|m_{\tau'} - m_{\nu'}| < 90$ GeV and $m_{t'} \simeq 500$ GeV, these observations can be summarised by the approximate upper bound (2.1.3) which the T parameter constraint translates to if $T \lesssim 0.3$ is fulfilled. As depicted in Fig. 2.1, it extends the approximation (2.1.2) and includes the mixing angle dependence between the two heavier generations, setting an upper limit on the allowed quark mass splitting from the T parameter.

The corrections to the U_4 parameter are known to be negligible if $T_4 < 0.4$ [72], so that we restrict our analysis to the two dimensional $S - T$ parameter space in the following. The S_4 parameter is sensitive to the mass scale of the new chiral fermions, whereas T_4 constrains the mass splitting between all isospin partners. Accordingly T_4 increases with $|V_{t'b}|$, while S_4 is CKM-independent. Besides the fermion contributions, the Higgs boson mass also affects the oblique corrections, which are known to depend logarithmically on the Higgs mass. In our analysis, the complete corrections computed at the Z pole given in [73] have been used. If larger than the SM reference, the Higgs boson mass m_H simultaneously lowers down the T parameter and increases S.

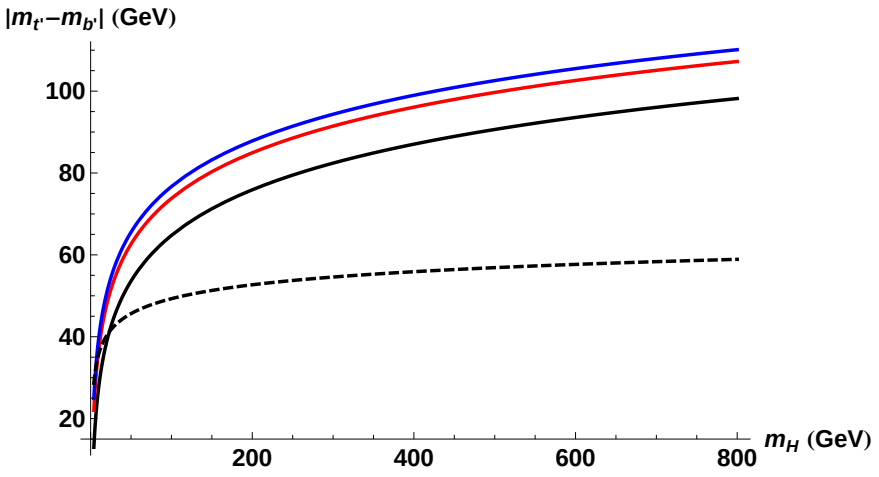

Figure 2.1: 95% CL upper bound on $|\Delta m_{q'}|$ versus m_H for $m_{t'} = 500$ GeV as given in (2.1.3) from the T parameter constraint, for the mixing values $|V_{t'b}| = 0.1$ (black), 0.05 (red) and 0.01 (blue). The dashed line depicts the value of the quark mass splitting as defined by the relation (2.1.2). No significant change is observed below $|V_{t'b}| < 10^{-2}$.

On the other hand, a smaller 3-4 mixing reduces the T parameter for a heavy Higgs mass without prejudicing the S parameter.

While small values are favored in the light Higgs case, fermion mass splittings larger than the W mass remain allowed in significant regions of the SM4 parameter space if $m_H \geq 450$ GeV. In the presence of a finite 3-4 CKM mixing element, the nondecoupling corrections to S and T imply a strong correlation between the fourth generation mass scale and the largest allowed value for $|V_{t'b}|$. The contour regions in the $S-T$ plane for a given confidence level CL are given by

$$\chi^2(S,T) = \frac{(S-S_0)^2}{\sigma_S^2(1-\rho^2)} + \frac{(T-T_0)^2}{\sigma_T^2(1-\rho^2)} + \frac{2(S_0T + ST_0 - ST - S_0T_0)}{\sigma_S\sigma_T(1-\rho^2)} < -2\ln(1-CL). \tag{2.2.17}$$

As an illustration, we compute the corresponding confidence levels for S and T, by varying the quark masses ($m_{t'}$,$m_{b'}$) within the range $[300, 800]$ GeV. Only evaluated for the Higgs reference mass $m_H^{ref} = m_Z$, the LEPEWWG fit results $S_0 \pm \sigma_S = 0.05 \pm 0.10$ and $T_0 \pm \sigma_T = 0.10 \pm 0.09$ are used for the central values and their related standard deviations ($\rho = 0.85$ gives the correlation coefficient between the two parameters) [74]. The top reference mass is defined as $m_t^{ref} = 173.2$ GeV. All relevant quantities, including $\alpha^{-1}(M_Z) = 128.89$ and $s_W^2(M_Z) = 0.22291$, are considered at the Z pole. We have checked that our results are in agreement with [72] at the permille level, yet very sensitive to the choice of (S_0, T_0). As a result, the upper limit on the 3-4 CKM mixing element yields

$$(|V_{t'b}|)_{S,T} \leq \frac{m_W}{m_{t'}}, \tag{2.2.18}$$

at the 95% CL, in agreement with [74], though weaker than (2.2.13). The minimization of Eq.(2.2.17) with respect to the t' mass and the mixing angle is shown in Fig. 2.2, as well as the upper bounds derived from R_b.

Although they provide additional insight on the SM4 parameters, we stress that flavour physics constraints are not considered in this analysis. However, both the electroweak precision and the flavour constraints are known to favour small mixing with a heavy fourth family [72]. As we neglect the 1-4 and 2-4 CKM mixing, the electroweak precision observables are found to give more severe constraints on the maximally allowed values for $|V_{t'b}|$.

2.3 Parameter space

In this section we interpret the previous constraints and present a systematic analysis of the SM4 parameter space. Parameter sets minimizing the values of the electroweak parameters S and T are purposely identified, considering the relative importance of the possible fermion mass hierarchies for the case of vanishing 2-4 and 1-4 family quark mixings. In the following, we will assume that the mixing between the third and the hypothetical fourth generation of quarks fully encodes the new flavour sector.

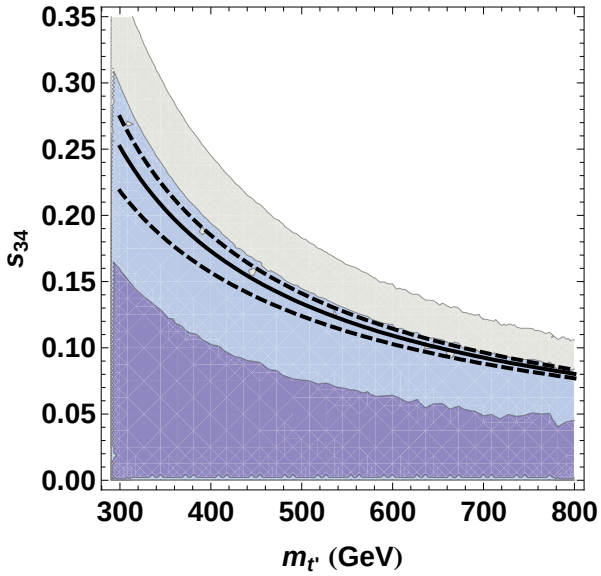

Figure 2.2: 68% (darker blue), 95% (blue) and 99% (grey) CL allowed regions from (2.2.17) for the $3-4$ CKM mixing element as a function of $m_{t'}$, with all other SM4 parameters unconstrained. We find that the mixing between the third and fourth generation quarks is restricted such that $|V_{t'b}| < 0.15$ (0.075) holds at the 2σ (1σ) level if $m_{t'} > 500$ GeV when considering the T parameter. The non-oblique correction arising from the $Z \to b\bar{b}$ rate at the 95% CL is given by the solid black line for $\Delta m_{q'} = 0$ GeV. The upper and lower dashed lines give the corresponding constraints for $\Delta m_{q'} = -80$ GeV and $\Delta m_{q'} = 80$ GeV, respectively.

As detailed in [40], none of the two quark mass differences $\Delta m_{q'} < 50$ GeV and $\Delta m_{q'} > 50$ GeV is disfavored if a small mixing is required. Regarding the possible mass hierarchies, the correlations between the fermion splittings $\Delta m_{q'} = m_{t'} - m_{b'}$ and $\Delta m_{l'} = m_{\nu'} - m_{\tau'}$ have been considered for various quark and lepton mass scales. For completeness, we briefly re-examine them here for a non-vanishing 3-4 CKM mixing. Fixing $m_H = 125$ GeV, we plot in Fig. 2.3 the corresponding 68%, 95% and 99% CL regions in the ($\Delta m_{q'}$, $\Delta m_{l'}$) plane for all possible mass differences and CKM mixing elements.

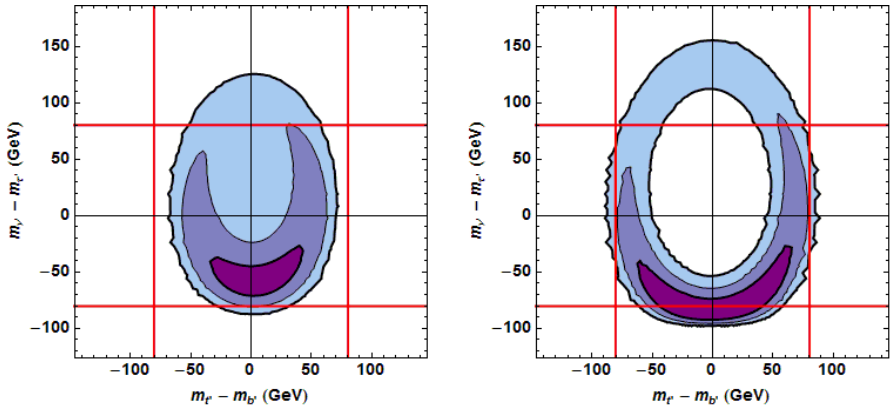

Figure 2.3: Contour regions in the $\Delta m_{q'} - \Delta m_{l'}$ plane as allowed from (2.2.17), for $m_H = 125$ GeV, and $|V_{t'b}| = 0.01$ (left), 0.1 (right). The three confidence levels 68%, 95% and 99% are given by the purple, dark blue and light blue areas, respectively, for $m_{t'} = 500$ GeV and $m_{\tau'} = 100$ GeV. The vertical (horizontal) red lines define the $\Delta m_{q'} = m_W$ ($\Delta m_{l'} = m_W$) threshold for the production of a real W in $t' \leftrightarrow b'$ ($\tau' \leftrightarrow \nu'$) decays.

Assuming a 500 (100) GeV scale for the fourth generation quarks (leptons), the χ^2 values given by (2.2.17) allow large areas for $\Delta m_{q'}, \Delta m_{l'} \geq 50$ GeV and $|V_{t'b}| \leq 10^{-1}$. Numerically, a strong correlation is confirmed between the quark and lepton mass splittings, with a weak yet relevant dependence on the 3-4 CKM mixing. Given the logarithmic dependence of S_4 on the ratio $m_{\nu'}/m_{\tau'}$, large lepton mass splittings can be allowed at the cost of a smaller quark mass difference balancing the T_4 parameter.

We observe that the lepton mass hierarchy $m_{\nu'} > m_{\tau'}$ occurs to be strongly disfavored in view of these results, whereas the quark splittings $\Delta m_{q'} > 0$ and $\Delta m_{q'} < 0$ are equally preferred if $m_{\nu'} < m_{\tau'}$. Assuming that $|V_{t'b}| \geq 10^{-2}$, small lepton mass splittings are allowed if $|\Delta m_{q'}|$ is larger than 50 GeV, while $|\Delta m_{q'}| < 40$ GeV defines a wide parameter region for which $m_{\tau'} - m_{\nu'} > 80$ GeV is possible. The oblique parameters thus allow the two-body decay mode $\tau' \to \nu' W$ for fourth generation leptons if the quark mass difference is small.

Considering $m_H = 125$ GeV, we extract in Tab. 2.2 various representative benchmark points for the two cases $m_{t'} > m_{b'}$ and $m_{t'} < m_{b'}$. We also note that quark mass splittings larger than 75 GeV are disfavored if $m_H < 400$ GeV, which confirms the non trivial correlation between the Higgs mass and the quark mass difference depicted in Fig. 2.3. Little change is noticed with respect to these conclusions when considering 3-4 CKM mixing smaller than 10^{-2}. As Fig. 2.1 indicates, there is not much gain in lowering down $|V_{t'b}|$ for the considered mass scales. We also observe that the upper bound on the quark mass splitting does not depend on any parameter other than the Higgs boson mass, unless the mixing angle saturates the upper bound required from R_b. If only the T constraint is satisfied, both the quark and the lepton mass scales can be increased without any effect on the S parameter.

2.4 Phenomenology at the LHC

The predominant production and decay modes for a fourth generation of quarks strongly depend on the quark mass splitting and hierarchy. Assuming a small 3-4 CKM mixing, we now consider the corresponding phenomenology in terms of LHC signatures.

Although pair production via the strong interaction is the main mechanism for producing new heavy quarks at the LHC, the electroweak production of a single top quark in the t-channel provides another relevant process to search for a fourth quark family [75], as shown on Fig. 2.4. For instance, the final state topologies expected from the electroweak $t'\bar{b}$ ($\bar{t}'b$) and $\bar{t}b'$ ($t\bar{b}'$) production have been used in [51] to set very restrictive bounds on a degenerate fourth generation. Benchmark cross-sections at NLO have been tabulated in [75] for various

$m_{t'}$	$\Delta m^{\max}_{\lvert V_{t'b}\rvert} = 0.1$	$\Delta m^{\max}_{\lvert V_{t'b}\rvert} = 0.05$	$\Delta m^{\max}_{\lvert V_{t'b}\rvert} = 0.01$
400	62	68	70
500	52	66	70
600	36	64	70
$m_{b'}$	$\Delta m^{\max}_{\lvert V_{t'b}\rvert} = 0.1$	$\Delta m^{\max}_{\lvert V_{t'b}\rvert} = 0.05$	$\Delta m^{\max}_{\lvert V_{t'b}\rvert} = 0.01$
400	-65	-72	-72
500	-55	-70	-72
600	-38	-66	-72

Table 2.2: Selected SM4 scenarios, allowed at the 95% CL by the S and T parameters, for $m_H = 125$ GeV, and $|V_{t'b}| = 0.1, 0.05, 0.01$. The shown benchmark points give the largest possible quark mass splittings when considering either the normal ($m_{t'} > m_{b'}$, top table) or the inverted ($m_{t'} < m_{b'}$, bottom table) mass hierarchy. All masses are given in GeV, with $m_{\nu'} = 60$ GeV and $\Delta m_{l'} = 40$ GeV being fixed.

fourth generation masses, PDF sets and LHC energies under the assumption $|V_{t'b^{(\prime)}}|^2 = 1$. However, these processes scale by a factor $|V_{t'b}|^2 \simeq |V_{tb'}|^2$ and are strongly suppressed if the 3-4 CKM mixing element is negligibly small (while pair production is independent of it). Considering small $|V_{t'b}|$ values as discussed in the previous section, single t' and b' production suffer strong CKM suppression, with cross sections below the femtobarn level for the considered mass scales and mixings. Would the phase space allow it with $|\Delta m_{q'}| \gtrsim m_W$, we highlight that the $t'\bar{b}'$ ($\bar{t}'b'$) electroweak pair production in the t-channel may provide an alternative without any CKM suppression, overtaking $t'b$ (tb') single production by two orders of magnitude if $|V_{t'b}|$ is smaller than 10^{-1}. In spite of the phase space suppression arising from the presence of two heavy particles in the final state, the interaction with the longitudinal W boson is proportional to the t' and b' Yukawa couplings, and may therefore provide a significant contribution to electroweak pair production of heavy quarks. If the fourth generation mixings with the lighter quarks are negligible, these channels actually feature the second dominant signal after strong pair production.

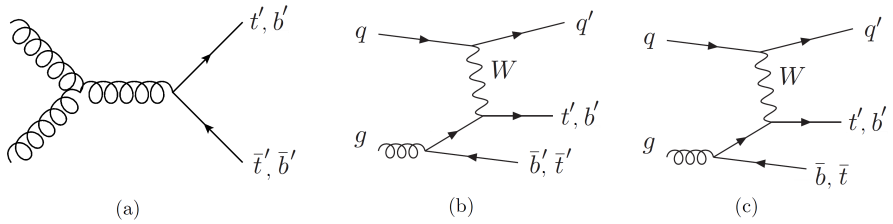

Figure 2.4: Representative diagrams for the production of fourth generation quarks. (a) Strong pair production of heavy quarks at leading order ; (b) $2 \to 3$ Born diagrams contributing to $t'\bar{b}'$ and $\bar{t}'b'$ electroweak production in the t-channel ; (c) $t'\bar{b}$ and $\bar{t}b'$ electroweak production (and the charge-conjugate processes) in the t-channel (suppressed if a small 3-4 CKM mixing is considered).

Tabs. 2.3, 2.4 and 2.5 present our predictions for selected choices of the t' and b' mass splittings. The $t'\bar{b}'$ ($\bar{t}'b'$) t-channel electroweak production, and the pair production cross-sections have been computed at 7, 8 and 14 TeV, with the CTEQ6.6 PDF set. The 6.0 version of the Monte-Carlo software MCFM [76] has been used for the calculations at NLO accuracy, following the conventions used previously in [75].

We now briefly discuss the possible decay signatures depending on their mass ordering for small values of $|V_{t'b'}|$. In the case of a normal quark mass hierarchy ($m_{t'} > m_{b'}$), up-like fourth generation quarks either decay via $t' \to bW$ or cascade through $t' \to b'W \to tWW \to bWWW$, with a real or a virtual W emission. Given the constraints established previously on $\Delta m_{q'}$, we conclude that the $t' \to b'W^*$ decay is unlikely to dominate over the $t' \to Wb$ mode due to strong phase space suppression, a case which is treated in detail in [40]. If we enforce that $\mathrm{BR}(t' \to bW) \gg \mathrm{BR}(t' \to b'W)$ and postulate that t' and b' decay promptly within the detector, the most likely final states for both a normal and an inverted mass hierarchy are

$m_{t'}$	$m_{b'}$	$\sigma^{7\,\mathrm{TeV}}_{t'\bar{b}'}(fb)$	$\sigma^{8\,\mathrm{TeV}}_{t'\bar{b}'}(fb)$	$\sigma^{14\,\mathrm{TeV}}_{t'\bar{b}'}(fb)$
400	350	(100) $120^{+12\,+13}_{-6\,-10}$	(155) $262^{+14\,+18}_{-6\,-16}$	(1162) $1395^{+55\,+69}_{-28\,-61}$
400	330	(111) $188^{+18\,+21}_{-9\,-15}$	(187) $223^{+22\,+26}_{-13\,-20}$	(1151) $1512^{+48\,+66}_{-31\,-64}$
400	310	(121) $203^{+15\,+17}_{-7\,-14}$	(201) $265^{+29\,+33}_{-18\,-25}$	(1218) $1720^{+60\,+81}_{-36\,-77}$
500	450	(32.9) $49.7^{+7.8\,+8.8}_{-4.6\,-6.1}$	(57.1) $92.6^{+11.1\,+12.6}_{-6.4\,-9.3}$	(468) $610^{+32\,+40}_{-17\,-35}$
500	430	(34.8) $50.1^{+8.7\,+9.7}_{-5.0\,-6.5}$	(67.2) $87.2^{+11.0\,+12.4}_{-6.2\,-8.6}$	(535) $653^{+34\,+42}_{-19\,-37}$
500	410	(40.9) $48.7^{+7.6\,+8.5}_{-4.5\,-6.0}$	(70.9) $113^{+12\,+14}_{-7\,-10}$	(614) $719^{+32\,+41}_{-16\,-37}$
600	550	(11.7) $19.1^{4.1\,+4.6}_{-2.2\,-2.9}$	(24.2) $33.6^{+5.8\,+6.5}_{-3.5\,-4.5}$	(278) $390^{+21\,+25}_{-9\,-22}$
600	530	(12.4) $16.7^{+3.8\,+4.2}_{-2.1\,-2.7}$	(26.1) $38.0^{+7.8\,+8.6}_{-4.3\,-5.5}$	(301) $367^{+19\,+23}_{-9\,-21}$
600	510	(14.1) $18.7^{+4.2\,+4.6}_{-2.4\,-3.0}$	(28.2) $36.2^{+6.3\,+6.9}_{-3.4\,-4.6}$	(321) $323^{+30\,+35}_{-17\,-26}$

Table 2.3: $\sqrt{s} =$ 7, 8 and 14 TeV NLO predictions for the $t'\bar{b}'$ t-channel electroweak production, with $|V_{t'b'}|^2 = 1$. LO predictions are given in parentheses for 50, 70 and 90 GeV mass splittings. The first uncertainty is calculated from the renormalisation and factorisation scales variation using the conventions detailed in [75], while the second gives the upper and lower PDF errors for the CTEQ6.6 PDF set. The central value is computed for $\mu = \mu_f = \mu_r = (m_{t'} + m_{b'})/2$. The assumed CP invariance and chirality of the $Wt'b'$ vertex lead to equal cross-sections when switching the t' and the b' masses, here given in GeV.

- (a) $t'\bar{t}' \to bWbW$
- (b) $b'\bar{b}' \to tWtW \to bWWbWW$
- (c) $t'b \to bWb$
- (d) $b't \to tWbW \to bWWbW$
- (e) $b't' \to tWbW \to bWWbW$

All the above decay modes require one to four W bosons in the final state, while two b-jets are systematically present in the decay of each signal. The above modes have been considered altogether in the combined search [51],

$m_{t'}$	$m_{b'}$	$\sigma^{7\,\text{TeV}}_{\bar{t}'b'}(fb)$	$\sigma^{8\,\text{TeV}}_{\bar{t}'b'}(fb)$	$\sigma^{14\,\text{TeV}}_{\bar{t}'b'}(fb)$
400	350	(39.7) $52.7^{+7.0\,+9.4}_{-2.5\,-4.6}$	(75.2) $102^{+11\,+14.6}_{-3\,-7}$	(537) $793^{+46\,+68}_{-18\,-36}$
400	330	(50.4) $78.0^{+10.4\,+13.3}_{-4.1\,-6.4}$	(84.8) $109^{+14\,+18}_{-5\,-9}$	(587) $602^{+40\,+57}_{-16\,-32}$
400	310	(52.0) $64.7^{+9.4\,+12.0}_{-4.0\,-6.2}$	(87.7) $112^{+14\,+18}_{-6\,-10}$	(676) $934^{+45\,+77}_{-20\,-44}$
500	450	(12.2) $18.9^{+4.0\,+5.0}_{-1.7\,-2.4}$	(23.4) $42.3^{+5.9\,+8.1}_{-1.6\,-3.8}$	(239) $300^{+23\,+32}_{-9\,-17}$
500	430	(13.9) $21.8^{+4.5\,+5.5}_{-2.0\,-2.7}$	(26.2) $44.2^{+6.2\,+8.0}_{-2.4\,-3.8}$	(287) $257^{+21\,+29}_{-8\,-16}$
500	410	(15.9) $48.6^{+6.3\,+8.3}_{-2.5\,-4.1}$	(31.2) $48.6^{+6.3\,+8.3}_{-2.5\,-4.1}$	(293) $327^{+25\,+35}_{-9\,-19}$
600	550	(4.07) $6.68^{+1.85\,+2.26}_{-0.81\,-1.10}$	(9.5) $12.8^{+2.7\,+3.3}_{-1.2\,-1.6}$	(117) $149^{+15\,+20}_{-5\,-10}$
600	530	(4.29) $6.72^{+1.74\,+2.08}_{-0.73\,-0.97}$	(9.8) $11.8^{+2.7\,+3.3}_{-1.2\,-1.6}$	(121) $142^{+14\,+19}_{-6\,-10}$
600	510	(5.23) $7.83^{+1.99\,+2.36}_{-0.86\,-1.11}$	(10.9) $15.0^{+3.2\,+3.9}_{-1.3\,-1.9}$	(142) $159^{+17\,+23}_{-6\,-12}$

Table 2.4: Same as Tab. 2.3 for t-channel $\bar{t}'b'$ electroweak production, with the CTEQ6.6 PDF set and $|V_{t'b'}|^2 = 1$.

which excluded t' and b' quark masses below 685 GeV at 95% confidence level. Both the $t'\bar{t}'$ and the $b'\bar{b}'$ pair production signals are covered by the direct searches [46, 47, 48, 49, 50] in multiple channels under the condition $\text{BR}(t' \to bW) = \text{BR}(b' \to tW) = 100\%$.

2.5 Summary

In this work, we considered the available parameter space for a perturbative fourth generation of fermions, as allowed by the current bounds. While exploring the still allowed mass spectra of fourth generation fermions, we evaluated the constraints from direct searches at the colliders and electroweak precision measurements. Our results showed that the relation (2.1.2) overconstrains the allowed SM4 scenarios if a small but non-zero CKM mixing between the two heaviest quark families is required. We also confirmed that the $Z \to b\bar{b}$ decay rate gives a stronger bound on the 3-4 family CKM mixing element than the oblique parameters, independently of the Higgs and lepton sectors. Considering the bound (2.1.3) and accounting for the observed value of 125 GeV

m_Q	$\sigma^{7\,\mathrm{TeV}}_{Q\bar{Q}}(fb)$	$\sigma^{8\,\mathrm{TeV}}_{Q\bar{Q}}(fb)$	$\sigma^{14\,\mathrm{TeV}}_{Q\bar{Q}}(fb)$
400	(955) $1329^{+240\,+280}_{-138\,-179}$	(1552) $2164^{+341\,+400}_{-202\,-267}$	(9206) $13033^{+1063\,-1169}_{-650\,-1028}$
425	(654) $907^{+175\,+202}_{-98\,-127}$	(1078) $1498^{+251\,+293}_{-147\,-192}$	(6675) $9414^{+836\,+1038}_{-511\,-784}$
450	(454) $629^{+127\,+148}_{-71\,-91}$	(761) $1054^{+188\,+218}_{-108\,-140}$	(4913) $6905^{+661\,+812}_{-404\,-604}$
475	(320) $442^{+95\,+109}_{-51\,-65}$	(544) $751^{+141\,+164}_{-80\,-103}$	(3665) $5131^{+526\,+641}_{-321\,-469}$
500	(228) $314^{+70.8\,+81}_{-37.1\,-48}$	(393) $542^{+107\,+124}_{-59\,-76}$	(2767) $3861^{+422\,+510}_{-257\,-368}$
525	(164) $226^{+53\,+61}_{-27\,-35}$	(287) $395^{+82\,+94}_{-44\,-57}$	(2112) $2938^{+340\,+408}_{-207\,-291}$
550	(119) $164^{+41\,+46}_{-20\,-26}$	(212) $291^{+63\,+73}_{-34\,-43}$	(1628) $2258^{+276\,+329}_{-167\,-232}$
575	(87.2) $120^{+31\,+35}_{-15\,-19}$	(158) $216^{+49\,+56}_{-25\,-33}$	(1266) $1750^{+225\,+267}_{-135\,-198}$
600	(64.4) $88.4^{+24\,+27}_{-11\,-14}$	(119) $162^{+38\,+44}_{-19\,-25}$	(993) $1369^{+184\,+218}_{-110\,-149}$

Table 2.5: (LO) NLO cross-sections for $Q = t', b'$ pair production at the LHC 7, 8 and 14 TeV. The first error gives the factorization and renormalization scales dependence, computed by setting $\mu = \mu_f = \mu_r$ and varying them between $m_Q/2$ and $2m_Q$ for the upper and lower deviations from the central value $\mu = m_Q$, respectively. The second error yields the CTEQ6.6 PDF uncertainties.

for the Higgs mass, we find that mass splittings $|m_{t'} - m_{b'}|$ larger than m_W are strongly disfavoured. This is a notable conclusion, as the heavy-to-heavy transitions $t' \to Wb'$ ($b' \to t'W$) are then unlikely to provide relevant decay modes if the 3-4 family CKM mixing element is small, so that only the production modes discussed in the previous section are expected to give a sizeable signal at the LHC.

Given the interest of excluding the largest possible spectrum from the direct searches, we have presented benchmark scenarios allowing for non-zero 3-4 CKM mixings, and non-degenerate SM4 quark masses. For extremely small values of $|V_{tb'}|$, long-lived quarks and bound states thereof might evade the direct searches, as we have shown in [41] that they require dedicated analyses. While the possibility for new families of chiral quarks remains allowed in the framework of additional scalar particles (see, e.g., [77, 78, 79, 80]), it is now acknowledged that a sequential fourth family is excluded for the minimal SM Higgs sector.

Chapter 3

Model Independent Framework for Searches of Top Partners

"The greatest challenge to any thinker is stating the problem in a way that will allow a solution"

Bertrand Russell

Based on:

M. Buchkremer, G. Cacciapaglia, A. Deandrea, L. Panizzi, "Model Independent Framework for Searches of Top Partners", *Nucl.Phys.*, vol. B876, pp. 376-417, 2013, 1305.4172.

In this chapter we propose a model-independent and general framework to study the LHC phenomenology of top partners, i.e. Vector-Like (VL) quarks including particles with different electro-magnetic charge. Focusing on the case of a single multiplet of the weak $SU(2)_L$, we scrutinise the electroweak single production of non-chiral states having standard Yukawa couplings to the Standard Model quarks. Based on this minimal assumption, we show that they may be studied in terms of a small amount of parameters in an effective Lagrangian description with a clear and simple connection with experimental

observables. We perform a numerical study and discuss the conclusions which can be drawn within such a description and the expected potential for discovery or exclusion at the LHC. Our main results are a clear connection between branching ratios and single production channels, and the identification of novel interesting channels to be studied at the LHC.

3.1 Introduction

Heavy partners of the top quark are a common feature of many New Physics scenarios beyond supersymmetry, including Little Higgs Models, Extra Dimensions, and Composite Higgs Models. Such new partners can be scalars, or new heavy coloured states, extra quarks with vector-like couplings, which are present in many extensions of the SM that offer alternative explanations for the dynamics of Electro-Weak Symmetry Breaking (EWSB) to the one embedded in the Brout-Englert-Higgs mechanism. In the so-called Little Higgs scenarios, these states arise as partners of the SM fields being promoted to larger multiplets, which are generally introduced in order to cancel the contributions of the quadratic divergences to the Higgs mass renormalisation [28, 81, 82, 83]. In extra-dimensional models, vector-like quarks are prevalent as Kaluza-Klein (KK) excitations of the SM quark fields in the bulk [84, 85], like in the Randall-Sundrum scenario [33, 86]. In composite Higgs [87, 34, 88] and composite top [89] models, they emerge as excited resonances of the bound states constituting the SM particles. Top-quark partners are also found in theories with gauge coupling unification where the new fermions are embedded into the simplest SU(5) representations [90], or top condensate models (see, e.g., [91, 92] and [93]). Modern incarnations of Technicolour, which have a light Higgs-like scalar in the spectrum [38, 39], should also be included in the list.

In all the above cases, a common prediction is the presence of partners of the top quark and more generally multiplets containing a top partner of the vector-like type [94], which have the same spin and only differ in the embedding into representations of the weak isospin, $SU(2)_L$. Contrary to sequential fourth family quarks which are severely constrained from the Higgs boson searches due to their non-decoupling properties [95], the indirect bounds on non-chiral quarks are much weaker. The forthcoming direct searches at the LHC will play

a fundamental role in testing the large number of models predicting the existence of these states. The motivation to concentrate on these states is due to the recent renewed interest for the presence of VL quarks (coloured fermions whose mass is not generated by the Brout-Englert-Higgs mechanism), following the exclusion of a fourth SM-like family of (chiral) quarks.

The importance of top partners, or generically new quarks, is also supported by the massive ongoing experimental effort for their discovery. A combination of the various searches available can be found on the public result pages of both ATLAS [96, 97, 98, 99] and CMS [100, 101, 102, 103] collaborations, with final states in the third generation. Couplings to light generation have also been considered in single production [104], and in some few cases in the decays (see for instance [96] for the case of a b-partner). The present limits on their masses are now close to 700 GeV, reaching the mass range of interest for the naturalness argument. At present most of the experimental searches assume that the new heavy quarks are QCD pair produced, while combining searches for quarks which are either produced singly or pairwise (also via EW interactions) will become a more effective option in the near future. Indeed, present limits from the LHC start to enter the region in which single production becomes relevant and this will be more and more the case if the bounds are raised. Experimental searches, such as e.g. [105], now focus on the electroweak single production of new heavy quarks, through channels that are sensitive to the size of the coupling to the standard quarks. However, most of the current studies are based on the assumption that the new quarks only couple to the first generation of quarks, and final states involving tops and/or bottoms have not been explored. We have therefore at present an incomplete picture, which will be for sure studied in more detail in the near future using more general analyses and a larger amount of data. While many decay channels and final states have been already considered by the experimental teams, little attempt has been done to combine the information extracted from the data in a systematic way: the main reason for this is the lack of a complete and model-independent framework to describe the interactions of such new particles.

In the following, we present a minimal Lagrangian which describes all the allowed couplings of VL quarks, and use it to define model-independent search strategies allowing to fully constrain the masses of top partners in any given

model. We propose to use this framework to find corners of the parameter space which are poorly covered by the present searches, and define new dedicated searches. The main guiding principle is the fact that the decays and single production of the new states are generated via mixing with the SM quarks [106], induced by standard Yukawa interactions with the $SU(2)_L$ scalar doublet Higgs.

Under this assumption, which requires the new particles to be fermions transforming as triplets of $SU(3)_c$, the only allowed decays are into a standard quark plus a boson, $W^{\pm}$, Z or Higgs. The minimal set of parameters we identify then consists of a set mainly describing the branching ratios into the massive bosons and the three Standard Model quark generations, plus a parameter describing the strength of the mixing. The connection between the branching ratios in different channels and the single production cross sections can be exploited to extend the searches to include both single and pair production channels, and extract a reliable bound on the mixing parameters with the standard quarks. It is important to emphasise that such new states cannot have arbitrary quantum numbers, since our assumption is that they can only mix with the SM quarks through a limited number of gauge-invariant terms. Classifying them into $SU(2)_L$ multiplets, their Yukawa couplings with the SM scalar doublet only allow for seven distinct possibilities, *i.e.*, the two singlets, the three doublets and the two triplets displayed in Tab. 3.1.

Q_q	$T_{\frac{2}{3}}$	$B_{-\frac{1}{3}}$	$\begin{pmatrix} X_{\frac{5}{3}} \\ T_{\frac{2}{3}} \end{pmatrix}$	$\begin{pmatrix} T_{\frac{2}{3}} \\ B_{-\frac{1}{3}} \end{pmatrix}$	$\begin{pmatrix} B_{-\frac{1}{3}} \\ Y_{-\frac{4}{3}} \end{pmatrix}$	$\begin{pmatrix} X_{\frac{5}{3}} \\ T_{\frac{2}{3}} \\ B_{-\frac{1}{3}} \end{pmatrix}$	$\begin{pmatrix} T_{\frac{2}{3}} \\ B_{-\frac{1}{3}} \\ Y_{-\frac{4}{3}} \end{pmatrix}$
T_3	0	0	$1/2$	$1/2$	$1/2$	1	1
Y	$4/3$	$-2/3$	$7/3$	$1/3$	$-5/3$	$4/3$	$-2/3$

Table 3.1: Vector-like multiplets allowed to mix with the SM quarks through Yukawa couplings. The electric charge is the sum of the third component of isospin T_3 and of $Y/2$, as defined from Eq.(1.1.1). Adapted from [106].

Vector-like quark singlets and triplets mix dominantly with the standard left-handed doublets, whereas doublets couple to the standard right-handed singlets[1]. The relative branching ratios are purely determined by the weak quantum numbers of the multiplet the new quark belongs to. Finally, we mention that though they are usually assumed to mix only with the third generation following hierarchy or naturalness arguments, we will see that the top partners can mix in a sizeable way with lighter quarks while remaining compatible with the current experimental constraints. Indeed, the top partners interactions with the electroweak and Higgs bosons are generically allowed through arbitrary Yukawa couplings, implying that the branching ratios into light quarks can be possibly competitive with the top quark.

Our work is organised as follows: in section 3.2 our general parametrisation is introduced, including all the VL quarks that are allowed to decay into standard quarks, thus covering all the quantum numbers present in multiplets that can couple to standard quarks via the Higgs. The effective Lagrangian is written in terms of the few relevant parameters which have a clear link to observable quantities at the LHC. In section 3.3 we use this parametrisation to study the production and decay modes of these states, and expand the single production cross sections in terms of model-independent coefficients. In section 3.5, we perform a numerical analysis using a Monte Carlo implementation of the model, and discuss a few outcomes reflecting the expected potential for discovery or exclusion at the LHC. Our conclusions are presented in section 3.6.

3.2 Complete and model independent parametrisation

3.2.1 Theoretical assumptions

In order to couple to the SM quarks through Yukawa interactions, the new top partners must have the same colour as the standard ones (thus belonging to the fundamental representation of $SU(3)_c$) and have four possible charge

[1] We highlight that this does not embed all the possible scenarios, a review of which can be found in [106, 107].

assignments, defining their allowed decay channels as

$$\begin{aligned} Q = 5/3 \quad &\Rightarrow \quad X \to W^+ u^i \,; \\ Q = 2/3 \quad &\Rightarrow \quad T \to W^+ d^i \,,\; Z u^i \,,\; H u^i \,; \\ Q = -1/3 \quad &\Rightarrow \quad B \to W^- u^i \,,\; Z d^i \,,\; H d^i \,; \\ Q = -4/3 \quad &\Rightarrow \quad Y \to W^- d^i \,; \end{aligned} \tag{3.2.1}$$

where $i = 1, 2, 3$ labels the 3 standard generations. Although top partners can have sizeable branching ratios to extended Higgs sectors, their decays to non-SM particles are generally expected to be subdominant in most scenarios due to phase space suppression. As long as the lightest states decay mainly to SM quarks via W, Z and Higgs bosons our formalism naturally extends to various classes of models. The parametrisation presented in the following will also be used in Chapter 4, in the context of one or multiple top partners.

In order to further simplify the analysis, we will limit our parametrisation to some reasonable and general assumptions on the couplings of the new quarks, mainly based on the search strategy followed by the LHC experiments. The first assumption we base our analysis on is that the signals, if any, arise from the presence of a single top partner. In fact, the bounds on new states are always based on the hypothesis that the new states can be studied as independent, either due to a large mass splitting or negligible mixing effects. The large mixing case can also be included under certain circumstances that will become clear later on. This is easily satisfied in the case where, for each kind of new quark, there is a single mass eigenstate that is significantly lighter than the others.

As mentioned previously, the second and main hypothesis leading to the effective Lagrangian we propose in the following is that the new states have standard Yukawa couplings to the SM quarks. Therefore the mixing is only generated by interactions involving a doublet of $SU(2)_L$. The assumption of a Standard Model Higgs field is directly motivated by the successful features of the CKM matrix so as to describe quark mixing in the SM. This fact also limits the size of the mass splitting which is related to the Higgs VEV. We note, however, that this is also valid for models with an extended Higgs sector: in fact, while additional doublets do not change the structure of the mixings,

other representations are forced to have a small vacuum expectation value to avoid too large corrections to the ρ parameter, thus we can generically safely neglect their contribution to the mixing.

As a direct consequence of the gauge structure of the Standard Model, the VL quarks belong to complete $SU(2)_L$ representations and are only allowed to decay to Standard Model quarks via standard gauge bosons. As summarised in Tab. 3.1, only 2 singlets, 3 doublets and 2 triplets are allowed, with varied hypercharge assignments. Finally, we highlight that the couplings of the new states are necessarily chiral. Singlets and triplets predominantly mix with the standard left-handed doublets, while the new doublets mix with the standard right-handed singlets. As shown in [109], this stays true in models with more than one VL multiplet, as long as the Yukawa couplings between VL multiplets are not too large. This is due to the fact that for singlets and triplets the mixing angles in the right-handed sector are suppressed with respect to the left-handed ones by the mass of the standard quarks over the new state mass [108], while for doublets the left-handed mixings which are the ones being suppressed.

As a comment, we also highlight that complete $SU(2)_L$ representations, with the exception of singlets, always contain more than one VL quark with different charge: they decay into different final states, therefore the assumption of an isolated new quark is still viable. Furthermore, decays of a VL quark into another, like for instance $X \to W^+T$, are generically not allowed kinematically because the mass splitting between two states in the same multiplet, which is generated by the Higgs VEV, is typically much smaller than the W mass.

3.2.2 The effective Lagrangian

Relying on the previous assumptions, we now describe a complete effective model apt to describe the phenomenology of the 4 aforecited kinds of VL quarks. For the sake of simplicity, only the final results will be presented in this Chapter, whereas a description of the underlying construction for the specific case of a T quark, and of all the associated parameters, can be found in Appendix A.

The most general Lagrangian contains the following 4 sets of interactions for leading left-handed mixing:

$$\begin{aligned}\mathcal{L} = \kappa_T &\left\{ \sqrt{\frac{\zeta_i \xi_W^T}{\Gamma_W^0}} \frac{g}{\sqrt{2}} \left[\bar{T}_L W_\mu^+ \gamma^\mu d_L^i\right] + \sqrt{\frac{\zeta_i \xi_Z^T}{\Gamma_Z^0}} \frac{g}{2c_W} \left[\bar{T}_L Z_\mu \gamma^\mu u_L^i\right] \right. \\ &\left. - \sqrt{\frac{\zeta_i \xi_H^T}{\Gamma_H^0}} \frac{M}{v} \left[\bar{T}_R H u_L^i\right] - \sqrt{\frac{\zeta_3 \xi_H^T}{\Gamma_H^0}} \frac{m_t}{v} \left[\bar{T}_L H t_R\right] \right\} \\ + \kappa_B &\left\{ \sqrt{\frac{\zeta_i \xi_W^B}{\Gamma_W^0}} \frac{g}{\sqrt{2}} \left[\bar{B}_L W_\mu^- \gamma^\mu u_L^i\right] + \sqrt{\frac{\zeta_i \xi_Z^B}{\Gamma_Z^0}} \frac{g}{2c_W} \left[\bar{B}_L Z_\mu \gamma^\mu d_L^i\right] \right\} \\ &\left. - \sqrt{\frac{\zeta_i \xi_H^B}{\Gamma_H^0}} \frac{M}{v} \left[\bar{B}_R H d_L^i\right] \right\} \\ + \kappa_X &\left\{ \sqrt{\frac{\zeta_i}{\Gamma_W^0}} \frac{g}{\sqrt{2}} \left[\bar{X}_L W_\mu^+ \gamma^\mu u_L^i\right] \right\} + \kappa_Y \left\{ \sqrt{\frac{\zeta_i}{\Gamma_W^0}} \frac{g}{\sqrt{2}} \left[\bar{Y}_L W_\mu^- \gamma^\mu d_L^i\right] \right\} \\ &+ h.c.\,, \quad (3.2.2)\end{aligned}$$

while it suffices to exchange the chiralities L $\leftrightarrow$ R for leading right-handed coupling. The mass of the VL quark will determine its production rates, especially for pair production which is dominated by QCD processes. The coupling strength factors κ_Q will drive the electroweak pair and single production cross sections, which are therefore sensitive to the overall strength of the coupling, similarly to the single top production processes in the Standard Model. Note that gauge couplings between two vector-like quarks and electroweak gauge bosons should also be present if multiple resonances are considered.

This effective Lagrangian has been implemented in FeynRules [110] for our analysis, and is described in more detail in Appendix B. The complete model, together with the CalcHEP and MadGraph outputs, are available on the FeynRules website for the general model [111] and also for more specific scenarios. See also the website of the HEP model database project [112].

In principle, the rates in the 3 generations may be different, however this is not the case in the simplest cases. The Lagrangian in Eq.(3.2.2) allows to express

the decay rates in a simple and intuitive form:

$$\begin{aligned} BR(T \to W^+ j) &= \zeta_{jet}\,, \qquad & BR(T \to W^+ b) &= \zeta_3 \xi_W^T\,, \\ BR(T \to Zj) &= \zeta_{jet}\xi_Z^T\,, \qquad & BR(T \to Zt) &= \zeta_3 \xi_Z^T\,, \\ BR(T \to Hj) &= \zeta_{jet}\xi_H^T\,, \qquad & BR(T \to Ht) &= \zeta_3 \xi_H^T\,, \end{aligned} \tag{3.2.3}$$

$$\begin{aligned} BR(B \to W^- j) &= \zeta_{jet}\xi_W^B\,, \qquad & BR(B \to W^- t) &= \zeta_3 \xi_W^B\,, \\ BR(B \to Zj) &= \zeta_{jet}\xi_Z^B\,, \qquad & BR(B \to Zb) &= \zeta_3 \xi_Z^B\,, \\ BR(B \to Hj) &= \zeta_{jet}\xi_H^B\,, \qquad & BR(B \to Hb) &= \zeta_3 \xi_H^B\,, \end{aligned} \tag{3.2.4}$$

where $\zeta_{jet} = 1 - \zeta_3$ and $\xi_H^{T/B} = 1 - \xi_W^{T/B} - \xi_Z^{T/B}$, so that the BR of the top and bottom partner only depend on 3 parameters each (ζ_{jet}, $\xi_W^{T/B}$ and $\xi_Z^{T/B}$), which take their values between 0 and 1. For the exotic-charge VL quarks:

$$BR(X \to W^+ j) = \zeta_{jet}\,, \qquad BR(X \to W^+ t) = (1 - \zeta_{jet})\,, \tag{3.2.5}$$

$$BR(Y \to W^- j) = \zeta_{jet}\,, \qquad BR(Y \to W^- b) = (1 - \zeta_{jet})\,, \tag{3.2.6}$$

so that each branching ratio also depends on the single parameter ζ_{jet}. Note that in the formulas above we neglected the top mass, as well as the effect of the coupling originating from the mass mixing between the VL and the SM quarks. Although possibly large model-independent corrections can be expected for the channels $T \to Ht$, $T \to Wb$, Zt, $B \to Wt$ and $X \to Wt$, as evaluated in [109]. The above formulas for the BRs will be used in the following to determine the parameters ζ_i and ξ_V, starting from the physical branching ratios in a specific model containing VL quarks.

3.2.3 Benchmark scenarios from flavour bounds

In all extensions of the Standard Model, the only consistent way to add VL quarks, independently on their number, is to introduce new complete $SU(2)_L$ representations. In the gauge basis, therefore, gauge interactions are diagonal and completely determined by the quantum numbers of the representations.

After the diagonalisation of the mass, mixing matrices will induce off-diagonal couplings in the form of Eq.(A.1.1) - this is a simple generalisation of the origin of the flavour-changing W couplings in the Standard Model. Thus, the physics of the new states can be completely encoded in mixing matrices V_L and V_R describing the mixing between standard and new quarks. The simplest scenario contains a single VL representation [106, 107], and this is the case that we will use as a starting point to study more general scenarios. The case of a new singlet was previously discussed in [113]. The 7 possibilities (2 singlets, 3 doublets and 2 triplets) can be recast in terms of our parametrisation. The branching ratios into the 3 generations can be expressed in terms of the mixing matrices as in (A.1.7), reported here for clarity with the parameters

$$\zeta_i = \frac{|V_{L/R}^{4i}|^2}{\sum_{j=1}^{3} |V_{L/R}^{4j}|^2}\,, \quad \sum_{i=1}^{3} \zeta_i = 1\,; \tag{3.2.7}$$

while the branchings into bosons, denoted by ξ_W, ξ_Z and ξ_H (A.1.8), are determined by the representation. The above quantities are given in Tab. 3.2, where each representation is identified by (n, Y), where n is the dimension of the SU(2) n-plet (2 for a doublet, and so on) and Y is the hypercharge. The simplicity of this parametrisation is based on the fact that only one set of Yukawa couplings generates all the new mixings. For the doublet with standard hypercharge ($Y = 1/6$) the situation is more complex, because there are two possible Yukawa couplings: one involving the up-singlets (λ_u) and one with the down-singlets (λ_d). Therefore, in general, such simple re-parametrisation is not possible. We can use our parametrisation only in 3 simple limits: when one of the two new Yukawas is set to zero or small, or when they are equal. The parametrisations in the 3 cases are listed in Tab. 3.3.

As the 4 parameters κ_Q, $\xi_{W,Z}$ and ζ_j play a crucial role in the phenomenology, it is important to have a handle on the reasonable value they may have. The mixing between the VL quarks and the standard ones is generated by Yukawa-type interactions, therefore such mixing will also modify the diagonalisation of the standard Yukawa matrices and potentially generate tree level flavour-changing couplings to the Z boson. The reason for this is the vector-like nature of the new quarks: either the left-handed or the right-handed chirality (or both)

	T			B		
	ξ_W^T	ξ_Z^T	κ_T/κ	ξ_W^B	ξ_Z^B	κ_B/κ
$(1,2/3)$	$\frac{1}{2}+\frac{\epsilon_H}{4}$	$\frac{1}{4}+\frac{\epsilon_H}{8}$	$\sqrt{2-\epsilon_H}$			
$(1,-1/3)$				$\frac{1}{2}+\frac{\epsilon_H}{4}$	$\frac{1}{4}+\frac{\epsilon_H}{8}$	$\sqrt{2-\epsilon_H}$
$(2,7/6)$	0	$\frac{1}{2}+\frac{\epsilon_H}{2}$	$\sqrt{1-\epsilon_H}$			
$(2,-5/6)$				0	$\frac{1}{2}+\frac{\epsilon_H}{2}$	$\sqrt{1-\epsilon_H}$
$(3,2/3)$	$\frac{1}{2}+\frac{\epsilon_H}{4}$	$\frac{1}{4}+\frac{\epsilon_H}{8}$	$\sqrt{2-\epsilon_H}$	0	$\frac{1}{2}+\frac{\epsilon_H}{2}$	$\sqrt{2-2\epsilon_H}$
$(3,-1/3)$	0	$\frac{1}{2}+\frac{\epsilon_H}{2}$	$\sqrt{1-\epsilon_H}$	$\frac{1}{2}+\frac{\epsilon_H}{4}$	$\frac{1}{4}+\frac{\epsilon_H}{8}$	$\sqrt{1-\frac{\epsilon_H}{2}}$

Table 3.2: Branching ratios into gauge bosons in the case of a single VL representation, where (n,Y) labels a SU(2) n-plet with hypercharge Y. Here we list the results at leading order in $1/M^2$, where $\Gamma^0_W \sim 2\Gamma^0_Z \sim 1$, and $\Gamma^0_H \sim 1/2-\epsilon_H = 1/2-\frac{m_H^2}{M^2}$. The coupling strengths are proportional to $\kappa=\sqrt{\sum_{j=1}^{3}|V^{4j}_{L/R}|^2}$.

of the new states will differ from the Standard Model quark ones. Therefore the presence of Z-mediated FCNC's is inevitable, unless tuned cancellations occur.

The same mechanism that generates the off diagonal couplings responsible for the decays of the VL quarks will also generate flavour changing couplings for the W, Z and Higgs. As mentioned previously, the couplings of the Higgs involve both right and left-handed mixing matrices, however it can be shown that one of the two will be suppressed by the mass of the light quarks, thus in general the flavour changing Higgs couplings are expected to be sufficiently suppressed. The most dangerous ones are the ones involving the Z, because they are absent in the Standard Model at tree level, thus very strong bounds on such couplings derive from flavour observables. As detailed in [108] and [109], the Z couplings for up- and down-like quarks (considering in general n

VL partners ψ_i) can be written in the gauge basis as :

$$g^{gauge}_{Z\bar{q}q} = \frac{g}{c_W}\left(T_3^{sm} - Qs_W^2\right)\delta^{ij} + \frac{g}{2c_W}\begin{pmatrix} 0 & & & & & & \\ & 0 & & & & & \\ & & 0 & & & & \\ & & & 2(T_3^{\psi_1} - T_3^{sm}) & & & \\ & & & & \ddots & & \\ & & & & & 2(T_3^{\psi_n} - T_3^{sm}) \end{pmatrix}. \tag{3.2.8}$$

The first term, proportional to the identity matrix, is the coupling of the standard quark (up or down type, $T_3^{sm} = \pm 1/2$ or 0). From this equation it is clear that the non-standard couplings are due to the weak isospin of the VL quarks, which must be different from the standard ones at least for one chirality. Once going to the mass eigenstate basis via the unitary matrices $V_{L/R}$, the first terms stay untouched, while the second term, sensitive to the difference in isospin, will generate off-diagonal couplings:

$$g^{mass}_{Z\bar{q}q} = \frac{g}{c_W}\left(T_3^{sm} - Qs_W^2\right)\delta^{ij} + \frac{g}{2c_W}\left(\sum_{k=4}^{n} 2(T_3^{\psi_k} - T_3^{sm}) V^{*,ki}_{L/R} V^{kj}_{L/R}\right). \tag{3.2.9}$$

In the case of a single VL representation, one can easily be convinced that the couplings with the largest mixing matrices (the other being suppressed by the mass of the standard quarks) has $2(T_3^{\psi_k} - T_3^{sm}) = \pm 1$. For instance, for singlets ($T_3^{\psi} = 0$), the large mixing takes place in the left-handed sector, where the standard quarks have isospin $\pm 1/2$. Using our previous re-parametrisation in terms of branching ratios, the couplings of the Z to the standard quarks can be rewritten as (ignoring phases)

$$\left(g^{sm}_{Z\bar{q}q}\right)_{ij} = \frac{g}{c_W}\left(T_3^{sm} - Qs_W^2\right)\delta^{ij} \pm \frac{g}{2c_W}\left(\kappa^2\sqrt{\zeta_i\zeta_j}\right), \tag{3.2.10}$$

$(2,1/6)$	T			B		
	ξ_W^T	ξ_Z^T	κ_T/κ	ξ_W^B	ξ_Z^B	κ_B/κ
$\lambda_d = 0$	0	$\frac{1}{2}+\frac{\epsilon_H}{2}$	$\sqrt{1-\epsilon_H}$	1	0	1
$\lambda_u = 0$	1	0	1	0	$\frac{1}{2}+\frac{\epsilon_H}{2}$	$\sqrt{1-\epsilon_H}$
$\lambda_u = \lambda_d$	$\frac{1}{2}+\frac{\epsilon_H}{4}$	$\frac{1}{4}+\frac{\epsilon_H}{8}$	$\sqrt{2-\epsilon_H}$	$\frac{1}{2}+\frac{\epsilon_H}{4}$	$\frac{1}{4}+\frac{\epsilon_H}{8}$	$\sqrt{2-\epsilon_H}$

Table 3.3: Branching ratios into gauge bosons for a doublet with standard hypercharge, in three limits: when one of the two Yukawa couplings is zero, or when they are equal.

with $i,j = 1,2,3$. The off-diagonal terms can therefore pose a bound on the product of two $\kappa\sqrt{\zeta_i}$ terms. As the Z is much heavier that any mesons, we can parametrise the bounds in terms of effective 4-fermion operators after integrating out the Z:

$$\frac{g^2\kappa^4}{4m_W^2}\sqrt{\zeta_{i1}\zeta_{i2}\zeta_{j1}\zeta_{j2}}\,(\bar{q}_{i1}\gamma_\mu q_{i2})\,(\bar{q'}_{j1}\gamma^\mu q'_{j2})\,, \tag{3.2.11}$$

where q and q' are up or down type quarks of the same chirality. To estimate the bounds from flavour, these expressions can be compared to the bounds in [114], which involve $\Delta F = 2$ operators in the left-handed sector (similar bounds apply to the right-handed operators):

$$\begin{aligned}
(\bar{s}_L\gamma^\mu d_L)^2 &: |c| < 9.0\cdot 10^{-7} \Rightarrow \kappa^4\zeta_1\zeta_2 < 5.5\cdot 10^{-8} \quad (\kappa < 0.015/(\zeta_1\zeta_2)^{1/4})\,,\\
(\bar{b}_L\gamma^\mu d_L)^2 &: |c| < 3.3\cdot 10^{-6} \Rightarrow \kappa^4\zeta_1\zeta_3 < 2.0\cdot 10^{-7} \quad (\kappa < 0.02/(\zeta_1\zeta_3)^{1/4})\,,\\
(\bar{b}_L\gamma^\mu s_L)^2 &: |c| < 7.6\cdot 10^{-5} \Rightarrow \kappa^4\zeta_1\zeta_2 < 4.6\cdot 10^{-6} \quad (\kappa < 0.045/(\zeta_2\zeta_3)^{1/4})\,,\\
(\bar{c}_L\gamma^\mu u_L)^2 &: |c| < 5.6\cdot 10^{-7} \Rightarrow \kappa^4\zeta_1\zeta_2 < 3.4\cdot 10^{-8} \quad (\kappa < 0.014/(\zeta_1\zeta_2)^{1/4})\,.
\end{aligned} \tag{3.2.12}$$

Here, the bounds on the coefficient $|c|$ assume a scale of 1 TeV, furthermore we only considered the bounds on the real parts as bounds on the imaginary parts of the coefficient are much stronger and would mainly affect the phases of the mixing matrices (that we ignored in our parametrisation).

While they are not discussed here, the possible contributions to $\Delta F = 1$ observables have been considered in previous works for specific models with a single VL quark representation. For instance, the impact of a T singlet on the rare decays of K, B and B_s mesons has been computed in [115] and [116] for $\zeta_3 = 1$, calling for corrections to the associated branching ratios in the range 20%-50%. Similarly, FCNC decays of D mesons have been considered in [108] for the exotic doublet (X, T), the $\Delta C = 1$ process $D^0 \to l^+ l^-$ leading to $\kappa^2(\zeta_1\zeta_2)^{1/2} < 3.2 \times 10^{-4}$. But while large effects in the rare decays amplitudes could be allowed due to the presence of new complex phases, the current experimental constraints in the $\Delta F = 1$ sector are generally known to be weaker than the above bounds (see, e.g., [117]).

From the expressions in (3.2.12), we can learn two things: the $\Delta F = 2$ flavour bounds only apply to the product of the coupling to two generations, therefore the bounds can be evaded by coupling the VL quarks mainly to one generation. Furthermore, in the down-sector, there are strong bounds on all three combinations, therefore we can conclude that in the presence of a VL down partner (B and Y), the coupling with a single generation is preferred. For the up-sector, there are no bounds involving the third generation, therefore one can evade bounds by allowing sizeable couplings with the top and one of the two light generations: this applies to all representations that do not contain a B partners (i.e., only T and X vector-like quarks). The coupling strength κ does not receive constraining bounds in this case: strong bounds are obtained if sizeable mixing with two generations are attained. In the case of maximal mixing (i.e. $\zeta_i = \zeta_j = 1/2$), the bounds range $\kappa < 0.02 \div 0.06$.

Considering other possible constraints, the mixing with the VL quarks also affects the diagonal couplings of the Z to the standard quarks. The corresponding corrections are of the order

$$\delta g_{Z\bar{q}_i q_i} = \pm \frac{g}{2c_W} \kappa^2 \zeta_i \,. \tag{3.2.13}$$

The couplings of the Z to light quarks have been precisely measured at LEP [118] and other low energy experiments, and they are proportional to the branching ratio to the given generation. This implies that these bounds allow to extract an absolute bound on the coupling strength κ. This story is true for all quarks, except for the top whose couplings to the Z are not known. In this case, therefore,

the only bound comes from loop corrections (mainly the T parameter) and corrections to the W coupling to the bottom, that mediates its decays. To extract bounds on the parameters κ and ζ_i, we take a very conservative approach: we assume that only one coupling is affected and compare the correction $\delta g_{Z\bar{q}_i q_i}$ to the error on the measurement, assuming therefore that the central value of the measurement agrees with the Standard Model prediction [2]. The bounds on κ from modifications of the Z couplings are listed below:

$$\begin{aligned}
Z\bar{u}u\,(APV) &\Rightarrow |\delta g_{L/R}| < 3\times 0.00069 \to \kappa < 0.074/\sqrt{\zeta_1}\,,\\
Z\bar{d}d\,(APV) &\Rightarrow |\delta g_{L/R}| < 3\times 0.00062 \to \kappa < 0.07/\sqrt{\zeta_1}\,,\\
Z\bar{s}s\,(LEP) &\Rightarrow \begin{array}{l} |\delta g_L| < 3\times 0.012 \to \kappa < 0.3/\sqrt{\zeta_2}\,,\\ |\delta g_R| < 3\times 0.05 \to \kappa < 0.6/\sqrt{\zeta_2}\,,\end{array}\\
Z\bar{c}c\,(LEP) &\Rightarrow \begin{array}{l} |\delta g_L| < 3\times 0.0036 \to \kappa < 0.17/\sqrt{\zeta_2}\,,\\ |\delta g_R| < 3\times 0.0051 \to \kappa < 0.20/\sqrt{\zeta_2}\,,\end{array}\\
Z\bar{b}b\,(LEP) &\Rightarrow \begin{array}{l} |\delta g_L| < 3\times 0.0015 \to \kappa < 0.11/\sqrt{\zeta_3}\,,\\ |\delta g_R| < 3\times 0.0063 \to \kappa < 0.23/\sqrt{\zeta_3}\,,\end{array}\\
Z\bar{t}t\,(T,\ \delta g_{Wtb}) &\Rightarrow \kappa < 0.1 \div 0.3/\sqrt{\zeta_3}\,.
\end{aligned} \tag{3.2.14}$$

The best bounds on the first generation couplings are coming from the measurement of the weak charge of the Cesium atom (Atomic Parity Violation) [119], while the others are determined from the LEP measurements of the hadronic cross sections and asymmetries. The bound in formula (3.2.14) is obtained from the electroweak precision tests as in [107]. The flavour diagonal bounds on κ are about one order of magnitude milder than the flavour violating ones.

From this simple analysis, we can derive a set of benchmark models than can be used to reduce the number of parameters in the first studies:

- in the presence of a bottom partner (B and Y), only the coupling to one family is allowed to be large: we therefore have 3 benchmark models with $\zeta_1 = 1$ ($\kappa \lesssim 0.07$), $\zeta_2 = 1$ ($\kappa \lesssim 0.2$) and $\zeta_3 = 1$ ($\kappa \lesssim 0.3$);

[2] A more detailed analysis would require a complete fit of the electroweak precision measurements, which depends on the details of the underlying model, and thus goes beyond the scope of our work.

- in the absence of a bottom partner (thus only T and X), one can allow for couplings to two generations: $\zeta_2 = 0$ ($\kappa \lesssim 0.1$) and $\zeta_1 = 0$ ($\kappa \lesssim 0.3$).

A scenario with significant couplings to all three generations is also allowed, however with an extra order of magnitude suppression on κ: in this case, single production will yield very small cross sections, and its relevance postponed to higher mass values. Note also that the bounds on the couplings have been extracted in a specific scenario (a single light VL representation), while the bounds may be weakened in more involved models, therefore they should only be considered as guiding points without limiting the validity of the parametrisation to more general scenarios.

3.3 Production processes

The production cross sections of VL quarks can be grouped in four classes:

- *pair production*: this class is largely dominated by QCD production, which is model independent and only depends on the mass of the new fermion;
- *single production in association with tops*;
- *single production in association with jets (where jet denotes any light quark)*;
- *single production in association with a boson*: including $W^{\pm}$, Z and the Higgs H.

The guiding thread of the model-independent approach taken in this work will be the following: to write the production cross sections explicitly in terms of model-independent cross sections, themselves multiplied by the parameters that also enter the branching ratios. This approach is similar to the one proposed in [120]. In this way, one can study all models at once by computing the efficiencies of each search in various channels, and given a model, correlate observations in various channels. In the following we discuss the 4 production

	$\bar{Q}Q$ (QCD)	$\bar{Q}Q'$ (W^+)	$\bar{Q}Q'$ (W^-)
$M = 600$ GeV	109(167)	3.95	1.12
$M = 800$ GeV	14.3(20.5)	0.646	0.165
$M = 1000$ GeV	2.37(3.24)	0.119	0.0285

Table 3.4: Pair production cross sections (in fb) at 8 TeV for processes dominated by QCD, and for s-channel W exchange (for a doublet). The values have been computed at LO with MadGraph, while the values in brackets are NLO+NNLL results from [121] with the MSTW2008 PDF set

mechanisms separately. All the inclusive single production cross sections will be reported in the next sections, while the corresponding model-independent expansion coefficients can be found in Appendix B.

3.3.1 Pair production

Pair production is dominated by QCD production via gluons:

$$\bar{q}q, gg \to \bar{Q}Q\,. \tag{3.3.15}$$

The cross section is model independent as it only depends on the mass of the VL quark, and it decreases quickly for higher masses due to PDF suppression, as shown in Tab. 3.4. There are also contributions from electroweak gauge bosons, which are sub-leading in terms of cross section. Production via neutral currents (Z and γ) have the same final states as QCD production, thus they are completely negligible.

Production via a W boson, on the other hand, can give rise to potentially interesting channels like:

$$\bar{q}q' \;\to\; W^+ \to \bar{T}X, \bar{B}T, \bar{Y}B \tag{3.3.16}$$

$$\bar{q}q' \;\to\; W^- \to \bar{X}T, \bar{T}B, \bar{B}Y \tag{3.3.17}$$

Such cross sections are however model-dependent, as they depend on the representation the VL quarks belong to. Another potentially relevant production process is represented by the production of a pair of VL quarks QQ', mediated by a W, Z or Higgs in the t-channel. This process is completely absent in QCD and, depending on subsequent decays, it can give rise to final states with peculiar kinematics or same-sign dileptons. It must be stressed however that this channel is proportional to κ_Q^4, because it requires both couplings of the gauge boson to be from Eq.(3.2.2), therefore rates are expected to be fairly small in realistic scenarios due to flavour bounds. While they are not discussed in the following, more details on the electroweak pair production modes can be found in [109].

3.3.2 Single production with tops and with jets

These final states can be obtained, at Leading Order (LO), by the exchange in t or s-channel of a W and/or a Z boson(s), due to the presence of the couplings ξ_W and/or ξ_Z in the Lagrangian in Eq.(3.2.2). Contributions of the Higgs will always be suppressed by the small masses of the light quarks. The corresponding cross sections can be expanded as in terms where we factor out powers of the parameters of our Lagrangian, the ζ_i and ξ_V (and an overall factor κ_Q^2), with coefficients that are model independent as they only depend on the mass of the VL quark via the kinematics. Here we will neglect contributions that are suppressed by extra factors of κ_Q, thus we cut the expansion to the leading κ_Q^2 terms. The cross sections for processes with a single top and a single VL

quark in the final state read:

$$\begin{aligned}
\sigma(T\bar{t}+\bar{T}t) &= \kappa_T^2\left(\xi_Z\zeta_3\,(\bar{\sigma}_{Z3}^{T\bar{t}}+\bar{\sigma}_{Z3}^{\bar{T}t})+\xi_W\sum_{i=1}^{3}\zeta_i\,(\bar{\sigma}_{Wi}^{T\bar{t}}+\bar{\sigma}_{Wi}^{\bar{T}t})\right),\\
\sigma(Bt+\bar{B}\bar{t}) &= \kappa_B^2\left(\xi_W\sum_{i=1}^{2}\zeta_i\,(\bar{\sigma}_{Wi}^{Bt}+\bar{\sigma}_{Wi}^{\bar{B}\bar{t}})\right),\\
\sigma(B\bar{t}+\bar{B}t) &= \kappa_B^2\left(\xi_W\zeta_3\,(\bar{\sigma}_{W3}^{B\bar{t}}+\bar{\sigma}_{W3}^{\bar{B}t})\right),\\
\sigma(X\bar{t}+\bar{X}t) &= \kappa_X^2\left(\xi_W\sum_{i=1}^{2}\zeta_i\,(\bar{\sigma}_{i}^{X\bar{t}}+\bar{\sigma}_{i}^{\bar{X}t})\right),\\
\sigma(Yt+\bar{Y}\bar{t}) &= \kappa_Y^2\left(\xi_W\sum_{i=1}^{3}\zeta_i\,(\bar{\sigma}_{i}^{Yt}+\bar{\sigma}_{i}^{\bar{Y}\bar{t}})\right). \qquad (3.3.18)
\end{aligned}$$

A similar expansion can be obtained for production in association with light jets (including the b):

$$\sigma(Qj+\bar{Q}j)=\kappa_Q^2\left(\xi_W\sum_{i=1}^{3}\zeta_i\,(\bar{\sigma}_{Wi}^{Qjet}+\bar{\sigma}_{Wi}^{\bar{Q}jet})+\xi_Z\sum_{i=1}^{3}\zeta_i\,(\bar{\sigma}_{Zi}^{Qjet}+\bar{\sigma}_{Zi}^{\bar{Q}jet})\right), \qquad (3.3.19)$$

where the numerical results for the coefficients $\bar{\sigma}$ are listed in Tab. 3.6. Generically, the production cross section with jets are much larger than with a top,

	$\bar{\sigma}_{Zi}^{T\bar{t}+\bar{T}t}$	$\bar{\sigma}_{Wi}^{T\bar{t}+\bar{T}t}$	$\bar{\sigma}_{Wi}^{B\bar{t}+\bar{B}t}$	$\bar{\sigma}_{Wi}^{Bt+\bar{B}\bar{t}}$	$\bar{\sigma}_{Wi}^{X\bar{t}+\bar{X}t}$	$\bar{\sigma}_{Wi}^{Yt+\bar{Y}\bar{t}}$
$\zeta_1=1$	-	1690	-	3791	3730	1760
$\zeta_2=1$	-	247	-	129	127	256
$\zeta_3=1$	12.6	78.2	12.4	-	13.5	85.3

Table 3.5: Coefficients for single production cross sections (in fb) in association with a top (and antitop) at 8 TeV for $M=600$ GeV. The values have been computed at LO with MadGraph.

and particularly large numbers are obtained for couplings to the first generation of quarks due to the valence quark enhancement. However, the bounds on κ_Q crucially depend on which generation the VL quark couples to, so this observation is not enough to quantify how large the single production can actually be. We will come back to this point at the end of this section.

We highlight that in these formulae we neglect the interference between W and Z exchange: in fact, we have verified numerically that they are small, the main reason being that interference is present only for a limited number of diagrams and between an s- and t-channel exchange. Quantitatively, the interference terms are always below the percent level, therefore the approximation is very accurate and allows for a great simplification of the formulae.

Relying on our FeynRules implementation of Eq.(3.2.2), we computed the coefficients in the above expansions: as an example, in Tab. 3.5, we list the results for a reference mass of $M = 600$ GeV and at a 8 TeV LHC. In the calculation, we use a 5F scheme (including the b quark in the PDFs) and use the CTEQ6L1 PDF set [122]. Tables of LO coefficients for different masses can be found at the end of Appendix B.

As an important comment, we point out that the above expansions are also valid once QCD corrections are included, and the effect can be completely included in the model-independent $\bar{\sigma}$ coefficients. The missing terms in the expansion, in fact, are not generated at any order in α_s. The inclusion of electroweak corrections is another story: in fact, even at leading order in κ_Q^2, terms that depend on the representation of the VL quark will be generated

	$\bar{\sigma}_{Zi}^{Tj+\bar{T}j}$	$\bar{\sigma}_{Wi}^{Tj+\bar{T}j}$	$\bar{\sigma}_{Zi}^{Bj+\bar{B}j}$	$\bar{\sigma}_{Wi}^{Bj+\bar{B}j}$	$\bar{\sigma}_{Wi}^{Xj+\bar{X}j}$	$\bar{\sigma}_{Wi}^{Yj+\bar{Y}j}$
$\zeta_1 = 1$	69200	51500	38100	62600	98600	37700
$\zeta_2 = 1$	5380	10700	8880	6350	6490	10440
$\zeta_3 = 1$	-	4230	3490	-	-	4110

Table 3.6: Coefficients for single production cross sections (in fb) in association with a light jet at 8 TeV for $M = 600$ GeV. The values have been computed at LO with MadGraph.

and furthermore the expansion in ζ_i and ξ_V will be affected. Such corrections are expected to be small, certainly much smaller that the QCD ones. These considerations apply to all the single production mechanisms here discussed. In the present work, we will limit ourselves to compute LO cross sections, even though NLO corrections in α_s may be relevant. One may be tempted to re-scale the NLO corrections from single top channels [123] to higher masses of the top quark, however this procedure is not justified here due to the presence of diagrams absent in the top case (for instance, processes mediated by the Z boson). As a complete NLO calculation is mandatory for the extraction of reliable numbers, we leave it for further investigation.

3.3.3 Single production with bosons (W, Z and H)

Here it is important to notice the presence of channels which are specific to VL quarks: single production in association with Z or H requires the presence of FCNC, absent in fourth chiral generation extensions. Such processes, at LO, are initiated by a gluon-quark fusion. The relevant cross sections can be

	$\bar{\sigma}_i^{TZ+\bar{T}Z}$	$\bar{\sigma}_i^{TH+\bar{T}H}$	$\bar{\sigma}_i^{TW+\bar{T}W}$	$\bar{\sigma}_i^{BZ+\bar{B}Z}$	$\bar{\sigma}_i^{BH+\bar{B}H}$	$\bar{\sigma}_i^{BW+\bar{B}W}$
$\zeta_1 = 1$	5480	3610	2430	2510	1820	5320
$\zeta_2 = 1$	202	133	374	386	267	196
$\zeta_3 = 1$	-	-	122	125	84.8	-

Table 3.7: Coefficients for single production cross sections (in fb) with a boson at 8 TeV for $M = 600$ GeV. The values have been computed at LO with MadGraph. The coefficients for $\bar{\sigma}_i^{XW+\bar{X}W}$ and $\bar{\sigma}_i^{YW+\bar{Y}W}$ are identical to those of $\bar{\sigma}_i^{BW+\bar{B}W}$ and $\bar{\sigma}_i^{TW+\bar{T}W}$, respectively.

written as:

$$\begin{aligned}
\sigma(QW^{\pm}+\bar{Q}W^{\mp}) &= \kappa_Q^2\left(\xi_W\sum_{i=1}^{3}\zeta_i\,(\bar{\sigma}_i^{QW}+\bar{\sigma}_i^{\bar{Q}W})\right), \\
\sigma(QZ+\bar{Q}Z) &= \kappa_Q^2\left(\xi_Z\sum_{i=1}^{3}\zeta_i\,(\bar{\sigma}_i^{QZ}+\bar{\sigma}_i^{\bar{Q}Z})\right), \\
\sigma(QH+\bar{Q}H) &= \kappa_Q^2\left(\xi_H\sum_{i=1}^{3}\zeta_i\,(\bar{\sigma}_i^{QH}+\bar{\sigma}_i^{\bar{Q}H})\right). \qquad (3.3.20)
\end{aligned}$$

The above expressions are general, and extendible to NLO in α_s. For $X_{5/3}$ and $Y_{-4/3}$ the production modes in association with Z or H are not present due to the absence of neutral currents. The relevant coefficients in the expansion can be found in Tab. 3.7 at LO. We highlight that the expressions (3.3.19), (3.3.18) and (3.3.20) should be complemented with the interference between W- and Z- mediated diagrams. The corresponding contributions, which are proportional to $\sqrt{\zeta_i\zeta_j}\,\sqrt{\xi_W\xi_Z}$, have been checked numerically to always be negligible with respect to the aforementioned coefficients. Finally, we comment that new non-zero complex phases resulting from the extension of the CKM mixing matrix might also affect this picture. Indeed, the definition (3.2.7) is not exhaustive as it carries no information on the phases, whereas the parameters $V_{L/R}^{4i}$ are imaginary quantities in general. This possibility goes beyond the scope of our analysis, and will be neglected in the following.

3.4 Single production in flavour-motivated benchmark models

In section 3.2.3, we used the simplified model with a single VL representation and bounds from flavour and electroweak precision physics to define a few benchmark points that allow to maximise the couplings in this minimal scenario. Such benchmark models can be used to have a realistic estimate of the single production cross sections. In the presence of a bottom partner B or Y, flavour constraints tend to prefer a sizeable coupling with a single generation, while generic couplings to the three generations would require significantly

stronger bounds on the overall couplings. For models without a bottom partner, on the other hand, sizeable couplings to two generations, one of which is the third, are allowed.

In Tab. 3.8 we listed the inclusive single VL quark production cross sections, computed starting from the values in Tabs. 3.5, 3.6 and 3.7. While the precise numbers are just indicative, they can be used to deduce some general properties of the VL quarks. In fact, from the second column, one can see that the case of sizeable couplings to all generation gives rise to smallish cross sections, amounting to a few fb at most, due to the strong suppression from flavour bounds. In such a case, therefore, the searches should focus on pair production. On the other hand, if exclusive coupling to a single generation is assumed, the cross sections grow to a few hundreds fb.

Interestingly, the values of the inclusive single production cross sections are close independently of which generation they couple to: in most cases, the suppression due to PDF effects is compensated by a weaker flavour bound on the couplings. There are exceptions in some cases for couplings to the third generation, mainly driven by the absence of couplings to the W boson: in fact, couplings of the Z to third generation leads to small cross sections as a top is always present in the final state. Models with sizeable couplings to the third generation and only one of the two light ones are only allowed for models without B and Y partners, i.e. the singlet $(1, 2/3)$ and doublet $(2, 7/6)$, and in the case of a standard doublet $(2, 1/6)$ when the mixing in the down sector is set to zero ($\lambda_d = 0$). In all cases, large cross sections are obtained.

We emphasise the relevance of the contribution of the channels of production in association with light quarks to the total cross section: when allowed, it always contributes to around 90% of the cross section. In Tab. 3.9 we show in more detail the contributions of all channels for a choice of some specific scenarios.

The benchmark points defined in Tab. 3.8 can be used to investigate the sensitivity of current searches at the LHC. To date, there is only one search for single production of vector-like quarks, and it has been performed by ATLAS

		Benchmark 1 $\kappa = 0.02$ $\zeta_1 = \zeta_2 = 1/3$	Benchmark 2 $\kappa = 0.07$ $\zeta_1 = 1$	Benchmark 3 $\kappa = 0.2$ $\zeta_2 = 1$	Benchmark 4 $\kappa = 0.3$ $\zeta_3 = 1$	Benchmark 5 $\kappa = 0.1$ $\zeta_1 = \zeta_3 = 1/2$	Benchmark 6 $\kappa = 0.3$ $\zeta_2 = \zeta_3 = 1/2$
$(1, 2/3)$	T	15 (91%)	464 (91%)	564 (94%)	399 (95%)	495 (91%)	834 (95%)
$(1, -1/3)$	B	14 (89%)	455 (88%)	457 (94%)	167 (94%)	-	-
$(2, 1/6)$	T	5.6 (89%)	191 (88%)	114 (94%)	0.6 (0%)	195 (88%)	128 (94%)
$\lambda_d = 0$	B	10 (88%)	351 (87%)	267 (95%)	1.1 (0%)	358 (87%)	301 (95%)
$(2, 1/6)$	T	9.5 (93%)	272 (93%)	451 (94%)	398 (95%)	-	-
$\lambda_u = 0$	B	3.7 (90%)	103 (90%)	190 (93%)	166 (94%)	-	-
$(2, 1/6)$	T	15 (91%)	464 (91%)	564 (94%)	399 (95%)	-	-
$\lambda_d = \lambda_u$	B	14 (89%)	455 (88%)	457 (94%)	167 (94%)	-	-
$(2, 7/6)$	X	15 (92%)	528 (92%)	272 (95%)	1.2 (0%)	538 (91%)	307 (95%)
	T	5.6 (88%)	191 (88%)	114 (94%)	0.6 (0%)	195 (88%)	128 (94%)
$(2, -5/6)$	B	3.7 (91%)	103 (90%)	190 (93%)	166 (94%)	-	-
	Y	7.6 (91%)	205 (90%)	443 (94%)	388 (95%)	-	-
$(3, 2/3)$	X	30.5 (92%)	1055 (92%)	545 (95%)	2.4 (0%)	-	-
	T	15 (91%)	464 (91%)	564 (94%)	399 (95%)	-	-
	B	7.4 (91%)	207 (90%)	380 (93%)	332 (94%)	-	-
$(3, -1/3)$	T	5.6 (89%)	191 (88%)	114 (94%)	0.6 (0%)	-	-
	B	7.1 (89%)	227 (88%)	228 (94%)	84 (94%)	-	-
	Y	7.6 (91%)	205 (90%)	443 (94%)	388 (95%)	-	-

Table 3.8: Inclusive single production cross sections (in fb) for a single VL multiplet in various benchmark points at 8 TeV and for $M = 600$ GeV. Within brackets, the relative contribution of the processes of production in association with light quarks.

	$\kappa = 0.02$ $\zeta_{1,2} = 1/3$	$\kappa = 0.07$ $\zeta_1 = 1$	$\kappa = 0.2$ $\zeta_2 = 1$	$\kappa = 0.3$ $\zeta_3 = 1$	$\kappa = 0.1$ $\zeta_{1,3} = 1/2$	$\kappa = 0.3$ $\zeta_{2,3} = 1/2$
σ_{Tq}	13.8	422	533	380	451	790
$\sigma_{T\bar{t}}$	0.3	8	10	8	9	15
σ_{TW^-}	0.4	12	15	11	13	22
σ_{TZ}	0.4	13	4	0	13	4
σ_{TH}	0.2	9	2	0	9	3
Total	15	464	564	399	495	834

Table 3.9: Contribution of different channels to the total cross sections (in fb) for a T singlet at 8 TeV for $M = 600$ GeV.

	600 GeV	800 GeV	1000 GeV
$(1, 2/3)$ $\kappa = 0.02 \quad \zeta_1 = \zeta_2 = 1/3$	15	7.3	3.8
$(1, 2/3)$ $\kappa = 0.3 \quad \zeta_2 = \zeta_3 = 1/2$	834	324	138

Table 3.10: Inclusive single production cross sections (in fb) for a T singlet mixing with all generations or mixing mostly with second and third generation and at 8 TeV, for 3 values of the VL mass.

under the hypothesis of mixing only with light generations [124]: in Fig. 3.1 we compare the upper bound on the coupling strength κ obtained considering the final state investigated by ATLAS in the neutral and charged current channels with the bound coming from flavour physics observables. In order to maximise the performance of the ATLAS search we have considered the second benchmark, in which the VLQ is coupled only to the first generation. The signal in the two channels has been obtained considering all the particles in the multiplet that can contribute to the final state (e.g., in the non-SM doublet $(X\ T)$ case, the CC channel receives a contribution only from the X, while the NC channel receives only the contribution of the T). The compar-

ison shows that, in the range of masses considered, the bounds coming from flavour physics are usually stronger than those coming from the direct search undertaken by ATLAS and that the only representation for which the ATLAS bound is competitive with flavour bounds is the triplet $(X\ T\ B)$. The ATLAS analysis considers also a channel where a negative lepton is required in the final state: including this channel we obtain stronger bounds for representations that contain a B or Y quark, however the limits from this channel are never competitive with the flavour bounds (again, in the range of masses considered), and therefore they have not been included in the plots.

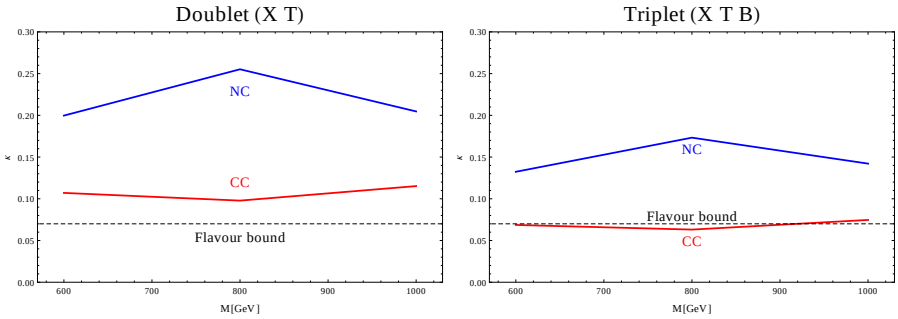

Figure 3.1: Comparison of the upper bounds on the coupling strength coming from ATLAS search in single production [124] and from flavour observables considering Benchmark 2 ($\kappa = 0.07$ and $\zeta_1 = 1$). The bound from ATLAS is competitive with the bound from flavour physics only for the triplet $(X\ T\ B)$ representation.

Finally, in Tab. 3.10 we show how the cross sections scale with the mass of the VL quark: we choose a representative case for illustration purposes. We can see here that the cross sections decrease with the mass slower than the pair production ones in Tab. 3.4, so that their relevance will be increased when higher mass regions are explored at the LHC.

3.5 Analysis of numerical results

The analysis presented in this Chapter allows us to highlight important conclusions that can be useful to drive searches of VL quark production in a model-independent fashion. Our main messages are the following:

- *Relevance of single production*: new vector-like top partners can have sizeable production rates regardless of their mixing structure with first, second or third generation quarks without conflicting with current experimental constraints. This is due to a compensation between suppression coming from PDFs and from flavour observables, as shown in Tab. 3.8. Processes like, for instance, production with a light jet followed by decays into third generation should therefore be considered.

- *Exclusive mixing hypotheses*: assuming exclusive (100%) branching ratios may forbid some single production channels. In the case of exclusive mixing with third generation, the channels Xj, XW, TZ, TH and BW are systematically forbidden. Therefore, considering a scenario with T mixing only with third generation, the Higgs and Z bosons may only appear in the T decay products. Analogous conclusion can be derived for the presence of a W boson in scenarios with B or X partners, coupling only to third generation. Furthermore, Bt and Bj (Tj) production are not allowed in the latter case if $\xi_W = 1$ ($\xi_Z = 1$), whereas $pp \to TH, TZ, BW, XW$ can only arise in scenarios where the VLQ mixes with either the first or second generation. The complete list of forbidden channels under different assumptions on mixings is in Tab. 3.11.

- *Associated production with top quarks*: VL quark single production in association with a top (antitop) quark provides a very interesting final state for the forthcoming searches. As shown in Tab.3.9, $pp \to Qt$ is worth exploring even in scenarios where the VL quark does not mix exclusively with the third family, due to the PDF enhancement in production.

	$\zeta_{1,2} = 1$	$\zeta_3 = 1$
$\xi_W = 1$	TZ, TH $B\bar{t}, BZ, BH$	Xj, XW TZ, TH $Bj, B\bar{t}, BW, BZ, BH$
$\xi_Z = 1$	$T\bar{t}, TW, TH$ $Bt, B\bar{t}, BW, BH$	Tj, TW, TZ, TH $Bt, B\bar{t}, BW, BH$
$\xi_H = 1$	all channels but TH all channels but BH	all channels all channels but BH

Table 3.11: Forbidden channels for single production under hypothesis of exclusive (100%) mixing patterns.

- *Distributions:* for $\zeta_{1,2} = 1$, the transverse momentum p_T and rapidity η distributions for inclusive T and B production, distinguishing amplitudes from W and Z exchanges, are hardly distinguishable at the level of production, as can be seen in Fig. 3.2, where distributions related to T have been considered for illustrative purpose. We can therefore infer that the production does not distinguish between couplings to first and second generation (while the value of the cross sections does depend on this), so that at the level of generation one can consider either one of them.

3.6 Summary

In this chapter we have developed a model-independent parametrisation that can be used to describe the phenomenology of pair- and singly-produced vector-like quarks with generic hypotheses about their mixing with SM quarks. The framework relies on a limited number of parameters which represent all possible mixings with SM quarks and couplings with SM bosons. The parametrisation is implemented in a publicly available FeynRules model [111], and has been adopted to perform an analysis of processes of production of vector-like

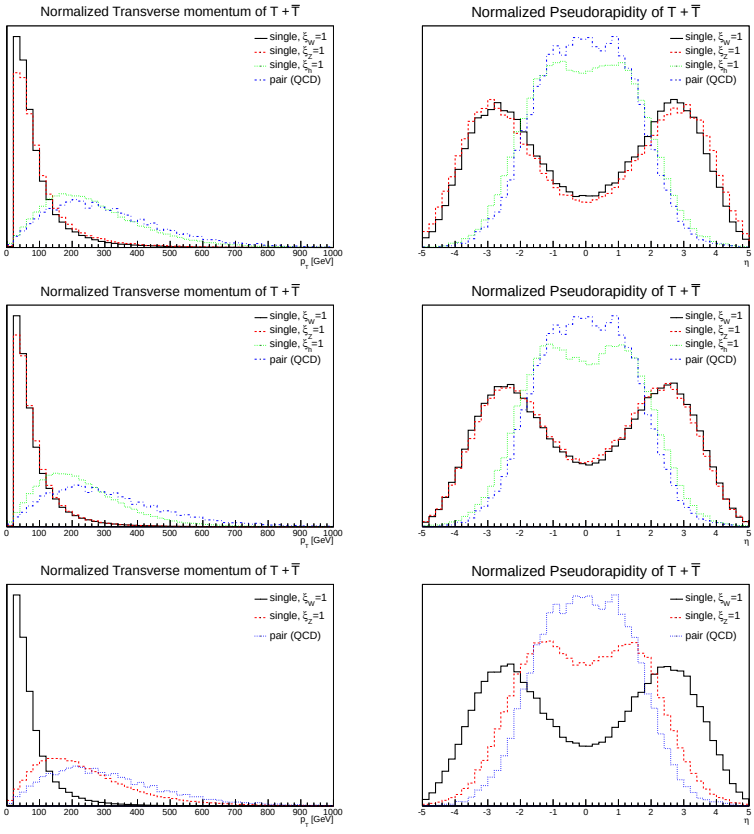

Figure 3.2: Normalised transverse momentum and pseudorapidity distributions for inclusive single production of T compared to QCD pair production with, from top to bottom, $\zeta_1 = 1$, $\zeta_2 = 1$, $\zeta_3 = 1$.

quarks: pair production, single production with tops, single production with jets and single production with a W, Z or H boson. The main result of the present analysis is to provide a theoretically consistent and general framework, where the various searches for VL or fourth generation quarks can be embedded in. In particular, our framework allows for a simple correlation of the branching ratios with the single production channels. We also provided a LO calculation of all the relevant single production cross sections, via model independent coefficients. All corresponding results for the VLQ species discussed in this work can be found in Tabs. B.1-B.6 in Appendix B.

To provide a concrete application of the parametrisation, we have applied this technique to obtain the production cross sections for some benchmark points which satisfy experimental constraints from flavour physics and other observables. In particular, we showed that:

- single production followed by decays to third generation should be considered, as the production rates are similar to the ones obtained through couplings to the first generation;
- single production with tops is relevant also in the case of decays into light generations;
- depending on the hypothesis on the branching ratios, some single production channels are forbidden, at leading order in the electroweak couplings.

A measure of the coupling is indeed essential to determine the nature of the VL quarks and, maybe, have a glimpse on the origin of the standard generations. The parametrisation proposed in this work can also be used for a systematic study of the flavour bounds on the mixing to light and heavy generations. This step is crucial in order to have an independent estimate of the maximum allowed couplings, and therefore the impact of single production to the future search strategies.

Our analysis, even if limited to production level, allows to highlight the potential relevance of scenarios which have been neglected in previous experimental searches, such as mixing only with second generation or presence of tops in

the final state in scenarios where the vector-like quark does not mix with third generation at all. These points deserve special attention as they may be the key to obtain hints of these vector-like states in realistic flavour mixing scenarios which go beyond the naïve expectations based on simplified single generation mixing.

Chapter 4

Analysis of Scenarios with Multiple Heavy Quarks

"At the heart of science is an essential balance between two seemingly contradictory attitudes–an openness to new ideas, no matter how bizarre or counterintuitive they may be, and the most ruthless skeptical scrutiny of all ideas, old and new."

Carl Sagan

Based on:

D. Barducci, A. Belyaev, M. Buchkremer, G. Cacciapaglia, A. Deandrea, S. De Curtis, J. Marrouche, S. Moretti, L. Panizzi, "Model Independent Framework for Analysis of Scenarios with Multiple Heavy Extra Quarks", submitted for publication in *JHEP*, 1405.0737.

In this chapter we detail an analysis strategy and a dedicated tool to determine the exclusion confidence level for any new physics scenario involving numerous top partners with generic decay channels. For this purpose, we present

a software called XQCAT (eXtra Quark Combined Analysis Tool), which is based on publicly available experimental data from direct searches for chiral and vector-like quarks, and from Supersymmetry inspired searches. By means of this code, which we have created and validated in [125], we recast the limits from selected searches by the CMS experiment on some simple scenarios with multiple vector-like quark states and general coupling assumptions. We conclude with possible perspectives for the following search strategies, so as to probe the remaining allowed parameter space for these particles.

4.1 Introduction

Since the start of its physics programme, the Large Hadron Collider (LHC) has delivered very high quality results on the discovery of the Higgs boson and the first characterisation of its properties, as well as a large set of new limits on searches for other particles, which may be present in extensions of the Standard Model (SM). New heavy quarks, in particular, receive a lot of attention from the experiments, as they naturally arise near the TeV scale in many extensions of new physics. In the next planned runs, the LHC will continue improving the existing limits, or else provide evidence of these new states. The search for new fermionic resonances, sometimes referred to as "top partners" when associated to the top quark, is also of growing interest for BSM phenomenology. New quarks appear in a large number of new physics scenarios, as they play a crucial role to soften the quadratic divergences contributing to the Higgs mass term, the origin of the SM hierarchy problem. Top partners coupled to the third generation of quarks have been thoroughly investigated from a phenomenological point of view in [106, 126, 127, 107], as well as the possibility to have sizeable couplings to the light generations, in [128, 108].

The key point to appreciate, though, is that many new physics models predicting the existence of such top partners contain in general more than one new heavy state. Up till now, this has gone against the approach of experimental searches for vector-like quarks, which are undertaken under the simplifying assumption that only one new state beside the SM spectrum is present, and constraints are given on this sole object (on its mass and/or couplings). These bounds cannot be easily re-interpreted in models containing two or more new

quarks, which can contribute to the signal events in the very same channel. Recasting consistently the available limits under the assumption of multiple resonances, or considering the possibility for non-zero couplings to the lighter quark generations [109], often requires an elaborated strategy so as to take into account all allowed signatures for a given benchmark point (or region). We are quick to point out, however, that progress on this front is currently underway in the experimental community, in both designing new searches and interpreting these in the context of models where the couplings of the top partners are either to heavy or light flavour quarks as well as to a linear combination of the two. Some studies and related codes have attempted to tackle this problem on more general grounds, such as the tools CheckMATE [129], SModelS [130] or Fastlim [131]. Each code has its own specific way to prepare the input model spectrum (i.e., masses and couplings) and address the comparison with existing data analyses, the former adopting a rather generic model independent approach while the others optimise performance for SUSY scenarios, yet in both cases the 'full spectrum' of a BSM realisation is tested.

On general grounds, performing a detailed simulation and analysing the results against experimental data from different studies is a challenging task, at times not feasible. Further, different top partners can decay into the same final state through different decay chains and therefore with different topologies. For either of these reasons, experimental efficiencies would therefore be different and a rescaling of mass bounds is not trivial. Finally, unknown input parameters in the new physics Lagrangian usually affect both the spectrum of the new quarks and their branching ratios (BRs).

The focus of the `XQCAT`, as described in this work, is precisely to provide an automated tool able to considerably simplify the comparison for general spectra of new heavy quarks. Its design allows the user to determine the exclusion Confidence Level (eCL) of any given scenario with multiple partners of the top, referred to as eXtra Quarks (XQs) in [125]. Based on this implementation, we will apply our software to specific benchmark models, reinterpreting a selected subset of direct and indirect searches by CMS as an input. As we will see, the obtained results highlight the importance of combining multiple topology searches to obtain accurate re-interpretations of the existing searches,

as well as the potential reach of the SUSY analyses so as to set bounds on new resonances.

4.2 Analysis Strategy

As introduced, the purpose of XQCAT is to address the analysis of scenarios with multiple top partners that can decay into any SM quark together with a Higgs or gauge boson. It is designed so as to allow the user to establish excluded regions of the corresponding parameter space, based on a comprehensive kinematical and statistical analysis. This parameter space is defined by the mass spectrum and the branching ratios (BRs) of the various quark states, provided as input to the tool. Model independency is achieved considering only strong pair production, which is induced by Quantum Chromo-Dynamics (QCD) interactions, so that the emerging cross section is only sensitive to the masses of the new quarks. Sub-leading pair production channels provided by electroweak processes can be safely neglected, since their cross sections are much smaller than the QCD ones. In fact, as no experimental search targeted at EW pair production is available, including their effect would only give a minor improvement in our bounds. Another interesting production channel is given by the single production of such top partners [128, 109]. As discussed in the previous chapter, large cross sections can be expected even after imposing flavour and EW precision bounds on the mixing parameters. It is well understood that single production can be relevant, especially for large masses, as it is less suppressed by the phase space of the final state and Parton Distribution Functions (PDFs) of the proton. While the details of its implementation will not be discussed in the following, the inclusion of single production to our tool strategy is straightforward, e.g., by following [109].

Starting from the QCD pair production followed by the decays of the new heavy quarks which mix with the SM quarks via Yukawa interactions, one can estimate the number of signal events that survive the selection cuts for any given signature and specific search strategy that is finding the respective efficiencies for each subprocess that contributes to the given final state. Under this assumption, the cross sections of various final states can be decomposed in model-independent subsets, which contain all the kinematic information from

the decays. Thanks to this observation, and considering the provided input on the masses and BRs, it is finally possible to reconstruct the signal coming from general scenarios by combining, with the appropriate "weights", the different model-independent topologies which generate the signal and the different kinematic distributions. Therefore, the main strategy employed in XQCAT is to express the overall signal as a weighted sum of signals from each of these subprocesses.

The most general scenario we consider covers the case of the following quark species, which can be simultaneously present in the generic model:

$$n_X X_{5/3} + n_T T_{2/3} + n_B B_{-1/3} + n_Y Y_{-4/3} \tag{4.2.1}$$

where the sub-script indicate the electric charge. T and B are top and bottom partners, respectively, while X and Y are exotic particles with charge 5/3 and $-4/3$, respectively. We limit the code to these four species of top partners because they are the only ones which can couple directly to SM quarks, as discussed in the previous chapters. Furthermore, the requirement for QCD to be asymptotically free sets an upper bound on the maximum number of active flavours that we will consider in our analysis. Under the assumption of the Standard Model gauge group, the restriction $(n_X + n_T + n_B + n_Y) \leq 10$ is enforced at leading order on the number of new color triplet quarks. In the following, the new states will be assumed to decay promptly, otherwise their signatures would be that of long-lived heavy objects (or of bound states thereof), depending on their lifetime. General mixings with the SM quarks will be considered, thus allowing the complete set of decays

- $X \to W^+ u_i$,
- $T \to W^+ d_i\,,\ Z u_i\,,\ H u_i$,
- $B \to W^- u_i\,,\ Z d_i\,,\ H d_i$,
- $Y \to W^- d_i$,

where $i = 1, 2, 3$ labels the SM family. It is further assumed that none of the new particles decay into each other, which is a reasonable expectation for

members of a vector-like multiplet with a common mass scale m and small mass splittings. Decay modes into another top partner plus a SM boson will not be addressed in the following, as they may be significant only in the case of large mass splitting. Even in this case though, the phenomenology is usually dominated by the lightest state(s) in the model, providing the above decay patterns[1].

For the purpose of our implementation, we have simulated signals for each subprocess for different values of the masses of the top partners. Using these signals as inputs, a dedicated analysis code is then applied to evaluate the respective efficiencies for all the subprocesses contributing to each individual signature and the respective search. These efficiencies, which are stored in the database of `XQCAT`, allow the user to automatically evaluate predictions for any desired model and channel. As an output, the respective eCL for the input point is provided for each implemented search. Moreover, when possible, searches are statistically combined, in order to obtain a more stringent exclusion bound. Using this strategy based on the use of pre-simulated data, the program also allows to flexibly study cases with multiple states. For the sake of brevity, the determination of the eCLs, the validation of the different parts of the code, as well as the restrictions for its applicability are detailed in Appendix C.

To illustrate our strategy in practice, we can consider a simple example with a single B quark and assume that it decays only to Wu and Wt. Following $B\bar{B}$ pair production, these decays would lead to the signatures:

$$pp \to B\bar{B} \to \begin{cases} W^+W^-u\bar{u} \\ W^+W^-u\bar{t} \to W^+W^-W^-u\bar{b} \\ W^+W^-t\bar{u} \to W^+W^+W^-b\bar{u} \\ W^+W^-t\bar{t} \to W^+W^+W^-W^-b\bar{b} \end{cases} \tag{4.2.2}$$

which we will denote as: $WWjj$, $WWWj\bar{b}$, $WWWjb$ and $WWWWb\bar{b}$. In a specific model, the weight of events coming from each channel will be

[1] As discussed in Appendix C.3, these additional decay chains introduce model-dependence and will only strengthen the bounds given that they would increase the inclusive production cross section of the lightest states.

determined by the Branching Ratios (BRs) BR_{Wu} and BR_{Wt}. If we distinguish these signals according to W-boson multiplicity as WW, WWW and $WWWW$ channels, then the relative rates are given by BR^2_{Wu}:$(2\,\mathrm{BR}_{Wu}\mathrm{BR}_{Wt})$:$\mathrm{BR}^2_{Wt}$ respectively. In addition to different rates, these three different channels have different kinematics for the final state fermions (after the W-bosons decays) and in turn different efficiencies upon the application of the analysis cuts. This complication is taken into account in our code, in which we have considered each channel independently and derived the respective efficiencies as a function of the top partner mass. Thus, considering the various BRs of as independent parameters and using the efficiencies mentioned above, one can evaluate the overall signal rate as a weighted sum of all channels under study.

In the following, this approach is extended to models with more than one top partner. For completeness, we also deal with the possibility for two or more different states to contribute to the same final state signature. Such a situation can be illustrated, for instance, with NP scenarios such as the one presented in [120],[128] and [88], allowing simultaneously for B and X quarks. If one would like to study the sensitivity of an experimental search for events with same-sign di-leptons, more than 2 jets and more than 2 b-jets, then the following channels can contribute to the above final state [88]: $pp \to B\bar{B} \to W^+\bar{t}W^-t$ and $pp \to X\bar{X} \to W^-\bar{t}W^+t$. In such a case, our tool weights the efficiencies of different channels by the different cross sections and BRs (that depend on the masses m_X and m_B), providing an eCL for the combined signal.

4.3 Generation of the efficiency database

The simulation of QCD pair production for each quark and for each mass has been performed with MadGraph5, v.1.5.8 [132]. The subsequent decays of the top partners into SM quarks and bosons have been computed with BRIDGE, v.2.24 [133]. The version v.2.1.21 of PYTHIA [134] has been used to compute the decays of SM particles, subsequent hadronisation and parton shower. The detector simulation has been performed by Delphes2, v.2.0.2 [135] with suitable detector cards for both ATLAS and CMS experiments. The calculation of the search efficiencies is performed in a framework built on the Delphes [135]

detector simulation as an input. This framework has been validated and used previously [136, 137] and is described in [137]. Since the pair production of the heavy quarks is here assumed to be a QCD-driven process, jet-matching has also been considered and appropriate matching parameters have been chosen for each mass of the quarks. Therefore, the processes simulated in MadGraph5 are $pp \to Q\bar{Q} + \{0, 1, 2\}$ jets, where $Q = T, B, X, Y$.

The corresponding number of simulated processes depends on the number of considered masses, on the possible decay channels and on the dominant chirality of the couplings[2]. Each T and B quark can decay into 9 channels, corresponding to combinations of three SM bosons and three SM quarks. However, since light generation quarks cannot be distinguished at the LHC and are experimentally seen as jets, the effective observable decays are just 6 for both T and B (assuming the bottom quark to be tagged, while we are not considering the possibility to tag a charm quark). Since the states are pair-produced, the total number of combinations is $6 \times 6 = 36$ for both T and B. Exotic quarks X and Y can only decay through charged currents, and therefore the possible combinations for pair production are $2 \times 2 = 4$ for both X and Y. Considering two chiralities for each combination, the total number of channels for each mass scale is equal to $2 \times 2 \times (6 \times 6 + 2 \times 2) = 160$. The simulation has been performed considering masses in the range $\{400, 2000\}$ GeV with steps of 100 GeV.

For the purpose of our analysis, we considered two different kinds of searches, all corresponding to CMS studies:

- *Direct searches of vector-like quarks* We implemented the CMS analysis B2G-12-015 [100], at $\sqrt{s} = 8$ TeV with a 19.5 fb^{-1} dataset, for a pair produced T quark that mixes only with third-generation SM quarks and can decay to W^+b, Zt or Ht with variable BRs. The CMS collaboration presents the 95% CL lower limits on the T quark mass for different combinations of its BRs using six mutually exclusive channels: two single lepton (single electron and single muon), three di-lepton (two opposite-sign and one same-sign) and one tri-lepton channel, all con-

[2] As detailed in [109] for vector-like quarks, the couplings of such states to SM quarks and bosons depend on the $SU(2)$ representation the quark belongs to, and are dominantly chiral.

taining tagged b-jets in the final state. No deviations from the SM expectations were observed when considering a large number of benchmark points among the allowed parameter space for the BRs. Since the sensitivity of the search is mostly driven by the multi-lepton channels, in the present version of the tool we have only implemented three bins: the opposite-sign (OS1, as denoted in [100]), the same-sign (SS) and the tri-lepton channels. More details about this choice will be explained in the validation section below. The limits for the multi-lepton channels only can be found in the twiki page of the search [138] and the quoted observed bounds are in the range $592 - 794$ GeV depending on the assumed BRs.

- *SUSY searches* We implemented four searches inspired by SUSY scenarios, characterised by the presence of different numbers of leptons in the final state and large missing transverse energy: the 0-lepton (α_T) [139], the mono-lepton (L_p) [140], the opposite-sign dilepton (OS) [141] and the same-sign dilepton (SS) [142], considering the entire 4.98 fb^{-1} 2011 dataset at $\sqrt{s} = 7$ TeV. We have also included the updated α_T [143] and same-sign [144] searches at 8 TeV, with 11.7 fb^{-1} and 10.5 fb^{-1}, respectively. It has been verified that the selected searches are uncorrelated and, therefore, it is possible to statistically combine them, yielding 95% CL bounds at 7 TeV (combination of 4 searches), 8 TeV (combination of 2 searches) and 7+8 TeV (combination of 6 searches).

We highlight, however, that this selection of analyses is arbitrary, while many other searches of vector-like quarks are available in the literature. For example, same-sign dilepton final states were accounted for in [145], searching for exotic partners with electric charge $5/3$ decaying exclusively to W bosons and tops, excluding $m_X < 770$ GeV at the 2σ level. For the same integrated luminosity at $\sqrt{s} = 8$ TeV, the multilepton search [102] excluded B quark masses below 520-785 GeV for non-nominal branching fractions to Wt, Zb and Hb. The present ATLAS direct limits also reach mass bounds of 585 (645) GeV for the T (B) vector-like singlet scenario with 14 fb^{-1} of data, while a mass bound of 680 (725) GeV is now excluded at the 95% CL for the branching ratio assumptions corresponding to weak-isospin doublets [96, 97, 98, 99]. Yet, it must be kept in mind that such priors do not include the possibility for

new partners having large couplings to the u, d, c and s quarks. While they fully cover the parameter space corresponding to top partners, non-zero mixings with the first two SM generations remain a likely possibility, and require careful treatment.

The validation of XQCAT has been performed by comparing our results to experimental data for some specific channels. For this purpose, we have considered the CMS inclusive search [100, 138] and analysed the same benchmark points (i.e., T masses and BRs) considered in the search. As described in Appendix C.2, the validation was performed for the two main sections of our framework: the limit code that computes the eCLs starting from the number of signal events obtained from input, and the code that extracts the efficiencies considering the selection and kinematics cuts of the implemented searches. We refer the reader to [137] for the case of SUSY searches.

4.4 Constraints on selected scenarios

4.4.1 Analysis of one T singlet mixing only with the top quark

As a critical step to the validation of our tool and of the implementation of an experimental search, we compute in this section the 95% CL mass bound obtained with XQCAT for a T singlet under different hypotheses for its BRs into third generation quarks and SM bosons. All the results presented in the following sections assume as an input the NLO-NNLL order cross sections for $pp \to Q\bar{Q}$ production at the LHC, as given in [146].

In Fig. 4.1 we show the eCLs for a T singlet with $\mathrm{BR}(Wb) = 50\%$ and $\mathrm{BR}(Zt) = \mathrm{BR}(Ht) = 25\%$. To extract the corresponding mass bound, we use the two first methods described in Appendix C.1. With a linear interpolation of the eCLs we obtain a 2σ mass bound of 614 GeV while a linear interpolation of the efficiencies yields a 2σ mass bound of 634 GeV. These results show that the numerical value of the mass bound is not very sensitive to the interpolation method in use, at least in a typical situation. These values can also be compared with the quoted value of 668 GeV in the multi-lepton channels only [138]. In

Fig. 4.1 we also plot the eCLs obtained from the combination of all SUSY searches, at $\sqrt{s} = 7$ and 8 TeV. In such a case, we observe that the direct search is more sensitive than the SUSY combination. The bound provided by linearly interpolating the eCLs of the SUSY searches combination is 525 GeV (560 GeV if interpolating the efficiencies). Taking into consideration that SUSY searches were not designed to be sensitive to this kind of final states, it is remarkable that the obtained bound is not too far from the one reproduced by the direct searches [100, 138]. We therefore emphasise the important role that the SUSY searches may have so as to explore scenarios where tentative top partners do not decay to heavy generations and for which direct searches of chiral and vector-like quarks (that usually require b-jets in the final states) might not be as sensitive. We will further explore this possibility in the following section.

To further validate our implementation, we computed the mass bounds on a T quark varying all the BRs between 0 and 1 in steps of 0.2. Our results in the BR(Wb)-BR(Ht) plane are shown in Fig. 4.2. Again, to be able to compare with the experimental results, the 95% CL contours on the T quark mass are obtained by linear interpolation of the eCLs between the simulated points. The comparison with the experimental values of the CMS search in the multi-lepton channels [138] shows that our results are consistent within a 60 GeV range for most BRs configurations.

In Appendix C.4, Tab. C.1 provides the numerical results for selected benchmark scenarios. The bounds have been obtained by interpolating either the eCLs or the efficiencies between simulated points, following the methods discussed in Appendix C.1. We have considered the nominal points with fixed ratios between decays through charged and neutral current, as well as specific scenarios with 100% BR into one channel, possibly relaxing the assumption of exclusive mixing with one generation.

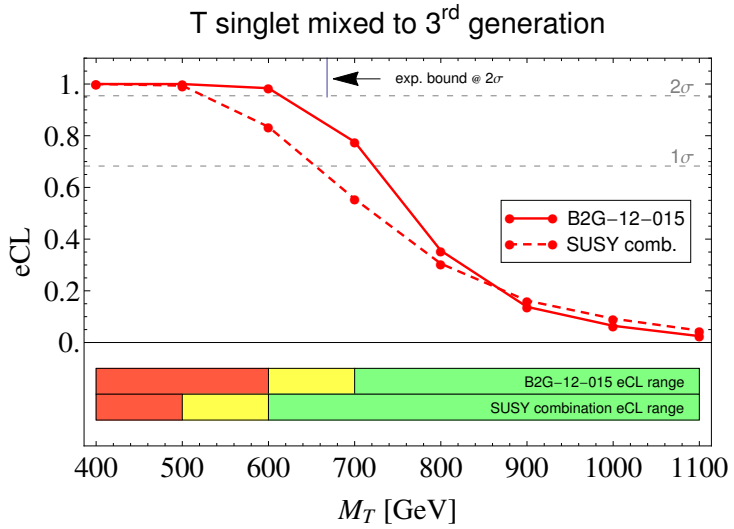

Figure 4.1: Exclusion confidence levels for a T singlet mixing only with the top quark, that is with $\mathrm{BR}(Zt) = \mathrm{BR}(Ht) = 0.25$ and $\mathrm{BR}(Wb) = 0.5$. The dots correspond to the simulated points, whereas the lines are linear interpolations of the eCLs (method 3 in Appendix C.1). The solid line corresponds to the eCLs obtained using the direct search [100], while the dashed line corresponds to the combination of the SUSY searches at $\sqrt{s} = 7$ and 8 TeV. The strips below the plot correspond to method 2 of Appendix C.1: the red region is excluded at 95% CL, the yellow region is where the 2σ mass bound can be found, the green region is not excluded at 95% CL.

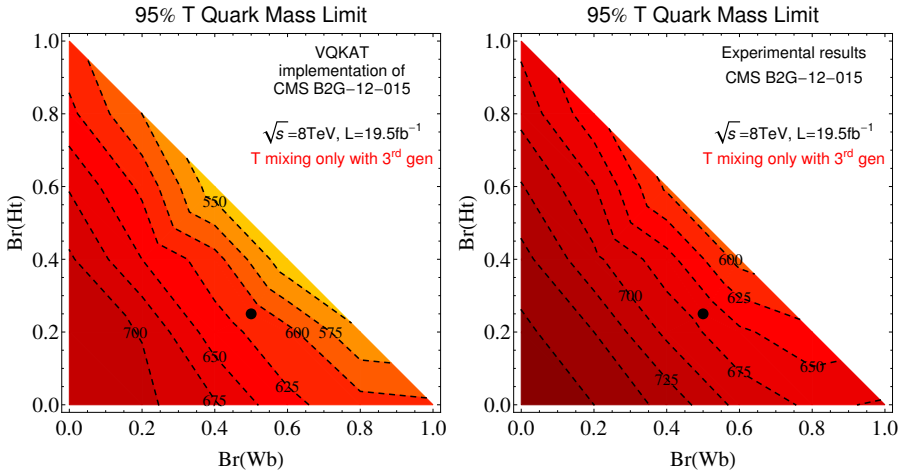

(a)

(b)

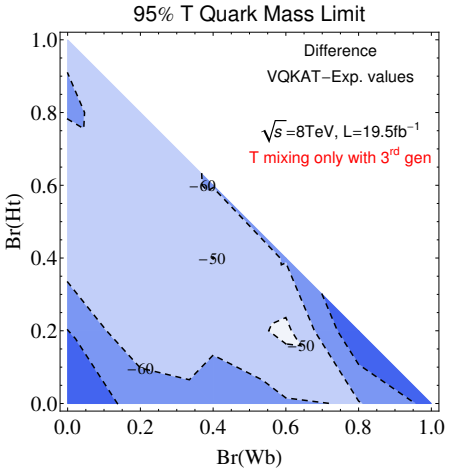

(c)

Figure 4.2: 95 % CL mass limit on the T quark mass in the BR($T \to Wb$)-BR($T \to Ht$) plane for the results obtained with XQCAT (a) and the experimental results of [138] (b). The difference between our results and the experimental results are shown in (c). The 95% contours have been obtained through linear interpolation of the eCLs for the simulated masses, i.e. from 400 GeV to 1000 GeV with steps of 100 GeV. The black dot represents the nominal point for a T singlet with $\mathrm{BR}(Zt) = \mathrm{BR}(Ht) = 0.25$ and $\mathrm{BR}(Wb) = 0.5$.

4.4.2 Constraints on scenarios with multiple top partners

In this section, we present the ability of XQCAT to set bounds on scenarios with multiple top partners in selected toy models. Re-interpreting the experimental results in models where more than one new fermion is present is not an easy task, as already intimated. It is even more involved when the new states are degenerate in mass. The main difficulty in such a re-interpretation of the searches is found in the fact that signals coming from different states can contribute to the same signal bin, therefore one needs to calculate the efficiencies and number of events that pass all the cuts before calculating the eCL. This is exactly what our program XQCAT does. In general, signal bins can receive contributions from different physical states in the following two cases:

- the model contains two states with the same decay channels which therefore produce the same final state;
- the model contains states with different decay channels, however, the signal features are (even partially) sensitive to the different final states.

To illustrate how the combined limits affect the excluded parameter space, we will here consider top partners which mix only to the third generation and exploit the bounds given by the CMS B2G-12-015 searches [100], which are specifically designed for pair produced T vector-like quarks decaying to Wb, Zt and Ht. For the purpose of setting representative bounds on models with extended quark sectors, we consider two simplified scenarios:

- two T singlets;
- a doublet (X, T) with exotic hypercharge, $Y = 7/6$.

If all quarks are pair-produced, the two cases above can be described in terms of 3 free parameters: the masses of the quarks, and a parameter encoding the BR into the third generation quarks. We also highlight that the T singlet and the (X, T) doublet scenarios above were identified in [109] as being among the least constrained vector-like quark representations from flavour observables, whenever assuming general mixing with the three SM quark families.

Let us start with the first simplified scenario of two T singlets, with arbitrary mass and similar decays: $\sim 50\%$ in Wb and $\sim 25\%$ in Zt and Ht. Using these BRs as inputs, we show on Fig. 4.3(a) the calculated eCLs for each value of the two masses $\{m_{T_1}, m_{T_2}\}$. The crossing points in the grid of the figure correspond to the mass values that we simulated are neglected in the following. The most conservative way to set bounds is to calculate the eCLs on the simulated masses, which are therefore fully reliable. Shown in red on the plot are the squares whose corners are all excluded at 95% CL, in green the squares whose corners are allowed. The yellow regions contain the intermediate situation, i.e., squares where only some of the corners are excluded: we can then affirm that the exclusion limit must be a line crossing the yellow squares. This is proven by the two black curves: the solid one corresponds to the bound one obtains by interpolating the eCL calculated on the simulated points, as it is usually done in experimental results. The dashed curve corresponds to a finer scan on the masses, using efficiencies which are interpolated between simulated points. This procedure, in general, gives rise to different values for the bounds, nevertheless we see that the corresponding dashed line falls very close to the solid one. From the displayed results, interesting conclusions can be drawn: the obtained bound is mostly sensitive to the presence of the two states when their mass differs by less than 200 GeV. In contrast, for larger mass differences, the presence of the second heavier state becomes irrelevant and the bound coincides with the one obtained with one state only, i.e., in the 600–700 GeV range at 95% CL. This toy model can therefore be excluded at the 2σ level from the considered set of searches if any of the two T singlets occurs to be lighter than 600 GeV.

To study the impact of the presence of multiple top partners with different charge and decay channels, we present in Fig. 4.3(b) the case of a vector-like quark doublet with non-standard hypercharge, (X, T), which contains a charge $5/3$ state X and a charge $2/3$ state T [108]. The T quark decays $\sim 50\%$ in Zt and Ht, while the exotic charge state only decays into Wt. This mode has been searched for in final states with two same sign leptons plus jets [147, 145], giving a bound of 670 GeV (ATLAS, pair production only) or 800 GeV (CMS). Although large mass differences between X and T do not correspond to physically realistic situations as the latter splitting can only be generated by

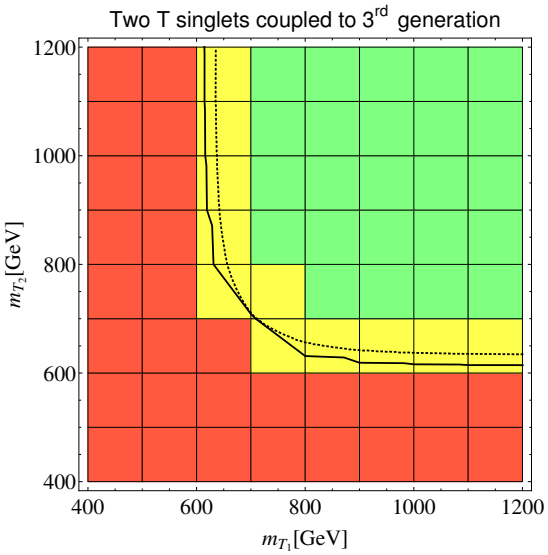

(a)

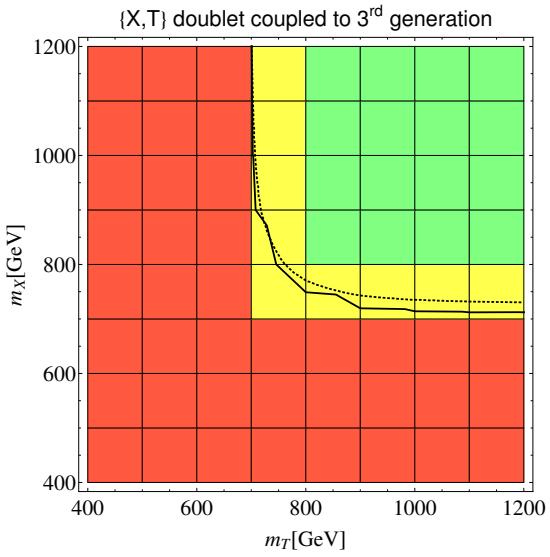

(b)

Figure 4.3: eCLs considering the CMS search [100] for a configuration of (a) 2 T singlets or (b) (X, T) doublet with masses ranging between 400 GeV and 1200 GeV coupled only to third generation SM quarks. The excluded (red), boundary (yellow) and non-excluded (green) regions at 95% CL are shown. The solid (dashed) contour corresponds to the 95% CL bound obtained by linear interpolation of the eCLs (efficiencies) for the simulated points.

mixing via the Higgs boson, we consider the bounds for two masses ranging independently between 400 to 1200 GeV. These results show again that an interplay between the two masses emerges when the mass splitting is smaller than 200 GeV, like in the case of the two T singlets. However, the most striking result is that the searches for T states can already pose bounds on the X state. This highlights the fact that, even in models where a single T state is present, one cannot simply utilise directly the experimental bounds: the other partners in the same multiplet as T can contribute to the signal rate and thus increase the bound on its mass.

4.4.3 Interplay and complementarity with other searches

A last but important issue that we want to address with the `XQCAT` code is the complementarity between direct searches for new extra quarks and other searches performed at the LHC. We here discuss the results obtained on the case where a single T partner mixes with the light generation quarks. This scenario has recently received great attention by the experiments, as it may give rise to large single production cross sections [128]. It has also been shown that the flavour bounds do not disfavour cases where significant mixing to both the top and either the up or the charm quarks is turned on [108]. Nevertheless, no specific search focused on pair production followed by decays to light jets is available. In the following, we show that SUSY data samples already set significant bounds on such scenarios.

In Fig. 4.4(a), we first consider the simple case of a singlet T, which is allowed to mix with light quarks only, with the following decay rates: $\mathrm{BR}(Wj) = 0.5$ and $\mathrm{BR}(Zj) = \mathrm{BR}(Hj) = 0.25$. We find, as expected, that the sensitivity of the B2G-12-015 direct searches are strongly reduced: this is not a surprise as the final state loses many jets and leptons from the top-decays, and is depleted of b-jets which are used systematically to tag the signal region. It is remarkable that, despite a sensible drop in sensitivity, the combination of the SUSY searches still yields a 95% eCL mass limit above 400 GeV, compared to the case of dominant coupling to third generation quarks. The corresponding mass limits are displayed in Appendix C.4 for different combinations of the BRs. The obtained results indicate that the SUSY searches combined at $\sqrt{s} = 7$ and

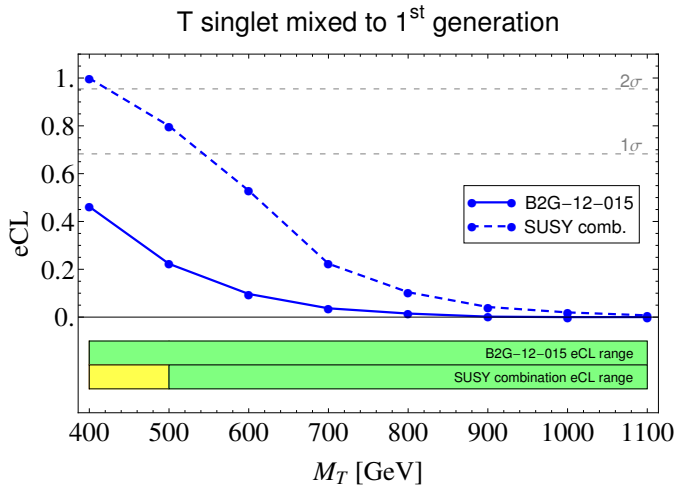

(a)

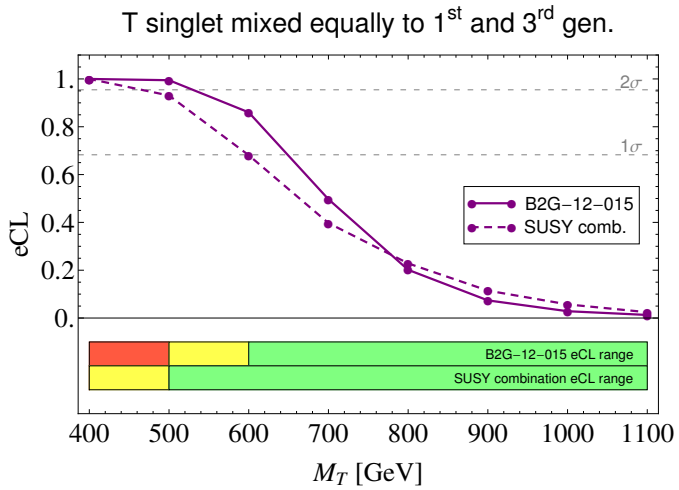

(b)

Figure 4.4: eCLs (a) for a T quark coupled only to the SM up quark such that $\mathrm{BR}(Zu) = \mathrm{BR}(Hu) = 0.25$ and $\mathrm{BR}(Wu) = 0.5$ and (b) for a T quark mixing equally with the first and the third generations, with $\mathrm{BR}(Wb) = \mathrm{BR}(Wd) = 0.25$ and $\mathrm{BR}(Zt) = \mathrm{BR}(Zu) = \mathrm{BR}(Ht) = \mathrm{BR}(Hu) = 0.125$. The dots correspond to the simulated points while the lines are linear interpolations of the eCLs (method 3 in Appendix C.1). The strips below the plot correspond to the method 2 discussed in Appendix C.1. The red region is excluded, the yellow region is where the 95% eCL mass bound can be found and the green region is not excluded.

8 TeV lead to a mass bound in the ballpark 400–500 GeV, except in the case of exclusive decays into Higgs boson. As an illustration, Fig. 4.4(b) displays the sensitivity of the two sets of searches if mixed decay modes are present, e.g., if equal couplings to the up and top quarks are allowed. In this specific situation, corresponding to the configuration $\mathrm{BR}(Wb) = \mathrm{BR}(Wd) = 0.25$ and $\mathrm{BR}(Zt) = \mathrm{BR}(Zu) = \mathrm{BR}(Ht) = \mathrm{BR}(Hu) = 0.125$, the combination of the SUSY searches only set mild constraints. On the other hand, the direct search [100] displays a much better sensitivity compared to the previous case.

From a channel-by-channel analysis, the interpolated eCLs and efficiencies indicate that the most sensitive handle on T quarks coupling exclusively to the light generations consists in looking for top partners decaying to Z bosons and jets. This implies that the forthcoming searches for pair-produced states would certainly benefit from the inclusion of such decay modes, as the assumption $\mathrm{BR}(Zj) = 1$ points at the next most interesting hypothesis for such scenarios. The Wj channels provide otherwise sensitive decay modes for the forthcoming searches, under the requirement of including more data. Finally, we highlight that no conclusions can be drawn for scenarios with a single T quark decaying exclusively to Higgs bosons and jets, as $\mathrm{BR}(Hj) = 1$ remains a very challenging hypothesis to probe at the LHC. Dedicated searches might however reach an impressive sensitivity by relying on EW single production to access the corresponding topologies (see, e.g., [148, 149]).

4.5 Summary

Depending on the new physics model at hand, new heavy quarks may come numerous, while experimental searches only look for one of such states. Although this approach is well motivated from the experimental point of view, it becomes a non trivial task to translate the bounds in scenarios with multiple resonances. Given the fact that multiple states may contribute to the same signal topologies and kinematic regions, reinterpreting the most recent analyses so as to provide bounds on multiple quark states is not straightforward. In order to remedy this obvious drawback, we presented in this chapter the `XQCAT` code, a tool which we designed so as to recast the available results from the aforementioned experimental searches into those applicable to any spectrum

of heavy quark states decaying to W, Z and H bosons plus jets, top and/or bottom quarks. Validating our code against the inclusive search CMS-B2G-12-015 [100] for a vector-like T quark and, as a novelty, the indirect SUSY searches of [139, 140, 141, 142, 143, 144] , we presented a re-interpretation of scenarios with one or multiple top partners, the latter being pair-produced via $pp \to Q\bar{Q}+$ jets, with Q having general couplings to the light and third generations of SM quarks. The eCLs were determined using various methods beyond the most customary and simplest approach of interpolating linearly the efficiencies. While conservative, this approach is accurate and fully model-independent.

The inclusion of indirect searches in the data sample exploited by `XQCAT` proved a crucial ingredient in furthering the scope of the available experimental information, as we show that recasting a selected subset of SUSY searches (e.g., zero-lepton, one-lepton, opposite-sign and and same-sign dilepton signals) gives robust hints regarding exclusion of new heavy quarks below the TeV scale at the LHC. Limits on the corresponding parameter spaces have been set from the analysis of recent direct and indirect searches, and we reported on the possibility to set bounds on various benchmark scenarios with non-exclusive couplings to the third generation. Further, their re-interpreted limits from these and from the combination of several SUSY searches (i.e., in an approach combining multiple topologies) appear to be in the same ballpark for pair-produced top partners coupling dominantly to the third generation. Doing so, we insist on the importance of combining multiple topology searches to obtain more accurate (model-independent) re-interpretations of standard single heavy quark searches. This remains true no matter the assumptions on their couplings, yielding a scope comparable and, in some cases, complementary to the one afforded by direct searches for chiral and vector-like quarks.

Conclusion

Since the start of its physics programme, the Large Hadron Collider (LHC) has delivered very high quality results on the Higgs boson, as well as a large set of new limits on searches for other particles. With the last building block of the SM successfully identified by the searches at the LHC, high energy physics now reaches a crossroads: an unprecedented situation where our theoretical paradigms can only speculate on the existence of tentative new physics. Similarly to the so-called "UV catastrophe" of 19th century physics, most of the current observations seem to indicate that particle physics is now close to being worked out, would no new particles and/or forces show up around the corner. Hopefully, the forthcoming Run 2 of the LHC in 2015 will provide theorists with clues to define what could possibly lie ahead the discovery of the Higgs particle. In the next planned runs, the experiments will continue improving the existing limits on novel particles beyond those predicted, or else provide evidence of these states. In this spirit, models should be built by considering both the theoretical ideas and their experimental scope, with the aim of making the former testable via the latter.

Now that the possible existence of a fourth generation of SM-like (i.e., chiral) quarks has essentially been ruled out by the LHC in the light of the latest Higgs data, an inevitable shift of focus in the search for new extra heavy quarks has been occurring. Prime candidates in playing a center-stage role in this renewed quest are heavy vector-like quarks, as these arise in a variety of well-motivated scenarios going beyond the Standard Model. While the Col-

lider searches are now collecting a large amount of data, the unprecedented sensitivity in the measurement of rare processes in Flavour physics allows to set stringent constraints on the corresponding parameter space. This work provides an overview on the current phenomenology of these states, which are predicted in many models of new physics.

After reviewing in Chapter 2 the constraints which allowed to exclude a perturbative family of new chiral quarks, we developed in Chapter 3 a model-independent parametrisation that can be used to describe the phenomenology of pair- and singly-produced vector-like quarks at the LHC, considering generic hypotheses on their Yukawa couplings to the SM quarks. Relying on a limited number of parameters, our framework has been adopted to perform a comprehensive analysis of the electroweak production modes of non-chiral top partners at the LHC. Given the interest of excluding the largest possible spectrum from the forthcoming experimental searches, these processes have been shown to play an essential role to constrain their possible couplings to the standard quarks and electroweak bosons. As a concrete application, we evaluated the corresponding production cross sections at leading order, and defined a set of benchmark scenarios which saturate the experimental constraints obtained from flavour physics and other observables. Considering the addition of a single vector-like quark partner beyond the SM, our analysis allowed to highlight the potential relevance of scenarios which have not been considered yet by the experimental collaborations, and suggest novel strategies for the forthcoming searches.

New heavy quarks, however, may come numerous depending on the considered BSM scenario. In this context, establishing a direct link between experimental and theoretical particle physics is not always an easy task. In fact, the presence of various decay modes means that channels with mixed decays can also contribute to the signal regions of the experimental searches, with an unknown experimental efficiency: a simple rescaling of the cross section with the branching ratios, therefore, is not sufficient to extract a reliable bound on realistic New Physics scenarios. Although this approach is well motivated from the experimental point of view, it is a non trivial effort to translate the bounds in scenarios with multiple resonances. Conversely, we have seen in the recent years that the extra knowledge brought in by the recent collider data is shift-

ing the focus of the particle theory community from established new physics models of which we have no evidence (like SUSY) to new ones which may be promptly testable by experiment. We therefore asked the question: given the still allowed parameter space for hypothetical extended fermion sectors, is it possible to estimate the bounds set by the current searches for new extra quarks in the context of general new physics scenarios ?

Attempting to answer this question, our final chapter aimed at developing a dedicated tool, so as to determine the exclusion confidence level for any scenario with multiple heavy quarks and generic decay channels. Under simplifying assumptions, our software reconstructs conservatively the signal coming from input scenarios, taking into account the different topologies that generate the signal and the different kinematic distributions. Based on a simple cut-and-count approach, we reported on the possibility to set bounds on benchmark scenarios with numerous top partners, with and without exclusive couplings to the third generation, considering a selection of direct and indirect analyses published by the CMS experiment. Considering QCD-driven pair production, we insisted on the importance of combining multiple topology searches to obtain more accurate re-interpretations of standard searches for benchmark models containing a single heavy quark. This remains true no matter the assumptions on their couplings, yielding a scope comparable and, in some cases, complementary to the one afforded by the current analyses. This proved a crucial ingredient in furthering the scope of the available experimental information, as we showed that recasting selected subsets of searches already gives robust hints regarding the exclusion of new heavy quarks below the TeV scale at the LHC.

Appendix A

Effective Lagrangian for a top partner T

A.1 Parametrisation

As an illustration of Eq.(3.2.2), we present in this appendix the construction of the most general effective Lagrangian for a top partner T, i.e., a single vector-like quark T with the same electric charge (and colour) as the top quark. The most general couplings with the electroweak gauge bosons can be parametrised as

$$\begin{aligned}\mathcal{L} &= \kappa_W V^{4i}_{L/R}\frac{g}{\sqrt{2}}\left[\bar{T}_{L/R}W^+_\mu\gamma^\mu d^i_{L/R}\right] + \kappa_Z V^{4i}_{L/R}\frac{g}{2c_W}\left[\bar{T}_{L/R}Z_\mu\gamma^\mu u^i_{L/R}\right] \\ &- \kappa_H V^{4i}_{L/R}\frac{M}{v}\left[\bar{T}_{R/L}H u^i_{L/R}\right] + h.c., \end{aligned} \tag{A.1.1}$$

where we omitted the couplings with gluon and photon, dictated by gauge invariance[1]. This is a generalisation of the Lagrangian in [128] by the inclusion of couplings with the Higgs [149], and to all the generations of quarks at the same time. In this formula, M is the mass of the VL quark, $V_{L/R}^{4i}$ represent the mixing matrices between the new quarks and the three Standard Model generations labelled by i, while the parameters κ_V ($V = W$, Z, H) encode the representation-dependent coupling of the T quark to the three bosons. The normalisation is chosen so that for $\kappa_W = \kappa_Z = \kappa_H = 1$, the T quark decays 25% to Z and H and 50% to W in the asymptotic limit where the mass M goes to infinity, in agreement with what is expected from the Goldstone boson equivalence theorem (see, e.g., [150, 151, 152]). The values of the κ_V's are determined by the $SU(2)_L$ representation T belongs to, and eventually by mixing to other VL representations.

In the most general set-up, T may have sizeable couplings to both left- and right-handed Standard Model quarks q. However, in the case of one single light VL quark, which is the simple case studied here, it is easy to show that only one of the two mixing angles is large, the other being suppressed by a factor of m_q/M [107]. Following this observation, we simplify the parametrisation by neglecting the suppressed mixing angles, so that (A.1.1) will only contain one of the two chiral couplings: this approximation may not be precise for the top quark, but is numerically well justified for all other quarks. A discussion of the terms suppressed by the top mass m_t, which are generally model-dependent, is detailed in [109].

[1] Couplings to the Z, to the W and other VL quarks, are also in general present but depend on the representation of $SU(2)_L$ T belongs to.

From the Lagrangian in Eq.(A.1.1), the partial widths in the various channels are given by

$$\begin{aligned}
\Gamma(T \to W d_i) &= \kappa_W^2 |V_{L/R}^{4i}|^2 \frac{M^3 g^2}{64\pi m_W^2} \Gamma_W(M, m_W, m_{d_i}) \,, \\
\Gamma(T \to Z u_i) &= \kappa_Z^2 |V_{L/R}^{4i}|^2 \frac{M^3 g^2}{64\pi m_W^2} \Gamma_Z(M, m_Z, m_{u_i}) \,, \\
\Gamma(T \to H u_i) &= \kappa_H^2 |V_{L/R}^{4i}|^2 \frac{M^3 g^2}{64\pi m_W^2} \Gamma_H(M, m_H, m_{u_i}) \,, \qquad \text{(A.1.2)}
\end{aligned}$$

where the kinematic functions are

$$\begin{aligned}
\Gamma_W &= \lambda^{\frac{1}{2}}(1, \frac{m_q^2}{M^2}, \frac{m_W^2}{M^2}) \left[\left(1 - \frac{m_q^2}{M^2}\right)^2 + \frac{m_W^2}{M^2} - 2\frac{m_W^4}{M^4} + \frac{m_W^2 m_q^2}{M^4} \right] , \\
\Gamma_Z &= \frac{1}{2}\lambda^{\frac{1}{2}}(1, \frac{m_q^2}{M^2}, \frac{m_Z^2}{M^2}) \left[\left(1 - \frac{m_q^2}{M^2}\right)^2 + \frac{m_Z^2}{M^2} - 2\frac{m_Z^4}{M^4} + \frac{m_Z^2 m_q^2}{M^4} \right] , \\
\Gamma_H &= \frac{1}{2}\lambda^{\frac{1}{2}}(1, \frac{m_q^2}{M^2}, \frac{m_H^2}{M^2}) \left[1 + \frac{m_q^2}{M^2} - \frac{m_H^2}{M^2} \right] ; \qquad \text{(A.1.3)}
\end{aligned}$$

and the function $\lambda(a, b, c)$ is given by

$$\lambda(a, b, c) = a^2 + b^2 + c^2 - 2ab - 2ac - 2bc \,. \qquad \text{(A.1.4)}$$

We expressed the partial width in a fashion that underlines the universal coupling factor, so that the difference between various channels only depends on the values of the masses. For the light quarks, the mass dependence is very mild, therefore we can assume that the numbers are the same for all generations. This is not true in general for the top quark, for which the effect of its mass may be important: as we neglected it in the mixing angles, we will consistently neglect it here.

Neglecting the SM quark masses, the branching ratios can be written as:

$$BR(T \to V q_i) = \frac{\kappa_V^2 |V_{L/R}^{4i}|^2 \Gamma_V^0}{\left(\sum_{j=1}^3 |V_{L/R}^{4j}|^2\right)\left(\sum_{V'=W,Z,H} \kappa_{V'}^2 \Gamma_{V'}^0\right)} \tag{A.1.5}$$

where Γ_V^0 are the kinematic functions for zero quark mass $m_q = 0$:

$$\begin{aligned}
\Gamma_W^0 &= \left(1 - 3\frac{m_W^4}{M^4} + 2\frac{m_W^6}{M^6}\right) \sim 1 + \mathcal{O}(M^{-4})\,, \\
\Gamma_Z^0 &= \frac{1}{2}\left(1 - 3\frac{m_Z^4}{M^4} + 2\frac{m_Z^6}{M^6}\right) \sim \frac{1}{2} + \mathcal{O}(M^{-4})\,, \\
\Gamma_H^0 &= \frac{1}{2}\left(1 - \frac{m_H^2}{M^2}\right)^2 \sim \frac{1}{2} - \frac{m_H^2}{M^2} + \mathcal{O}(M^{-4})\,.
\end{aligned} \tag{A.1.6}$$

These branching ratios can be defined in terms of four independent parameters which contain all the necessary information:

$$\zeta_i = \frac{|V_{L/R}^{4i}|^2}{\sum_{j=1}^3 |V_{L/R}^{4j}|^2}\,, \quad \sum_{i=1}^3 \zeta_i = 1\,, \tag{A.1.7}$$

$$\xi_V = \frac{\kappa_V^2 \Gamma_V^0}{\sum_{V'=W,Z,H} \kappa_{V'}^2 \Gamma_{V'}^0}\,, \quad \sum_{V=W,Z,H} \xi_V = 1\,; \tag{A.1.8}$$

so that

$$BR(T \to V q_i) = \zeta_i \xi_V\,. \tag{A.1.9}$$

For experimental purposes, the decays into first or second generation cannot be distinguished: so that all the results can be written in terms of the decay rates into light generations via $\zeta_{jet} = \zeta_1 + \zeta_2 = 1 - \zeta_3$. From these definitions, we can express the branching ratios as

$$\begin{aligned}
BR(T \to Zj) &= \zeta_{jet}\xi_Z\,, & BR(T \to Zt) &= \zeta_3 \xi_Z\,, \\
BR(T \to Hj) &= \zeta_{jet}\xi_H\,, & BR(T \to Ht) &= \zeta_3 \xi_H\,, \\
BR(T \to W^+ j) &= \zeta_{jet}\xi_W\,, & BR(T \to W^+ b) &= \zeta_3 \xi_W\,.
\end{aligned} \tag{A.1.10}$$

where $\zeta_{jet} = 1 - \zeta_3$ and $\xi_H = 1 - \xi_W - \xi_Z$. When studying pair production of T, which is dominated by model-independent QCD processes only sensitive to the mass of the VL quark, the phenomenology of the T can be therefore completely described in terms of 4 independent parameters: the mass M, and three additional parameters which we will choose as ξ_W, ξ_Z and ζ_{jet}. We note that single production processes may be sensitive to the separate values of ζ_1 and ζ_2, so the number of relevant parameters can be increased by one unit.

We can finally re-express the Lagrangian in Eq.(A.1.1) in terms of the relevant parameters as follows:

$$\begin{aligned}\mathcal{L} &= \kappa_T \left\{ \sqrt{\frac{\zeta_i \xi_W}{\Gamma^0_W}} \frac{g}{\sqrt{2}} \left[\bar{T}_{L/R} W^+_\mu \gamma^\mu d^i_{L/R}\right] + \sqrt{\frac{\zeta_i \xi_Z}{\Gamma^0_Z}} \frac{g}{2c_W} \left[\bar{T}_{L/R} Z_\mu \gamma^\mu u^i_{L/R}\right] \right. \\ &- \left. \sqrt{\frac{\zeta_i (1 - \xi_Z - \xi_W)}{\Gamma^0_H}} \frac{M}{v} \left[\bar{T}_{R/L} H\, u^i_{L/R}\right] \right\} + h.c. \end{aligned} \tag{A.1.11}$$

Recalling that $\xi_H = 1 - \xi_Z - \xi_W$, one finally recovers the contribution of a T quark to Eq.(3.2.2). The new parameter κ_T is an overall coupling strength measure: it is not relevant for the branching ratios, nor for pair production (which is to a very good approximation due to QCD processes), however it will determine the strength of single production. It can be written in terms of the parameters in the starting Lagrangian as

$$\kappa_T = \sqrt{\sum_{i=1}^{3} |V^{4i}_{L/R}|^2} \sqrt{\sum_V \kappa^2_V \Gamma^0_V}\,. \tag{A.1.12}$$

It is important to notice that the $V^{4i}_{L/R}$ matrix elements are, in general, complex quantities. Since the parameters ζ_i are proportional to the square of mixing matrix entries, the information about phases is lost in the parametrisation in Eq.(A.1.11). Such phases may be present in the mixing with light quarks, and are crucial when considering the flavour bounds on the couplings ; however they will play a minor role in the LHC phenomenology which is the main focus of this parametrisation.

Appendix B

Numerical results for VLQ single production

B.1 FeynRules model and validation

In this appendix we summarise the implementation and the validation of the model-independent parametrisation provided by Eq.(3.2.2) in FeynRules [111]. As detailed in Section 3.2.1, we restrict the present analysis to the case of the four generic states $X_{5/3}$, $T_{2/3}$, $B_{-1/3}$ and $Y_{-4/3}$ which decay directly into a pair of standard model particles. The common procedure for introducing such new states is to define new class members within a given $SU(2)_L$ representation, with appropriate `Indices` definitions for each particle class. In the present study, we start from the Standard Model implementation and add them as the new coloured spin 1/2 objects:

```
F[5] == {
ClassName->xq,
ClassMembers->{x},
SelfConjugate->False,
Indices->{Index[Colour]},
QuantumNumbers->{Q->5/3},
Mass->{MX,600},
PDG->{6000005},
},

F[7] == {
ClassName->bpq,
ClassMembers->{bp},
SelfConjugate->False,
Indices->{Index[Colour]},
QuantumNumbers->{Q->-1/3},
Mass->{MBP,600},
PDG->{6000007}
},

F[6] == {
ClassName->tpq,
ClassMembers->{tp},
SelfConjugate->False,
Indices->{Index[Colour]},
QuantumNumbers->{Q->2/3},
PDG->{6000006},
},

F[8] == {
ClassName->yq,
ClassMembers->{y},
SelfConjugate->False,
Indices->{Index[Colour]},
QuantumNumbers->{Q->-4/3},
Mass->{MY,600},
PDG->{6000008}
}
```

Here each `ClassName` defines a specific VL quark class with a given electric charge. Such definitions are made without any assumptions on the other quantum numbers. Any change in the above PDG codes should not interfere with the existing assignments. The masses are set to 600 GeV by default, while the total widths should be systematically evaluated within MadGraph and given as inputs in the corresponding parameter cards. For an appropriate evaluation of the $2 \to 2$ processes cross-sections, all light quarks included in the proton definition are restricted to be massless (5F scheme). In addition to the VL quark masses and widths, the remaining parameters are divided into the three `External` classes `KAPPA`, `XI` and `ZETA`, combined internally in FeynRules to match the effective couplings defined in Eq.(3.2.2).

Having defined the new quark fields and all relevant parameters, the interactions given in Eq.(3.2.2) have been added to the Standard Model Lagrangian of FeynRules, together with the corresponding kinetic and mass terms for all quark species. The electromagnetic and strong currents are implemented as

well. All the model files are provided in the Universal Feynrules Output (UFO) format and support the unitary gauge (`Set FeynmanGauge = False`). We comment that, depending on the representation they belong to, the new VL quarks can induce sizeable corrections to the Standard Model quark mixings, which are not included here. However, for the LHC phenomenology, they are irrelevant so that we restrict the implementation to the model independent couplings involving a single vector-like quark, without limiting the utility of such implementation.

As a first step of the validation procedure, all the tree-level decay rates have been checked to match the results from the analytical formulae (A.1.2) for various benchmark points. The particles decay widths and branching ratios have also been calculated with BRIDGE [133], and successfully compared to the analytical formulae. As a second step, a comparison of the leading order coefficients $\bar{\sigma}^{Qt}$ and $\bar{\sigma}^{QV}$ has been performed between MadGraph5 [132] and an independent model implementation of Eq. (3.2.2) in CalcHEP 3.4 [153], for similar parameter choices. Although deviations up to 10% can be obtained for particular cases of $\bar{\sigma}^{Qq}$ between MadGraph5 and CalcHEP, the Qq channels rates obtained from the UFO output have been verified to be consistent with [128]. Considering the case of exclusive couplings to the first generation, $\zeta_1 = 1$, cross-sections agree at the percent level when comparing $\sigma(pp \to Qq)$ versus $\sigma(pp \to \bar{Q}q)$ for all four VL quark types and the two benchmark points given in the reference. Finally, we have checked that the MadGraph cross-sections for pair and electroweak single production of top partners at the LHC at $\sqrt{s} = 7, 8$ and 14 TeV match the leading order predictions for the top quark in the Standard Model, when adjusting the mass and width values. Overall consistency at the % level is obtained.

B.2 Tables of cross sections

In Tabs. B.1-B.6 we provide the expansion coefficients for the single production cross sections of all the VLQ species discussed in Chapter 3. The cross sections have been computed at different LHC energies for particles with mass $M = 600$, 800, and 1000 GeV.

	7 TeV			8 TeV			14 TeV		
	$i=1$	$i=2$	$i=3$	$i=1$	$i=2$	$i=3$	$i=1$	$i=2$	$i=3$
$\bar{\sigma}_{Wi}^{T\bar{t}}$	893	68.4	20.7	1441	123	39.1	7580	985	373
$\bar{\sigma}_{Zi}^{T\bar{t}}$	–	–	4.22	–	–	6.28	–	–	2.47
$\bar{\sigma}_{Wi}^{Bt}$	2314	34.5	–	3605	64.5	–	16700	588	–
$\bar{\sigma}_{Wi}^{B\bar{t}}$	–	–	2.04	–	–	3.14	–	–	13.8
$\bar{\sigma}_{Wi}^{X\bar{t}}$	2277	33.9	7.01	3546	63.2	10.0	16640	578	33.6
$\bar{\sigma}_{Wi}^{Yt}$	936	71.2	22.3	1507	128	42.7	7911	1021	405
$\bar{\sigma}_{Wi}^{Tj}$	34150	4943	1906	45420	7316	2957	125000	29400	13970
$\bar{\sigma}_{Zi}^{Tj}$	48000	1770	–	63200	2760	–	171000	13400	–
$\bar{\sigma}_{Wi}^{Bj}$	39500	1140	–	53000	2090	–	152000	10800	–
$\bar{\sigma}_{Zi}^{Bj}$	22500	3030	1130	30400	4550	1790	91000	19600	9080
$\bar{\sigma}_{Wi}^{Xj}$	72900	2950	–	94000	4520	–	232000	20400	–
$\bar{\sigma}_{Wi}^{Yj}$	18600	2290	831	25600	3510	1340	80500	16200	7250
$\bar{\sigma}_{Wi}^{TW}$	1300	106	32.9	2070	187	60.9	10700	1420	545
$\bar{\sigma}_{Wi}^{BW}$	3270	53.5	–	5040	97.9	–	23400	840	–
$\bar{\sigma}_{Wi}^{XW}$	3270	53.5	–	5040	97.9	–	23400	840	–
$\bar{\sigma}_{Wi}^{YW}$	1300	106	33.0	2070	187	60.9	10700	1420	545
$\bar{\sigma}_{Zi}^{TZ}$	3370	55.0	–	5200	101	–	24200	869	–
$\bar{\sigma}_{Zi}^{BZ}$	1340	109	33.9	2130	193	62.6	11100	1470	563
$\bar{\sigma}_{Hi}^{TH}$	2460	34.5	–	3610	64.5	–	16900	588	–
$\bar{\sigma}_{Hi}^{BH}$	965	74.1	22.5	1560	133	42.4	8560	1090	409

Table B.1: Coefficients (in fb) for single production of VL quarks with mass $M = 600$ GeV. $\bar{\sigma}_C^{AB}$ is the coefficient in the expansion, corresponding to the production of a VL quark A in association with a particle B due to the exchange of C, where j labels a jet (including the b quark). Bottom quarks have been included among proton components and as final states in Qj processes. Contributions of interference terms are neglected as we have checked they give a negligible effect.

	7 TeV			8 TeV			14 TeV		
	$i=1$	$i=2$	$i=3$	$i=1$	$i=2$	$i=3$	$i=1$	$i=2$	$i=3$
$\bar{\sigma}^{\bar{T}t}_{Wi}$	138	68.7	20.7	244	124	39.1	1800	992	373
$\bar{\sigma}^{\bar{T}t}_{Zi}$	–	–	4.21	–	–	6.28	–	–	24.7
$\bar{\sigma}^{\bar{B}t}_{Wi}$	105	34.4	–	186	64.5	–	1410	590	–
$\bar{\sigma}^{\bar{B}t}_{Wi}$	–	–	6.36	–	–	9.21	–	–	32.3
$\bar{\sigma}^{\bar{X}t}_{Wi}$	103	34.0	2.31	184	63.8	3.51	1390	581	14.9
$\bar{\sigma}^{\bar{Y}t}_{Wi}$	143	71.2	22.5	254	128	42.6	1860	1020	405
$\bar{\sigma}^{\bar{T}j}_{Wi}$	4010	2160	783	6040	3330	1270	25600	15500	6950
$\bar{\sigma}^{\bar{T}j}_{Zi}$	4010	1680	–	5990	2620	–	25300	12900	–
$\bar{\sigma}^{\bar{B}j}_{Wi}$	6510	2780	–	9590	4260	–	37400	19500	–
$\bar{\sigma}^{\bar{B}j}_{Zi}$	5240	2870	1080	7720	4330	1700	30500	19000	8720
$\bar{\sigma}^{\bar{X}j}_{Wi}$	3030	1240	–	4640	1970	–	20900	10400	–
$\bar{\sigma}^{\bar{Y}j}_{Wi}$	8380	4660	1780	12100	6930	2770	44400	28300	13300
$\bar{\sigma}^{\bar{T}W}_{Wi}$	210	106	33.0	365	187	60.9	2570	1420	545
$\bar{\sigma}^{\bar{B}W}_{Wi}$	158	53.7	–	275	98.1	–	1990	848	–
$\bar{\sigma}^{\bar{X}W}_{Wi}$	158	53.7	–	275	98.1	–	2000	846	–
$\bar{\sigma}^{\bar{Y}W}_{Wi}$	210	106	33.0	365	187	60.9	2570	1420	545
$\bar{\sigma}^{\bar{T}Z}_{Zi}$	163	55.2	–	283	101	–	2060	870	–
$\bar{\sigma}^{\bar{B}Z}_{Zi}$	216	109	33.9	376	193	62.6	2650	1470	563
$\bar{\sigma}^{\bar{T}H}_{Hi}$	111	36.8	–	198	68.8	–	1540	637	–
$\bar{\sigma}^{\bar{B}H}_{Hi}$	148	73.9	22.5	263	134	42.44	1990	1090	409

Table B.2: The same as Tab. B.1 for VL antiquarks.

	7 TeV			8 TeV			14 TeV		
	$i=1$	$i=2$	$i=3$	$i=1$	$i=2$	$i=3$	$i=1$	$i=2$	$i=3$
$\bar{\sigma}^{T\bar{t}}_{Wi}$	398	24.8	7.07	692	49.0	14.6	4520	508	183
$\bar{\sigma}^{T\bar{t}}_{Zi}$	–	–	1.06	–	–	1.69	–	–	8.28
$\bar{\sigma}^{Bt}_{Wi}$	1090	11.8	–	1820	24.1	–	10400	289	–
$\bar{\sigma}^{B\bar{t}}_{Wi}$	–	–	0.485	–	–	0.803	–	–	4.42
$\bar{\sigma}^{X\bar{t}}_{Wi}$	1080	11.7	1.90	1810	23.9	2.92	10300	287	12.1
$\bar{\sigma}^{Yt}_{Wi}$	418	25.9	7.59	724	50.9	15.7	4710	525	196
$\bar{\sigma}^{Tj}_{Wi}$	16910	1915	674	23750	3040	1130	75400	14900	6670
$\bar{\sigma}^{Tj}_{Zi}$	24400	618	–	33700	1040	–	104000	6290	–
$\bar{\sigma}^{Bj}_{Wi}$	19200	436	–	27200	748	–	90500	4940	–
$\bar{\sigma}^{Bj}_{Zi}$	10680	1130	392	15300	1830	665	53000	9700	4230
$\bar{\sigma}^{Xj}_{Wi}$	38600	1060	–	52100	1740	–	147000	9880	–
$\bar{\sigma}^{Yj}_{Wi}$	8400	814	272	12300	1340	473	45400	7730	3270
$\bar{\sigma}^{TW}_{Wi}$	363	23.2	6.70	631	45.3	13.7	4260	470	170
$\bar{\sigma}^{BW}_{Wi}$	984	11.0	–	1650	22.2	–	9850	264	–
$\bar{\sigma}^{XW}_{Wi}$	984	11.0	–	1650	22.2	–	9850	264	–
$\bar{\sigma}^{YW}_{Wi}$	363	23.2	6.70	631	45.3	13.7	4260	470	170
$\bar{\sigma}^{TZ}_{Zi}$	1010	11.2	–	1690	22.8	–	10100	270	–
$\bar{\sigma}^{BZ}_{Zi}$	372	23.7	6.85	646	46.3	14.0	4360	480	174
$\bar{\sigma}^{TH}_{Hi}$	794	8.18	–	1350	16.9	–	8460	216	–
$\bar{\sigma}^{BH}_{Hi}$	289	17.6	4.98	511	35.0	10.4	3630	388	138

Table B.3: The same as Tab. B.1 for $M = 800$ GeV.

	7 TeV			8 TeV			14 TeV		
	$i=1$	$i=2$	$i=3$	$i=1$	$i=2$	$i=3$	$i=1$	$i=2$	$i=3$
$\bar{\sigma}_{Wi}^{\bar{T}t}$	50.7	25.0	7.11	99.0	49.2	14.7	953	509	183
$\bar{\sigma}_{Zi}^{\bar{T}t}$	–	–	1.05	–	–	1.69	–	–	8.28
$\bar{\sigma}_{Wi}^{\bar{B}t}$	39.0	11.8	–	75.2	24.2	–	734	290	–
$\bar{\sigma}_{Wi}^{\bar{B}t}$	–	–	1.68	–	–	2.62	–	–	11.3
$\bar{\sigma}_{Wi}^{\bar{X}t}$	38.8	11.7	0.563	74.7	24.0	0.920	727	287	4.86
$\bar{\sigma}_{Wi}^{\bar{Y}t}$	52.6	25.8	7.56	103	50.9	15.7	988	525	196
$\bar{\sigma}_{Wi}^{\bar{T}j}$	1510	778	259	2440	1290	452	12900	7500	3160
$\bar{\sigma}_{Zi}^{\bar{T}j}$	1550	591	–	2480	994	–	12800	6120	–
$\bar{\sigma}_{Wi}^{\bar{B}j}$	2610	1010	–	4100	1670	–	19500	9510	–
$\bar{\sigma}_{Zi}^{\bar{B}j}$	2080	1090	374	3290	1760	636	15900	9440	4100
$\bar{\sigma}_{Wi}^{\bar{X}j}$	1120	414	–	1830	714	–	10200	4770	–
$\bar{\sigma}_{Wi}^{\bar{Y}j}$	3450	1820	638	5350	2910	1070	23900	14400	6420
$\bar{\sigma}_{Wi}^{\bar{T}W}$	46.9	23.2	6.70	90.8	45.3	13.7	882	471	170
$\bar{\sigma}_{Wi}^{\bar{B}W}$	35.9	11.0	–	68.8	22.3	–	673	266	–
$\bar{\sigma}_{Wi}^{\bar{X}W}$	35.9	11.0	–	68.8	22.3	–	673	266	–
$\bar{\sigma}_{Wi}^{\bar{Y}W}$	46.9	23.2	6.70	90.8	45.3	13.7	882	471	170
$\bar{\sigma}_{Zi}^{\bar{T}Z}$	36.7	11.3	–	70.4	22.8	–	689	272	–
$\bar{\sigma}_{Zi}^{\bar{B}Z}$	48.1	23.7	6.85	93.0	46.4	14.0	902	482	174
$\bar{\sigma}_{Hi}^{\bar{T}H}$	27.4	8.23	–	53.6	17.0	–	556	215	–
$\bar{\sigma}_{Hi}^{\bar{B}H}$	35.6	17.6	4.98	70.5	35.0	10.4	731	387	138

Table B.4: The same as Tab. B.2 for $M = 800$ GeV.

	7 TeV			8 TeV			14 TeV		
	$i=1$	$i=2$	$i=3$	$i=1$	$i=2$	$i=3$	$i=1$	$i=2$	$i=3$
$\bar{\sigma}^{T\bar{t}}_{Wi}$	183	9.44	2.56	343	20.4	5.80	2800	275	95.1
$\bar{\sigma}^{T\bar{t}}_{Zi}$	–	–	0.302	–	–	0.526	–	–	3.23
$\bar{\sigma}^{Bt}_{Wi}$	534	4.27	–	955	9.56	–	6700	150	–
$\bar{\sigma}^{B\bar{t}}_{Wi}$	–	–	0.133	–	–	0.239	–	–	1.66
$\bar{\sigma}^{X\bar{t}}_{Wi}$	528	4.23	0.577	947	9.50	0.965	6650	150	4.99
$\bar{\sigma}^{Yt}_{Wi}$	192	9.83	2.72	360	21.2	6.17	2920	285	101
$\bar{\sigma}^{Tj}_{Wi}$	8830	800	261	13100	1370	470	48700	8250	3490
$\bar{\sigma}^{Tj}_{Zi}$	13100	236	–	19100	428	–	68000	3260	–
$\bar{\sigma}^{Bj}_{Wi}$	9850	158	–	14800	296	–	57600	2470	–
$\bar{\sigma}^{Bj}_{Zi}$	5380	460	148	8160	800	272	33200	5250	2170
$\bar{\sigma}^{Xj}_{Wi}$	21400	414	–	30500	739	–	98900	5220	–
$\bar{\sigma}^{Yj}_{Wi}$	4040	316	97.8	6280	566	185	27700	4070	1630
$\bar{\sigma}^{TW}_{Wi}$	116	5.94	1.63	220	12.9	3.70	1940	183	62.6
$\bar{\sigma}^{BW}_{Wi}$	337	2.68	–	613	6.03	–	4700	98.2	–
$\bar{\sigma}^{XW}_{Wi}$	337	2.68	–	613	6.03	–	4700	98.2	–
$\bar{\sigma}^{YW}_{Wi}$	116	5.94	1.63	220	12.9	3.70	1940	183	62.6
$\bar{\sigma}^{TZ}_{Zi}$	343	2.73	–	625	6.16	–	4780	99.8	–
$\bar{\sigma}^{BZ}_{Zi}$	118	6.06	1.66	225	13.2	3.76	1970	186	63.7
$\bar{\sigma}^{TH}_{Hi}$	283	2.10	–	524	4.84	–	4190	83.6	–
$\bar{\sigma}^{BH}_{Hi}$	96.2	4.73	1.28	186	10.5	2.96	1720	158	53.2

Table B.5: The same as Tab. B.1 for $M = 1000$ GeV.

	7 TeV			8 TeV			14 TeV		
	$i=1$	$i=2$	$i=3$	$i=1$	$i=2$	$i=3$	$i=1$	$i=2$	$i=3$
$\bar{\sigma}^{\bar{T}t}_{Wi}$	19.4	9.49	2.58	41.7	20.5	5.83	529	276	95.4
$\bar{\sigma}^{\bar{T}t}_{Zi}$	–	–	0.302	–	–	0.526	–	–	3.23
$\bar{\sigma}^{\bar{B}t}_{Wi}$	15.3	4.26	–	32.1	9.59	–	402	151	–
$\bar{\sigma}^{\bar{B}t}_{Wi}$	–	–	0.499	–	–	0.850	–	–	4.63
$\bar{\sigma}^{\bar{X}t}_{Wi}$	15.3	4.26	0.158	32.1	9.55	0.280	400	150	1.85
$\bar{\sigma}^{\bar{Y}t}_{Wi}$	20.1	9.81	2.71	43.3	21.2	6.14	549	285	101
$\bar{\sigma}^{\bar{T}j}_{Wi}$	606	303	93.8	1070	544	178	7040	3950	1580
$\bar{\sigma}^{\bar{T}j}_{Zi}$	654	227	–	1120	414	–	7030	3180	–
$\bar{\sigma}^{\bar{B}j}_{Wi}$	1130	398	–	1900	710	–	11000	5080	–
$\bar{\sigma}^{\bar{B}j}_{Zi}$	881	445	142	1500	775	262	8930	5120	2110
$\bar{\sigma}^{\bar{X}j}_{Wi}$	450	152	–	793	285	–	5470	2400	–
$\bar{\sigma}^{\bar{Y}j}_{Wi}$	1500	769	249	2530	1320	450	13800	8020	3380
$\bar{\sigma}^{\bar{T}W}_{Wi}$	12.2	5.98	1.63	26.3	13.0	3.70	351	183	62.6
$\bar{\sigma}^{\bar{B}W}_{Wi}$	9.63	2.69	–	20.3	6.04	–	266	98.7	–
$\bar{\sigma}^{\bar{X}W}_{Wi}$	9.63	2.69	–	20.3	6.04	–	266	98.7	–
$\bar{\sigma}^{\bar{Y}W}_{Wi}$	12.2	5.98	1.63	26.3	13.0	3.70	351	183	62.6
$\bar{\sigma}^{\bar{T}Z}_{Zi}$	9.80	2.74	–	20.7	6.15	–	271	101	–
$\bar{\sigma}^{\bar{B}Z}_{Zi}$	12.4	6.09	1.66	26.7	13.2	3.76	358	187	63.7
$\bar{\sigma}^{\bar{T}H}_{Hi}$	7.72	2.11	–	16.6	4.84	–	230	84.0	–
$\bar{\sigma}^{\bar{B}H}_{Hi}$	9.68	4.75	1.28	21.4	10.5	2.96	304	157	53.2

Table B.6: The same as Tab. B.2 for $M = 1000$ GeV.

Appendix C

Description of the XQCAT code

In this appendix we provide complementary information on the software XQCAT presented in Chapter 4. We present successively the methods used for the determination of the exclusion CLs, the validation of the different parts of the code, and the limitations regarding its applicability to selected New Physics scenarios.

C.1 Determination of the eCLs

In the presented version of the XQCAT code, we are quick to point out that the interpolation of mass points is among the main factors that could affect our conservative estimate of the simulated mass limits within a given scenario. Since the efficiencies can only be computed for a limited number of quark masses, caution must be exercised when extracting limits on the full mass range of interest. When computing the eCL for a given mass between two simulated values, we interpolate the result by relying on several methods, described in the following. We have checked that they lead to similar results.

Once the number of background events (including their uncertainty) is estimated from our tool for a given number of observed events, the eCL for a specific signature and a given number of signal events is expressed via ratio

of p-values of the Poissonian distributions for the background-only hypothesis and signal-plus-background hypothesis,

$$eCL = 1 - \frac{CL(s+b)}{CL(b)} = 1 - \frac{1 - \text{p-value}(s+b)}{1 - \text{p-value}(b)}. \tag{C.1.1}$$

This formula can be extended to the case of multiple channels (or bins of the analysis) by introducing products of p-values. Such an approximation is quite reasonable to reproduce as accurately as possible the experimental bounds by the CMS collaboration, and obtain results without performing a full analysis. Although our objective is to carry out an accurate yet conservative analysis, several points need attention.

As an illustration, we consider a general scenario where the masses of the top partners are different from the simulated ones, i.e., masses in the range $400 - 2000$ GeV with steps of 100 GeV. In such a case, the accuracy in the determination of the eCL is limited by two factors: firstly, the impossibility of fully reproducing the experimental selection and kinematical cuts; secondly, the size of the gaps between the simulated masses. The first factor can only be quantified by performing validation steps as described in the following. The second factor is a technical limitation that can be reduced by performing scans in the quark masses with smaller mass gaps. However, one needs to be careful when trying to determine eCLs for generic mass values: even if assuming a smooth behaviour of the efficiency as a function of the mass, there may be non-trivial effects in the mass range, like a sudden change in the efficiency. Since we do not have information about the selection efficiencies and kinematics cuts, one cannot be sure to have a correct estimate of the efficiency. A very fine scan in the masses not being possible due to the computational weight of the Monte Carlo (MC) generation, there are however methods to determine a reliable eCL in the general case. In order to provide results as accurate as possible, we adopted different combinations of these methods depending on the considered situation.

1. *Linear interpolation of efficiencies* The simplest approach is to determine the number of events for a generic mass configuration by linearly interpolating the efficiencies between the closest simulated mass values for each pair-produced quark in the given scenario. Supposing that we

want to analyse the case for a single top partner with its mass m_Q in the interval $[m^{\downarrow}, m^{\uparrow}]$, where $m^{\downarrow}$ and $m^{\uparrow}$ are the masses for which the simulated efficiencies are known, the number of events corresponding to m_Q, in the search bin k,are

$$\#\text{ events}(k, m_Q) = L\,\sigma_{\text{pair}}(m_Q)\,\sum \text{BR}(Q \to F)\,\text{BR}(Q \to F')\,\epsilon^{FF'}(k, m_Q) \tag{C.1.2}$$

where L is the integrated luminosity, $\sigma_{\text{pair}}(m_Q)$ the pair production cross section at the mass m_Q, F and F' are the possible final states Q decays into, and

$$\epsilon(k, m_Q) = \epsilon(k, m^{\downarrow})\frac{m^{\uparrow} - m_Q}{m^{\uparrow} - m^{\downarrow}} + \epsilon(k, m^{\uparrow})\frac{m_Q - m^{\downarrow}}{m^{\uparrow} - m^{\downarrow}}. \tag{C.1.3}$$

This approach assumes that the fluctuations in the efficiencies are small between the simulated values and that the number of signal events is mostly driven by the decrease in the production cross section. This can be a quite strong requirement, especially if the total number of events comes from the interplay of a large number of channels.

2. *Determination of a range for confidence levels* For any given scenario with N top partners with masses m_{Q_i}, $i = 1, \dots N$, it is possible to compute the eCLs in all the vertices of the N-dimensional cube obtained by raising or lowering the input masses to the closest simulated values. For each quark of mass m_{Q_i}, we define $m_i^{\downarrow}$ ($m_i^{\uparrow}$) the closest simulated mass which is lower (higher) than the the i^{th} quark mass (so that $m_i^{\downarrow} \leq m_{Q_i} \leq m_i^{\uparrow}$). Thus

$$\begin{aligned}
\text{eCL}_{\text{min}} &= \min\left(\text{eCL}(m_1^{\downarrow}, m_2^{\downarrow}, \dots, m_N^{\downarrow}), \dots, \text{eCL}(m_1^{\uparrow}, m_2^{\uparrow}, \dots, m_N^{\uparrow})\right), \\
\text{eCL}_{\text{max}} &= \max\left(\text{eCL}(m_1^{\downarrow}, m_2^{\downarrow}, \dots, m_N^{\downarrow}), \dots, \text{eCL}(m_1^{\uparrow}, m_2^{\uparrow}, \dots, m_N^{\uparrow})\right);
\end{aligned}$$

where the eCLs in the right-hand side of the equations are obtained with the simulated efficiencies. Assuming that the fluctuations of the efficiencies between the simulated values are not too large and that efficiencies do not drastically increase for increasing masses, the eCL of the tested scenario will lie within the minimum and maximum values. As

an illustration, we can consider the case of 2 extra quarks, with masses $m_{Q_1} = 650$ GeV and $m_{Q_2} = 750$ GeV. The simulations have been performed in XQCAT with steps of 100 GeV: therefore, the eCL for this scenario is between the minimum and maximum values of the exclusion eCLs for the $\{m_1, m_2\}$ combinations $\{600, 700\}$, $\{600, 800\}$, $\{700, 700\}$ and $\{700, 800\}$ GeV.

3. *Interpolation of* eCL*s* From the calculation of the eCLs in all corners of the N-dimensional cube, it is possible to perform an Inverse-Distance-Weighted (IDW) interpolation [154] and extract an eCL for the input configuration. This approach still assumes that the efficiencies between the simulated mass values have a smooth behaviour, and can be generalised to the case of multiple top partners. More details on the implementation of this interpolation procedure can be found in [125].

The first method is by far the less computationally expensive, as the other methods require the calculation of eCLs in every corner of an N-dimensional cube, which can be challenging for scenarios with many top partners, as the number of eCLs that must be computed scales as 2^N. Conversely, these more involved methods provide a more accurate, though conservative, determination of the eCL range for a given scenario. It must be added, however, that an increase in the density of the mass scan for the simulation makes the first approach more and more equivalent to the other approaches. Method 2, in fact, will result in smaller and smaller eCL intervals as the scan density increases. The limitation in the density of point that can be coded is due to the heavy MC simulation involved, as many final state channels need to be populated. Nevertheless, in all of the analyses presented in Chapter 4, we have checked that the 3 methods give mass bounds which are very close to each other and within the intrinsic systematic uncertainties of this approach, like the approximate implementation of detector effects and experimental cuts.

C.2 Validation of the framework

C.2.1 Validation of the limit code

The limit code implemented in `XQCAT` has been validated by computing the expected and observed limits using the information provided in the experimental search documentation. This test allows us to determine any discrepancies between the statistical method used in our approach and the one in the CMS analysis [100, 138]. The uncertainty on the signal events has been assumed to be 20%. The results of this test indicate that we can reproduce the experimental expected (observed) mass bounds with a discrepancy of -8% (-6%) considering only the multi-lepton channels. However, due to a different analysis technique, our code is unable to reproduce the mass bounds considering the single lepton-channels in combination with the multi-lepton channels. For these reasons, only the multi-lepton channels has been considered in the implementation of this search in our framework.

C.2.2 Validation of the efficiency extraction code

The extraction of the efficiencies depends on the interplay of different parameters: the most relevant ones are the accuracy of the MC simulation, the correct reproduction of the true detector effects using a fast detector simulation and the correct reproduction of the experimental selection and kinematic cuts. The offset between our computed number of events and the values quoted in the experimental search can be explained by unavoidable differences in the modeling of the detector and in the implementation of the selection cuts. A further exploration of these discrepancies would require a more precise knowledge of the details of the measurements and a more accurate simulation of detector effects, which are not possible with the information and tools currently available. For this reason, we have decided to omit one of the opposite-sign lepton channel (OS2) from the implementation as – in essence – it cannot be accurately reproduced. The channels used to extract our results with the search [100] are only the first opposite-sign di-lepton (OS1), the same-sign di-lepton (SS) and the tri-lepton (3l) channels. The uncertainty in the number of events has been

set to 30% to take into account both the uncertainty in the efficiencies and the uncertainty in the NLO-NNLL production cross section computed following [146].

C.3 Code restrictions

In this subsection, we discuss various effects that may affect the calculation of eCLs in our implementation of the XQCAT code. Since the main point in our framework is to establish exclusion limits on new heavy quarks in a conservative and robust way, it is extremely important to identify and deal with all possible effects that can reduce the number of predicted signal events. Conversely, an over-conservative estimate would result in too weak bounds, so it is also relevant to take into account any enhancing effect. The main factors which could affect the conservative estimate of the number of signal events and the respective limits are the following.

- *Chain decays between heavy quarks* Decays like $Q \to Q'V$ (where V is any SM boson, W, Z or H) have not been included in the analysis. In principle, their inclusion is straightforward, even though it would require a scan over two masses. However, we have decided not to include them in order to keep the tool simple. Furthermore, even when kinematically allowed, decays directly to SM states tend to always dominate when a sizeable mixing to the standard quarks is allowed, as it is common in explicit models.

- *Decays into other states in the model* Decays like $Q \to qV_{BSM}$, where $V_{\rm BSM}$ is a new boson present in the considered model, have not been included as they are model dependent. Further, typical mass limits on $V_{\rm BSM}$ states may be higher than those on new heavy quarks (especially if their leptonic decays are not suppressed, in which case they can be accessed in Drell-Yan processes), so that such decays are not kinematically possible.

- *Interference effects* In the presence of multiple top partners, there is the possibility that the decays of different states would lead to identical final

states, so that we need to separate the various channels. While interference between the various signal processes may occur, this effect has not been included in the analysis presented in Chapter 4. Interference may occur in the following two situations:

  - two or more top partners with same charge decay into the same channel, such as $T_{1,2}\bar{T}_{1,2} \to ZtZ\bar{t}$: the effect becomes sizeable when the masses of the heavy quarks are close enough compared to their decay width;
  - two or more top partners of different kind produce the same final states: this can only occur for the charged current decays of heavy quarks, if their electric charge is separated by two units. The channels in question are $X\bar{X} \to (W^+u_i)(W^-\bar{u}_j)$ and $B\bar{B} \to (W^-u_i)(W^+\bar{u}_j)$, as well as $Y\bar{Y} \to (W^-d_i)(W^+\bar{d}_j)$ and $T\bar{T} \to (W^+d_i)(W^-\bar{d}_j)$. In this case, however, the interference is always extremely small due to the very different kinematics of the final state.

  The only relevant interference effects, therefore, arise when two or more same-charge states are degenerate enough. A first quantitative estimate of these effects is provided in [155].

- *Loop corrections to masses and mixing* A potentially relevant effect comes from NLO corrections to the masses and mixings of the top partners, as they may, for instance, remove or add degeneracies, or change the BRs. However, such effects are highly model dependent and it is left to the user to check whether they are relevant in the model of interest: loop corrected masses and BRs can be provided as input to `XQCAT`. While not discussed in Chapter 4, a detailed and quantitative treatment of this dynamics may be included into the code by applying the technique proposed in [156] to fermion propagators and its implementation will be considered in a future upgrade of the code.

- *Higher order cross section* The pair production cross section receives sizeable QCD corrections. Under the approximation that the kinematics is unaffected by the latter, the effect can be added via a model independent k-factor. Therefore, we have considered for our simulation the cross

sections computed at Next-to-Leading Order supplemented by Next-to-Next-Leading-Logarithmic resummation (NLO-NNLL) in QCD in [146]. Electroweak loop corrections may also be relevant, however, they are model dependent and they are expected to be smaller than the QCD ones.

C.4 Numerical results

Scenario	eCLs interpolation		efficiencies interpolation	
	B2G-12-015	SUSY combination	B2G-12-015	SUSY combination
T singlet mixing with 1^{st} generation only $\mathrm{BR}(Wb) = 0$ $\mathrm{BR}(Zt) = 0$ $\mathrm{BR}(Ht) = 0$ $\mathrm{BR}(Wd) = 0.5$ $\mathrm{BR}(Zu) = 0.25$ $\mathrm{BR}(Hu) = 0.25$	×	422	×	469
T singlet mixing with 3^{rd} generation only $\mathrm{BR}(Wb) = 0.5$ $\mathrm{BR}(Zt) = 0.25$ $\mathrm{BR}(Ht) = 0.25$ $\mathrm{BR}(Wd) = 0$ $\mathrm{BR}(Zu) = 0$ $\mathrm{BR}(Hu) = 0$	614	525	634	560
T singlet mixing with 1^{st} and 3^{rd} generation $\mathrm{BR}(Wb) = 0.25$ $\mathrm{BR}(Zt) = 0.125$ $\mathrm{BR}(Ht) = 0.125$ $\mathrm{BR}(Wd) = 0.25$ $\mathrm{BR}(Zu) = 0.125$ $\mathrm{BR}(Hu) = 0.125$	529	465	564	493
T quark decaying 100% to W + jet	×	406	×	425
T quark decaying 100% to Z + jet	×	566	×	590
T quark decaying 100% to H + jet	×	×	×	×
T quark decaying 100% to W + b	605	427	615	475
T quark decaying 100% to Z + top	720	638	743	671
T quark decaying 100% to H + top	608	542	624	577
T quark decaying 50% to W + jet, 50% to W + b	529	409	564	438
T quark decaying 50% to Z + jet, 50% to Z + top	637	608	667	623
T quark decaying 50% to H + jet, 50% to H + top	520	479	553	494

Table C.1: 95% CL mass bounds in GeV for a pair-produced vector-like quark T, considering representative benchmark scenarios for the branching ratios to first generation quarks, third generation quarks, or both. The explicit numerical values of the limits are obtained through the linear interpolation of the eCLs and of the efficiencies, respectively.

Bibliography

[1] S.L. Glashow, "Partial Symmetries of Weak Interactions", *Nucl.Phys.*, vol. 22, pp. 579–588, 1961.

[2] Steven Weinberg, "A Model of Leptons", *Phys.Rev.Lett.*, vol. 19, pp. 1264–1266, 1967.

[3] Murray Gell-Mann, "A Schematic Model of Baryons and Mesons", *Phys.Lett.*, vol. 8, pp. 214–215, 1964.

[4] H. Fritzsch, Murray Gell-Mann, and H. Leutwyler, "Advantages of the Color Octet Gluon Picture", *Phys.Lett.*, vol. B47, pp. 365–368, 1973.

[5] David J. Gross and Frank Wilczek, "Ultraviolet Behavior of Nonabelian Gauge Theories", *Phys.Rev.Lett.*, vol. 30, pp. 1343–1346, 1973.

[6] H. David Politzer, "Reliable Perturbative Results for Strong Interactions?", *Phys.Rev.Lett.*, vol. 30, pp. 1346–1349, 1973.

[7] J. Beringer et al., "Review of Particle Physics (RPP)", *Phys.Rev.*, vol. D86, pp. 010001, 2012.

[8] ATLAS Collaboration; CDF Collaboration; CMS Collaboration; D0 Collaboration, "First combination of Tevatron and LHC measurements of the top-quark mass", ATLAS-CONF-2014-008, CDF-NOTE-11071, CMS-PAS-TOP-13-014, D0-NOTE-6416, 2014.

[9] Chen-Ning Yang and Robert L. Mills, "Conservation of Isotopic Spin and Isotopic Gauge Invariance", *Phys.Rev.*, vol. 96, pp. 191–195, 1954.

[10] Peter W. Higgs, "Broken symmetries, massless particles and gauge fields", *Phys.Lett.*, vol. 12, pp. 132–133, 1964.

[11] Peter W. Higgs, "Broken Symmetries and the Masses of Gauge Bosons", *Phys.Rev.Lett.*, vol. 13, pp. 508–509, 1964.

[12] F. Englert and R. Brout, "Broken Symmetry and the Mass of Gauge Vector Mesons", *Phys.Rev.Lett.*, vol. 13, pp. 321–323, 1964.

[13] J. Goldstone, "Field Theories with Superconductor Solutions", *Nuovo Cim.*, vol. 19, pp. 154–164, 1961.

[14] Jeffrey Goldstone, Abdus Salam, and Steven Weinberg, "Broken Symmetries", *Phys.Rev.*, vol. 127, pp. 965–970, 1962.

[15] Abdelhak Djouadi, "The Anatomy of electro-weak symmetry breaking. I: The Higgs boson in the standard model", *Phys.Rept.*, vol. 457, pp. 1–216, 2008.

[16] K. Nakamura et al., "Review of particle physics", *J.Phys.*, vol. G37, pp. 075021, 2010.

[17] ATLAS Collaboration, "Observation of a new particle in the search for the Standard Model Higgs boson with the ATLAS detector at the LHC", *Phys.Lett.*, vol. B716, pp. 1–29, CERN-PH-EP-2012-218, 2012.

[18] CMS Collaboration, "Observation of a new boson at a mass of 125 GeV with the CMS experiment at the LHC", *Phys.Lett.*, vol. B716, pp. 30–61, CMS-HIG-12-028, 2012.

[19] Nicola Cabibbo, "Unitary Symmetry and Leptonic Decays", *Phys.Rev.Lett.*, vol. 10, pp. 531–533, 1963.

[20] Makoto Kobayashi and Toshihide Maskawa, "CP Violation in the Renormalizable Theory of Weak Interaction", *Prog.Theor.Phys.*, vol. 49, pp. 652–657, 1973.

[21] B. Pontecorvo, "Mesonium and anti-mesonium", *Sov.Phys.JETP*, vol. 6, pp. 429, 1957.

[22] Ziro Maki, Masami Nakagawa, and Shoichi Sakata, "Remarks on the unified model of elementary particles", *Prog.Theor.Phys.*, vol. 28, pp. 870–880, 1962.

[23] S.L. Glashow, J. Iliopoulos, and L. Maiani, "Weak Interactions with Lepton-Hadron Symmetry", *Phys.Rev.*, vol. D2, pp. 1285–1292, 1970.

[24] Martin Schmaltz, "Physics beyond the standard model (theory): Introducing the little Higgs", *Nucl.Phys.Proc.Suppl.*, vol. 117, pp. 40–49, 2003.

[25] S. Dawson, "Introduction to electroweak symmetry breaking", pp. 1–83, Proceedings of the ICTP Summer School in High-Energy Physics and Cosmology, Trieste, 1998.

[26] Christopher F. Kolda and Hitoshi Murayama, "The Higgs mass and new physics scales in the minimal standard model", *JHEP*, vol. 0007, pp. 035, 2000.

[27] Stephen P. Martin, "A Supersymmetry primer", *Adv.Ser.Direct.High Energy Phys.*, vol. 21, pp. 1–153, 2010.

[28] Martin Schmaltz and David Tucker-Smith, "Little Higgs review", *Ann.Rev.Nucl.Part.Sci.*, vol. 55, pp. 229–270, 2005.

[29] Ignatios Antoniadis, K. Benakli, and M. Quiros, "Finite Higgs mass without supersymmetry", *New J.Phys.*, vol. 3, pp. 20, 2001.

[30] Yutaka Hosotani, Shusaku Noda, and Kazunori Takenaga, "Dynamical gauge-Higgs unification in the electroweak theory", *Phys.Lett.*, vol. B607, pp. 276–285, 2005.

[31] Kaustubh Agashe, Roberto Contino, and Alex Pomarol, "The Minimal composite Higgs model", *Nucl.Phys.*, vol. B719, pp. 165–187, 2005.

[32] Nima Arkani-Hamed, Savas Dimopoulos, and G.R. Dvali, "The Hierarchy problem and new dimensions at a millimeter", *Phys.Lett.*, vol. B429, pp. 263–272, 1998.

[33] Lisa Randall and Raman Sundrum, "A Large mass hierarchy from a small extra dimension", *Phys.Rev.Lett.*, vol. 83, pp. 3370–3373, 1999.

[34] Roberto Contino, Leandro Da Rold, and Alex Pomarol, "Light custodians in natural composite Higgs models", *Phys.Rev.*, vol. D75, pp. 055014, 2007.

[35] Christopher T. Hill and Elizabeth H. Simmons, "Strong dynamics and electroweak symmetry breaking", *Phys.Rept.*, vol. 381, pp. 235–402, 2003.

[36] G.F. Giudice, C. Grojean, A. Pomarol, and R. Rattazzi, "The Strongly-Interacting Light Higgs", *JHEP*, vol. 0706, pp. 045, 2007.

[37] Edward Farhi and Leonard Susskind, "Technicolor", *Phys.Rept.*, vol. 74, pp. 277, 1981.

[38] Shinya Matsuzaki and Koichi Yamawaki, "Is 125 GeV techni-dilaton found at LHC?", *Phys.Lett.*, vol. B719, pp. 378–382, 2013.

[39] Roshan Foadi, Mads T. Frandsen, and Francesco Sannino, "125 GeV Higgs from a not so light Technicolor Scalar", *Phys.Rev.*, vol. D87, pp. 095001, 2013.

[40] Mathieu Buchkremer, Jean-Marc Gerard, and Fabio Maltoni, "Closing in on a perturbative fourth generation", *JHEP*, vol. 1206, pp. 135, 2012.

[41] Mathieu Buchkremer and Alexander Schmidt, "Long-lived heavy quarks : a review", *Adv.High Energy Phys.*, vol. 2013, pp. 690254, 2013.

[42] B. Holdom, W.S. Hou, T. Hurth, M.L. Mangano, S. Sultansoy, et al., "Four Statements about the Fourth Generation", *PMC Phys.*, vol. A3, pp. 4, 2009.

[43] Johan Alwall, R. Frederix, J.-M. Gerard, A. Giammanco, M. Herquet, et al., "Is V($_{tb}$) $\simeq$ 1?", *Eur.Phys.J.*, vol. C49, pp. 791–801, 2007.

[44] Graham D. Kribs, Tilman Plehn, Michael Spannowsky, and Timothy M.P. Tait, "Four generations and Higgs physics", *Phys.Rev.*, vol. D76, pp. 075016, 2007.

[45] M. Baak, M. Goebel, J. Haller, A. Hoecker, D. Ludwig, et al., "Updated Status of the Global Electroweak Fit and Constraints on New Physics", *Eur.Phys.J.*, vol. C72, pp. 2003, 2012.

[46] CDF Collaboration, "Search for heavy bottom-like quarks decaying to an electron or muon and jets in $p\bar{p}$ collisions at $\sqrt{s} = 1.96$ TeV", *Phys.Rev.Lett.*, vol. 106, pp. 141803, FERMILAB-PUB-11-023-E, 2011.

[47] CDF Collaboration, "Search for Heavy Top-like Quarks $t' \to Wq$ Using Lepton Plus Jets Events in 1.96-TeV $p\bar{p}$ Collisions", FERMILAB-CONF-08-473-E, 2008.

[48] CMS Collaboration, "Search for heavy bottom-like quarks in 4.9 inverse femtobarns of pp collisions at $\sqrt{s} = 7$ TeV", *JHEP*, vol. 1205, pp. 123, CMS-EXO-11-036, 2012.

[49] CMS Collaboration, "Search for a Heavy Top-like Quark in the Dilepton Final State in pp Collisions at 7 TeV", CMS-PAS-EXO-11-050, 2011.

[50] CMS Collaboration, "Search for heavy, top-like quark pair production in the dilepton final state in pp collisions at $\sqrt{s} = 7$ TeV", *Phys.Lett.*, vol. B716, pp. 103–121, CMS-EXO-11-050, 2012.

[51] Serguei Chatrchyan et al., "Combined search for the quarks of a sequential fourth generation", *Phys.Rev.*, vol. D86, pp. 112003, 2012.

[52] Serguei Chatrchyan et al., "Search for heavy quarks decaying into a top quark and a W or Z boson using lepton + jets events in pp collisions at $\sqrt{s}$ = 7 TeV", *JHEP*, vol. 1301, pp. 154, 2013.

[53] Jens Erler and Paul Langacker, "Precision Constraints on Extra Fermion Generations", *Phys.Rev.Lett.*, vol. 105, pp. 031801, 2010.

[54] Akin Wingerter, "Implications of the Stability and Triviality Bounds on the Standard Model with Three and Four Chiral Generations", *Phys.Rev.*, vol. D84, pp. 095012, 2011.

[55] L3 Collaboration, "Search for heavy neutral and charged leptons in e^+e^- annihilation at LEP", *Phys.Lett.*, vol. B517, pp. 75–85, CERN-EP-2001-046, 2001.

[56] H. Lacker and A. Menzel, "Simultaneous Extraction of the Fermi constant and PMNS matrix elements in the presence of a fourth generation", *JHEP*, vol. 1007, pp. 006, 2010.

[57] Ozgur Cobanoglu, Erkcan Ozcan, Saleh Sultansoy, and Gokhan Unel, "OPUCEM: A Library with Error Checking Mechanism for Computing Oblique Parameters", *Comput.Phys.Commun.*, vol. 182, pp. 1732–1743, 2011.

[58] Giacomo Cacciapaglia, Aldo Deandrea, and Jeremie Llodra-Perez, "Higgs to Gamma Gamma beyond the Standard Model", *JHEP*, vol. 0906, pp. 054, 2009.

[59] S.A. Cetin, T. Cuhadar-Donszelmann, M. Sahin, S. Sultansoy, and G. Unel, "Impact of the relatively light fourth family neutrino on the Higgs boson search", *Phys.Lett.*, vol. B710, pp. 328–331, 2012.

[60] Linda M. Carpenter, "Higgs Search Constraints on Fourth Generation Scenarios with General Lepton Sectors", 2011, 1110.4895.

[61] Gang Guo, Bo Ren, and Xiao-Gang He, "LHC Evidence Of A 126 GeV Higgs Boson From $H \to \gamma\gamma$ With Three And Four Generations", 2011, 1112.3188.

[62] A. Denner, S. Dittmaier, A. Muck, G. Passarino, M. Spira, et al., "Higgs Production and Decay with a Fourth Standard-Model-Like Fermion Generation", *Eur.Phys.J.*, vol. C72, pp. 1992, 2012.

[63] Abdelhak Djouadi and Alexander Lenz, "Sealing the fate of a fourth generation of fermions", *Phys.Lett.*, vol. B715, pp. 310–314, 2012.

[64] Eric Kuflik, Yosef Nir, and Tomer Volansky, "Implications of Higgs Searches on the Four Generation Standard Model", *Phys.Rev.Lett.*, vol. 110, pp. 091801, 2013.

[65] Otto Eberhardt, Geoffrey Herbert, Heiko Lacker, Alexander Lenz, Andreas Menzel, et al., "Joint analysis of Higgs decays and electroweak precision observables in the Standard Model with a sequential fourth generation", *Phys.Rev.*, vol. D86, pp. 013011, 2012.

[66] Alexander Lenz, "Constraints on a fourth generation of fermions from Higgs Boson searches", *Adv.High Energy Phys.*, vol. 2013, pp. 910275, 2013.

[67] Patrick Gonzalez, Jurgen Rohrwild, and Martin Wiebusch, "Electroweak Precision Observables within a Fourth Generation Model with General Flavour Structure", *Eur.Phys.J.*, vol. C72, pp. 2007, 2012.

[68] Tomer Yanir, "Phenomenological constraints on extended quark sectors", *JHEP*, vol. 0206, pp. 044, 2002.

[69] J. Bernabeu, A. Pich, and A. Santamaria, "Top quark mass from radiative corrections to the Z b anti-b decay", *Nucl.Phys.*, vol. B363, pp. 326–344, 1991.

[70] Bernd A. Kniehl and Johann H. Kuhn, "QCD Corrections to the Z Decay Rate", *Nucl.Phys.*, vol. B329, pp. 547, 1990.

[71] Michael E. Peskin and Tatsu Takeuchi, "Estimation of oblique electroweak corrections", *Phys.Rev.*, vol. D46, pp. 381–409, 1992.

[72] Otto Eberhardt, Alexander Lenz, and Jurgen Rohrwild, "Less space for a new family of fermions", *Phys.Rev.*, vol. D82, pp. 095006, 2010.

[73] Jeffrey R. Forshaw, D.A. Ross, and B.E. White, "Higgs mass bounds in a triplet model", *JHEP*, vol. 0110, pp. 007, 2001.

[74] Michael S. Chanowitz, "Bounding CKM Mixing with a Fourth Family", *Phys.Rev.*, vol. D79, pp. 113008, 2009.

[75] John M. Campbell, Rikkert Frederix, Fabio Maltoni, and Francesco Tramontano, "Next-to-Leading-Order Predictions for t-Channel Single-Top Production at Hadron Colliders", *Phys.Rev.Lett.*, vol. 102, pp. 182003, 2009.

[76] John M. Campbell and R. Keith Ellis, "Next-to-leading order corrections to W^+ 2 jet and Z^+ 2 jet production at hadron colliders", *Phys.Rev.*, vol. D65, pp. 113007, 2002.

[77] Shaouly Bar-Shalom, Soumitra Nandi, and Amarjit Soni, "Two Higgs doublets with 4th generation fermions - models for TeV-scale compositeness", *Phys.Rev.*, vol. D84, pp. 053009, 2011.

[78] Xiao-Gang He and German Valencia, "An extended scalar sector to address the tension between a fourth generation and Higgs searches at the LHC", *Phys.Lett.*, vol. B707, pp. 381–384, 2012.

[79] Ning Chen and Hong-Jian He, "LHC Signatures of Two-Higgs-Doublets with Fourth Family", *JHEP*, vol. 1204, pp. 062, 2012.

[80] Leo Bellantoni, Jens Erler, Jonathan J. Heckman, and Enrique Ramirez-Homs, "Masses of a Fourth Generation with Two Higgs Doublets", *Phys.Rev.*, vol. D86, pp. 034022, 2012.

[81] N. Arkani-Hamed, A.G. Cohen, E. Katz, and A.E. Nelson, "The Littlest Higgs", *JHEP*, vol. 0207, pp. 034, 2002.

[82] Maxim Perelstein, Michael E. Peskin, and Aaron Pierce, "Top quarks and electroweak symmetry breaking in little Higgs models", *Phys.Rev.*, vol. D69, pp. 075002, 2004.

[83] Maxim Perelstein, "Little Higgs models and their phenomenology", *Prog.Part.Nucl.Phys.*, vol. 58, pp. 247–291, 2007.

[84] Thomas Appelquist, Hsin-Chia Cheng, and Bogdan A. Dobrescu, "Bounds on universal extra dimensions", *Phys.Rev.*, vol. D64, pp. 035002, 2001.

[85] Takuya Kakuda, Kenji Nishiwaki, Kin-ya Oda, and Ryoutaro Watanabe, "Universal extra dimensions after Higgs discovery", *Phys.Rev.*, vol. D88, pp. 035007, 2013.

[86] Tony Gherghetta and Alex Pomarol, "Bulk fields and supersymmetry in a slice of AdS", *Nucl.Phys.*, vol. B586, pp. 141–162, 2000.

[87] Roberto Contino, Yasunori Nomura, and Alex Pomarol, "Higgs as a holographic pseudoGoldstone boson", *Nucl.Phys.*, vol. B671, pp. 148–174, 2003.

[88] Oleksii Matsedonskyi, Giuliano Panico, and Andrea Wulzer, "Light Top Partners for a Light Composite Higgs", *JHEP*, vol. 1301, pp. 164, 2013.

[89] Christopher T. Hill, "Topcolor: Top quark condensation in a gauge extension of the standard model", *Phys.Lett.*, vol. B266, pp. 419–424, 1991.

[90] Can Kilic, Karoline Kopp, and Takemichi Okui, "LHC Implications of the WIMP Miracle and Grand Unification", *Phys.Rev.*, vol. D83, pp. 015006, 2011.

[91] Bogdan A. Dobrescu and Christopher T. Hill, "Electroweak symmetry breaking via top condensation seesaw", *Phys.Rev.Lett.*, vol. 81, pp. 2634–2637, 1998.

[92] Hong-Jian He, Timothy M.P. Tait, and C.P. Yuan, "New top flavor models with seesaw mechanism", *Phys.Rev.*, vol. D62, pp. 011702, 2000.

[93] Hidenori S. Fukano and Kimmo Tuominen, "A hybrid 4^{th} generation: Technicolor with top-seesaw", *Phys.Rev.*, vol. D85, pp. 095025, 2012.

[94] F. del Aguila and Mark J. Bowick, "The Possibility of New Fermions With Δ I = 0 Mass", *Nucl.Phys.*, vol. B224, pp. 107, 1983.

[95] Otto Eberhardt, Geoffrey Herbert, Heiko Lacker, Alexander Lenz, Andreas Menzel, et al., "Impact of a Higgs boson at a mass of 126 GeV on the standard model with three and four fermion generations", *Phys.Rev.Lett.*, vol. 109, pp. 241802, 2012.

[96] ATLAS collaboration, "Search for anomalous production of events with same-sign dileptons and b jets in 14.3 fb^{-1} of pp collisions at $\sqrt{s} = 8$ TeV with the ATLAS detector", ATLAS-CONF-2013-051, 2013.

[97] ATLAS Collaboration, "Search for pair production of new heavy quarks that decay to a $\mathbf{Z}$ boson and a third generation quark in $\mathbf{pp}$ collisions

at $\sqrt{\mathrm{s}} = \mathbf{8}$ TeV with the ATLAS detector", ATLAS-CONF-2013-056, 2013.

[98] ATLAS Collaboration, "Search for heavy top-like quarks decaying to a Higgs boson and a top quark in the lepton plus jets final state in pp collisions at $\sqrt{s} = 8$ TeV with the ATLAS detector", ATLAS-CONF-2013-018, 2013.

[99] ATLAS Collaboration, "Search for pair production of heavy top-like quarks decaying to a high-p_{T} W boson and a b quark in the lepton plus jets final state in pp collisions at $\sqrt{s} = 8$ TeV with the ATLAS detector", ATLAS-CONF-2013-060, 2013.

[100] CMS Collaboration, "Inclusive search for a vector-like T quark with charge 2/3 in pp collisions at sqrt(s) = 8 TeV", *Phys.Lett.*, vol. B729, pp. 149–171, CMS-B2G-12-015, 2014.

[101] CMS Collaboration, "Search for pair-produced vector-like quarks of charge -1/3 in lepton+jets final state in pp collisions at sqrt(s) = 8 TeV", CMS-PAS-B2G-12-019, 2012.

[102] CMS Collaboration, "Search for Vector-Like b' Pair Production with Multilepton Final States in pp collisions at sqrt(s) = 8 TeV", CMS-PAS-B2G-13-003, 2013.

[103] CMS Collaboration, "Search for pair-produced vector-like quarks of charge -1/3 in dilepton+jets final state in pp collisions at sqrt(s) = 8 TeV", CMS-PAS-B2G-12-021, 2013.

[104] ATLAS Collaboration, "Search for heavy vector-like quarks coupling to light quarks in proton-proton collisions at $\sqrt{s} = 7$ TeV with the ATLAS detector", *Phys.Lett.*, vol. B712, pp. 22–39, CERN-PH-EP-2011-193, 2012.

[105] ATLAS Collaboration, "Search for single b^*-quark production with the ATLAS detector at $\sqrt{s} = 7$ TeV", *Phys.Lett.*, vol. B721, pp. 171–189, CERN-PH-EP-2012-344, 2013.

[106] F. del Aguila, M. Perez-Victoria, and Jose Santiago, "Observable contributions of new exotic quarks to quark mixing", *JHEP*, vol. 0009, pp. 011, 2000.

[107] Giacomo Cacciapaglia, Aldo Deandrea, Daisuke Harada, and Yasuhiro Okada, "Bounds and Decays of New Heavy Vector-like Top Partners", *JHEP*, vol. 1011, pp. 159, 2010.

[108] Giacomo Cacciapaglia, Aldo Deandrea, Luca Panizzi, Naveen Gaur, Daisuke Harada, et al., "Heavy Vector-like Top Partners at the LHC and flavour constraints", *JHEP*, vol. 1203, pp. 070, 2012.

[109] Mathieu Buchkremer, Giacomo Cacciapaglia, Aldo Deandrea, and Luca Panizzi, "Model Independent Framework for Searches of Top Partners", *Nucl.Phys.*, vol. B876, pp. 376–417, 2013.

[110] Neil D. Christensen and Claude Duhr, "FeynRules - Feynman rules made easy", *Comput.Phys.Commun.*, vol. 180, pp. 1614–1641, 2009.

[111] All the models discussed throughout this thesis are publicly available on the FeynRules website, ", `http://feynrules.irmp.ucl.ac.be/wiki/VLQ`.

[112] High Energy Physics Model Database, ", `http://hepmdb.soton.ac.uk/`.

[113] J.A. Aguilar-Saavedra, "Effects of mixing with quark singlets", *Phys.Rev.*, vol. D67, pp. 035003, 2003.

[114] Gino Isidori, Yosef Nir, and Gilad Perez, "Flavor Physics Constraints for Physics Beyond the Standard Model", *Ann.Rev.Nucl.Part.Sci.*, vol. 60, pp. 355, 2010.

[115] P.N. Kopnin and M.I. Vysotsky, "Manifestation of a singlet heavy up-type quark in the branching ratios of rare decays K -> pi nu anti-nu, B -> pi nu anti-nu and B -> K nu anti-nu", *JETP Lett.*, vol. 87, pp. 517–523, 2008.

[116] Ivica Picek and Branimir Radovcic, "Nondecoupling of terascale isosinglet quark and rare K- and B-decays", *Phys.Rev.*, vol. D78, pp. 015014, 2008.

[117] Oram Gedalia, Jernej F. Kamenik, Zoltan Ligeti, and Gilad Perez, "On the Universality of CP Violation in Delta F = 1 Processes", *Phys.Lett.*, vol. B714, pp. 55–61, 2012.

[118] S. Schael et al., "Precision electroweak measurements on the Z resonance", *Phys.Rept.*, vol. 427, pp. 257–454, 2006.

[119] Aldo Deandrea, "Atomic parity violation in cesium and implications for new physics", *Phys.Lett.*, vol. B409, pp. 277–282, 1997.

[120] Andrea De Simone, Oleksii Matsedonskyi, Riccardo Rattazzi, and Andrea Wulzer, "A First Top Partner Hunter's Guide", *JHEP*, vol. 1304, pp. 004, 2013.

[121] Matteo Cacciari, Michal Czakon, Michelangelo Mangano, Alexander Mitov, and Paolo Nason, "Top-pair production at hadron colliders with next-to-next-to-leading logarithmic soft-gluon resummation", *Phys.Lett.*, vol. B710, pp. 612–622, 2012.

[122] J. Pumplin, D.R. Stump, J. Huston, H.L. Lai, Pavel M. Nadolsky, et al., "New generation of parton distributions with uncertainties from global QCD analysis", *JHEP*, vol. 0207, pp. 012, 2002.

[123] John M. Campbell, Rikkert Frederix, Fabio Maltoni, and Francesco Tramontano, "NLO predictions for t-channel production of single top and fourth generation quarks at hadron colliders", *JHEP*, vol. 0910, pp. 042, 2009.

[124] ATLAS Collaboration, "Search for Single Production of Vector-like Quarks Coupling to Light Generations in $4.64\ ifb$ of Data at $sqrts = 7$ TeV", ATLAS-CONF-2012-137, 2012.

[125] D. Barducci, A. Belyaev, M. Buchkremer, G. Cacciapaglia, A. Deandrea, et al., "Model Independent Framework for Analysis of Scenarios with Multiple Heavy Extra Quarks", 2014, 1405.0737.

[126] J.A. Aguilar-Saavedra, "Pair production of heavy Q = 2/3 singlets at LHC", *Phys.Lett.*, vol. B625, pp. 234–244, 2005.

[127] J.A. Aguilar-Saavedra, "Identifying top partners at LHC", *JHEP*, vol. 0911, pp. 030, 2009.

[128] Anupama Atre, Georges Azuelos, Marcela Carena, Tao Han, Erkcan Ozcan, et al., "Model-Independent Searches for New Quarks at the LHC", *JHEP*, vol. 1108, pp. 080, 2011.

[129] Manuel Drees, Herbi Dreiner, Daniel Schmeier, Jamie Tattersall, and Jong Soo Kim, "CheckMATE: Confronting your Favourite New Physics Model with LHC Data", 2013, 1312.2591.

[130] Sabine Kraml, Suchita Kulkarni, Ursula Laa, Andre Lessa, Wolfgang Magerl, et al., "SModelS: a tool for interpreting simplified-model results from the LHC and its application to supersymmetry", *Eur.Phys.J.*, vol. C74, pp. 2868, 2014.

[131] Michele Papucci, Kazuki Sakurai, Andreas Weiler, and Lisa Zeune, "Fastlim: a fast LHC limit calculator", 2014, 1402.0492.

[132] Johan Alwall, Michel Herquet, Fabio Maltoni, Olivier Mattelaer, and Tim Stelzer, "MadGraph 5 : Going Beyond", *JHEP*, vol. 1106, pp. 128, 2011.

[133] Patrick Meade and Matthew Reece, "BRIDGE: Branching ratio inquiry / decay generated events", 2007, hep-ph/0703031.

[134] Torbjorn Sjostrand, Stephen Mrenna, and Peter Z. Skands, "PYTHIA 6.4 Physics and Manual", *JHEP*, vol. 0605, pp. 026, 2006.

[135] S. Ovyn, X. Rouby, and V. Lemaitre, "DELPHES, a framework for fast simulation of a generic collider experiment", 2009, 0903.2225.

[136] O. Buchmueller, R. Cavanaugh, M. Citron, A. De Roeck, M.J. Dolan, et al., "The CMSSM and NUHM1 in Light of 7 TeV LHC, $B_s \to \mu^+\mu^-$ and XENON100 Data", *Eur.Phys.J.*, vol. C72, pp. 2243, 2012.

[137] O. Buchmueller and J. Marrouche, "Universal mass limits on gluino and third-generation squarks in the context of Natural-like SUSY spectra", *Int.J.Mod.Phys.*, vol. A29, pp. 1450032, 2014.

[138] Inclusive search for a vector-like T quark by CMS additional material, ", https://twiki.cern.ch/twiki/bin/view/CMSPublic/PublicResultsB2G12015AdditionalPlots.

[139] CMS Collaboration, "Search for supersymmetry in final states with missing transverse energy and 0, 1, 2, or at least 3 b-quark jets in 7 TeV pp collisions using the variable alphaT", *JHEP*, vol. 1301, pp. 077, CMS-SUS-11-022, 2013.

[140] CMS Collaboration, "Search for supersymmetry in final states with a single lepton, b-quark jets, and missing transverse energy in proton-proton collisions at $\sqrt{s} = 7$ TeV", *Phys.Rev.*, vol. D87, no. 5, pp. 052006, CMS-SUS-11-028, 2013.

[141] CMS Collaboration, "Search for new physics in events with opposite-sign leptons, jets, and missing transverse energy in pp collisions at $\sqrt{s} = 7$ TeV", *Phys.Lett.*, vol. B718, pp. 815–840, CMS-SUS-11-011, 2013.

[142] CMS Collaboration, "Search for new physics in events with same-sign dileptons and b-tagged jets in pp collisions at $\sqrt{s} = 7$ TeV", *JHEP*, vol. 1208, pp. 110, CMS-SUS-11-020, 2012.

[143] CMS Collaboration, "Search for supersymmetry in hadronic final states with missing transverse energy using the variables AlphaT and b-quark multiplicity in pp collisions at 8 TeV", *Eur.Phys.J.*, vol. C73, pp. 2568, CMS-SUS-12-028, 2013.

[144] CMS Collaboration, "Search for new physics in events with same-sign dileptons and b jets in pp collisions at $\sqrt{s} = 8$ TeV", *JHEP*, vol. 1303, pp. 037, CMS-SUS-12-017, 2013.

[145] CMS Collaboration, "Search for top-quark partners with charge 5/3 in the same-sign dilepton final state", CMS-B2G-12-012, 2013.

[146] Matteo Cacciari, Michal Czakon, Michelangelo Mangano, Alexander Mitov, and Paolo Nason, "Top-pair production at hadron colliders with next-to-next-to-leading logarithmic soft-gluon resummation", *Phys.Lett.*, vol. B710, pp. 612–622, 2012.

[147] ATLAS Collaboration, "Search for exotic same-sign dilepton signatures (b' quark, $T_{5/3}$ and four top quarks production) in 4.7/fb of pp collisions at sqrts=7 TeV with the ATLAS detector", ATLAS-CONF-2012-130, 2012.

[148] Adrian Carmona, Mikael Chala, and Jose Santiago, "New Higgs Production Mechanism in Composite Higgs Models", *JHEP*, vol. 1207, pp. 049, 2012.

[149] Anupama Atre, Mikael Chala, and Jose Santiago, "Searches for New Vector Like Quarks: Higgs Channels", *JHEP*, vol. 1305, pp. 099, 2013.

[150] John M. Cornwall, David N. Levin, and George Tiktopoulos, "Derivation of Gauge Invariance from High-Energy Unitarity Bounds on the s Matrix", *Phys.Rev.*, vol. D10, pp. 1145, 1974.

[151] C.E. Vayonakis, "Born Helicity Amplitudes and Cross-Sections in Non-abelian Gauge Theories", *Lett.Nuovo Cim.*, vol. 17, pp. 383, 1976.

[152] Michael S. Chanowitz and Mary K. Gaillard, "The TeV Physics of Strongly Interacting W's and Z's", *Nucl.Phys.*, vol. B261, pp. 379, 1985.

[153] Alexander Belyaev, Neil D. Christensen, and Alexander Pukhov, "CalcHEP 3.4 for collider physics within and beyond the Standard Model", *Comput.Phys.Commun.*, vol. 184, pp. 1729–1769, 2013.

[154] Donald Shephard, "A two-dimensional interpolation function for irregularly-spaced data", *Proc. 23rd Nat. Conf. ACM*, pp. 517–523, 1968.

[155] Daniele Barducci, Alexander Belyaev, Jacob Blamey, Stefano Moretti, Luca Panizzi, et al., "Model-independent approach to the analysis of interference effects in pair production of new heavy quarks", 2013, 1311.3977.

[156] Giacomo Cacciapaglia, Aldo Deandrea, and Stefania De Curtis, "Nearby resonances beyond the Breit-Wigner approximation", *Phys.Lett.*, vol. B682, pp. 43–49, 2009.